1. FHWA/RD-81/052

ES, EXPERIMENTAL STUDIES, AND ...TIONS OF CONTROL MEASURES FOR AIR FLOW AND AIR QUALITY ON AND NEAR HIGHWAYS

Vol. II. User Guidelines and Application Notes for Estimating Air Quality for Alternative Roadway Configurations

March 1981

Final Report

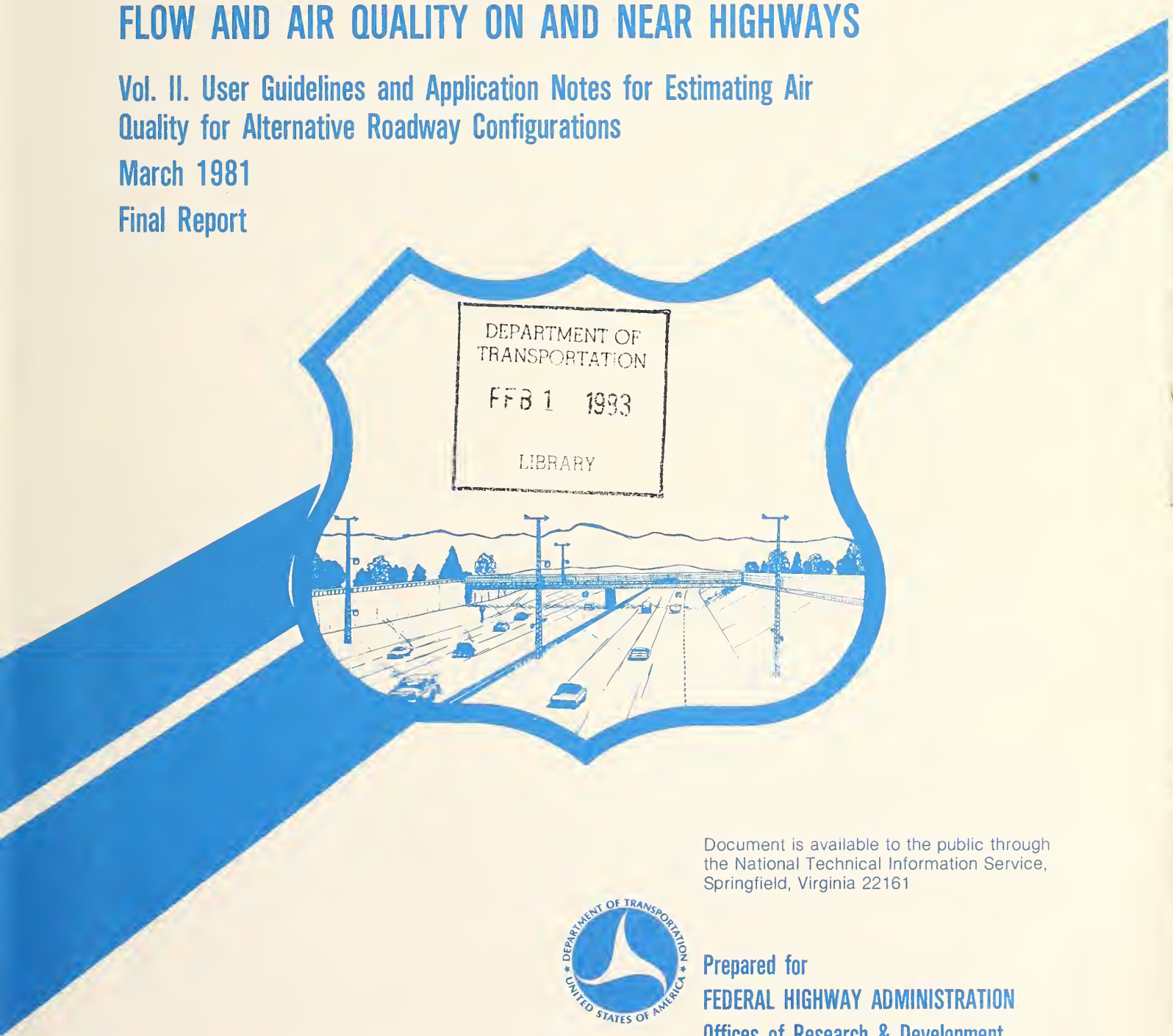

Document is available to the public through the National Technical Information Service, Springfield, Virginia 22161

Prepared for
FEDERAL HIGHWAY ADMINISTRATION
Offices of Research & Development
Environmental Division
Washington, D.C. 20590

FOREWORD

This report presents the development of concepts and guidelines to air contaminant entrainment and dispersion and the evaluation of air quality for generally uniform and steady traffic flows. From basic considerations, experimental results, and a simulation model, an assessment methodology was developed. Guidance for air quality near a highway is presented. This report will be of interest to researchers and advisors involved in air pollution and related environmental investigations.

Reports of this study, "Analyses, Experimental Studies, and Evaluations of Control Measures for Air Flows and Air Quality On and Near Highways," include:

FHWA/RD-81/051 Volume I, "Experimental Studies, Analyses, and Model Development"

FHWA/RD-81/052 Volume II, "User Guidelines and Application Notes for Estimating Air Quality for Alternative Roadway Configurations."

FHWA/RD-81/054 Volume III, "User's Manual for FHWA Data Base and Retrieval Programs" (Data Base on Magnetic Tapes)

FHWA/RD-81/053 An Executive Summary

Research in highway air pollution is included in the Federally Coordinated Program (FCP) of Highway Research and Development in Project 3F, "Pollution Reduction and Environmental Enhancement." Dr. H. A. Jongedyk is the FCP project manager.

One copy is being sent to each FHWA regional office. This report is also being given limited initial distribution to pertinent offices and specialists. A limited number of additional copies are available for official use upon request.

Charles F. Scheffey
Director, Office of Research
Federal Highway Administration

NOTICE

Technical Report Documentation Page

1. Report No.	2. Government Accession No.	3. Recipient's Catalog No.
FHWA/RD-81/052		

4. Title and Subtitle
ANALYSES, EXPERIMENTAL STUDIES, AND EVALUATIONS OF CONTROL MEASURES FOR AIR FLOW AND AIR QUALITY ON AND NEAR HIGHWAYS; VOL. II — User Guidelines and Applications Notes for Estimating Air Quality for Alternative Roadway Configuragions

5. Report Date: March 1981

6. Performing Organization Code:

8. Performing Organizotian Report No.: Final Report SRI Project 2761-1

7. Author(s): Walter F. Dabberdt

9. Performing Organization Name and Address:
SRI International
333 Ravenswood Avenue
Menlo Park, California 94025

10. Work Unit No. (TRAIS): 33F3082

11. Contract or Grant No.: DOT-FH-11-8125

13. Type of Report and Period Covered: Final Report (1973-1980)

12. Sponsoring Agency Name and Address:
U.S. Department of Transportation
Federal Highway Administration
Environmental Division
Washington, D.C. 20590
Offices of Research and Development

14. Sponsoring Agency Code:

15. Supplementary Notes

FHWA Contract Manager: Dr. Howard A. Jongedyk (HRS-42)

16. Abstract

A manual user-oriented methodology has been developed for estimating air quality conditions at each of a wide variety of simple and complex roadway configurations. The methodology is the result of experimental and theoretical investigations made at a number of atmospheric sites in addition to physical modeling studies made in Calspan Corporation's atmospheric simulation wind tunnel facility; experimental details, analyses, and results are presented in Volume I of this Final Report (No. FHWA/RD-81/051).

Guidelines are presented in four parts for the evaluation of air quality conditions at alternative roadway configurations. The first part presents a background discussion of principles of atmospheric dispersion and the emission of pollution (particularly carbon monoxide) by motor vehicles. In the second part the theory and application of the dispersion methodology is presented; the procedure is based on the roadway-atmospheric dispersion model of air pollution (ROADMAP) developed in Volume I of this report. To aid the user in applying the methodology, a worksheet format is used with accompanying tables and graphs. The applications of the methodology to some thirty site configurations in part three is intended to demonstrate the various tactical uses of the guidelines. The fourth part, on the other hand, presents some of the strategic considerations and limitations pertinent to the proper application of the guidelines for the purpose of air quality management.

In addition to the two-volume final report, two other reports and a movie dealing with various aspects of this study are available. The Executive Summary (FHWA/RD-81/053) presents the overall scope and the important technical results of the study. A user's manual for the experimental data collected in the field and wind tunnel tests is also available (FHWA/RD-81/054). The 20-minute 16-mm color movie, "Highway Pollution Dispersion: Air Quality in the Right-of-Way," uses sound, animation, graphics, and film sequences to present a comprehensive introduction to the causes and characteristics of microscale pollution dispersion near highways.

17. Key Words	18. Distribution Statement
Pollution, dispersion, highways, experimentation, wind tunnel, atmospheric testing, modeling, user guidelines, applications, limitations	This report is available through the National Technical Information Service, Springfield, Virginia 22161.

19. Security Classif. (of this report)	20. Security Classif. (of this page)	21. No. of Pages	22. Price
Unclassified	Unclassified	130	

TABLE OF CONTENTS

LIST OF ILLUSTRATIONS iv

LIST OF TABLES vii
METRIC CONVERSION FACTORS viii
I INTRODUCTION 1

A. Scope of the Study 1

B. Description of the User's Guide and Application Notes 5

C. Caveats 6

II BACKGROUND 8

A. Emissions 8

B. Pollutant Dispersion 10

1. Wind Transport 11
2. Diffusion by Ambient Wind 12
3. Terrain Effects 20
4. Traffic Effects 31

III ASSESSMENT METHODOLOGY 46

A. Introduction 46

B. Emissions from Uninterrupted Flow 47

C. Dispersion Methodology 53

1. Background 53
2. Application Procedure 62

IV APPLICATIONS 74

A. Introduction 74

B. Direct (Quantitative) Applications 75

C. Special Considerations 87

1. Variation in Median Width for Grade-Level Roads 87
2. Depressed Sections Resembling the ROADMAP Prototypes 88
3. Broad and Shallow Cut-Sections 89
4. Variations in Height and Width of Elevated Sections 89

TABLE OF CONTENTS (continued)

IV APPLICATIONS (Continued)

5. Stacked Viaducts 90
6. Curved Roadways 91
7. Grade Separations 92
8. Artificial Dispersion Control 95

D. Semi-quantitative Applications 101

1. Noise Barriers 102
2. Air-right Structure 102
3. Large Isolated Buildings Near Roadways 103
4. Traffic Congestion 104
5. Grade 104
6. Street Canyons and Cut Sections 106
7. Hillsides 109

E. Remarks 109

V AIR QUALITY MANAGEMENT THROUGH ROADWAY DESIGN AND LOCATION 112

A. Use of the ROADMAP Assessment Procedure 112

B. Guidelines for the Management of Local Air Quality . . 114

REFERENCES 120

ILLUSTRATIONS

1	Conceptual Framework for a Program to Develop a Rationale for the Assessment of the Impact of Vehicle, Meteorological, Roadway and Adjacent-Building Features on Microscale Air Quality	2
2	Vertical Diffusion According to Gaussian Formulation	17
3	Relationship Between σ_z and K	18
4	Influence of Terrain Upon Variation of Wind with Height (N. Hemisphere)	22
5	Idealized Representation of the Circulation That Might Be Expected in a Typical Valley on a Clear Night	23
6	Various Flow Patterns over Topographic Obstacles	24
7	The Airflow in the Vicinity of an Idealized Hill	25
8	Distortions of the Wind Flow by Topographic Obstacles	26
9	Schematic of Cross-street Circulation Between Buildings	27
10	Distribution of CO Concentration in Broadway Street Canyon	29
11	Variation of K_d and U_d with Distance from Vehicles for Drag Flow Corresponding to Different Vehicle Speeds	33
12	Schematic of Air Flow Over and Around a Vehicle Under Steady-State Flow Conditions	35
13	Schematic Illustration of Roadway-Shelterbelt Effect on Wind Flow and Turbulence	36
14	Wind Structure About a Small Shelter Consisting of Short Christmas Trees	38
15	Sheltering at Different Porosities	38
16	Average Effect of Speed on Automobile Fuel Consumption--1970/71 Models (4500 pounds)	40
17	Cumulative Frequency Distributions of Vertical Temperature Gradients Near a Freeway	42
18	Examples of Vertical Dispersion of Vehicle Exhaust Plume Due to Waste Heat Emission	43
19	Schematic Illustration of the Effects of Stability and Initial Mixing on Diffusion and Concentration	45
20	Relationships Between V/C Ratio and Operating Speed, in One Direction of Travel, on Freeways and Expressways, Under Uninterrupted Flow Conditions	50

21 Relationships Between V/C Ratio and Operating Speed, in One Direction of Travel, on Multilane Rural Highways, Under Uninterrupted Flow Conditions 50

22 Relationships Between V/C Ratio and Operating Speed, Overall for Both Directions of Travel, on Two-lane Rural Highways with Average Highway Speed of 50 mph, Under Uninterrupted Flow Conditions 51

23 Typical Relationships Between V/C Ratio and Average Overall Travel Speed, in One Direction of Travel, on Urban and Suburban Arterial Streets 51

24 Emission Density as a Function of Speed for 1975 Base Year. . 52

25 Coordinate System for ROADMAP 60

26 Variation of Dispersion Parameters with Cross-Roadway Distance for Grade-Level Roadway and Rough Terrain 67

27 Variation of Dispersion Parameters with Cross-Roadway Distance for Grade-Level Roadway and Smooth Terrain Upwind/Rough Downwind 67

28 Variation of Dispersion Parameters with Cross-Roadway Distance for Grade-Level Roadway and Rough Terrain Upwind/Smooth Downwind 68

29 Variation of Dispersion Parameters with Cross-Roadway Distance for Cut Section with Vertical Walls and Smooth Terrain 68

30 Variation of Dispersion Parameters with Cross-Roadway Distance for Street Canyon and Rough Terrain 69

31 Variation of Dispersion Parameters with Cross-Roadway Distance for Cut Section with Vertical Walls and Smooth Terrain 69

32 Variation of Dispersion Parameters with Cross-Roadway Distance for Cut Section with Sloping Walls and Smooth Terrain 70

33 Variation of Dispersion Parameters with Cross-Roadway Distance for Fill Section and Smooth Terrain 70

34 Variation of Dispersion Parameters with Cross-Roadway Distance for Viaduct Section and Smooth Terrain 71

35 Variation of Dispersion Parameters with Cross-Roadway Distance for Grade-Level Roadway, Smooth Terrain, and Stable Atmospheric Conditions 71

36 Variation of Dispersion Parameters with Cross-Roadway Distance for Grade-Level Roadway, Smooth Terrain, and Unstable Atmospheric Conditions 72

37 Schematic Illustration of the Use of a Virtual Roadway in Applying ROADMAP to a Gentle Curve 91

ILLUSTRATIONS (continued)

38	Schematic Illustration of Receptor Near Interchange of Grade-Level Roadway and Elevated Crossing on Fill	92
39	Schematic Illustration of Receptor Near Interchange of Grade-Level Roadway Intersected by a Depressed Roadway in a Sloped-Wall Cut Section	94
40	Normalized-Concentration Profiles for Various Median Belt Heights (p)	98
41	Slope Correction Factor for CO Emissions	106
42	Schematic of Cross-Street Circulation Between Buildings . .	108
43	Specification for Leeward and Windward Cases on the Basis of Receptor Location, Street Orientation, and Wind Direction	108
44	Wind Tunnel Results of Carbon Monoxide Concentrations (ppm) for a Roadway on a Hillside with a 3-m s^{-1} Ambient Crosswind and Moderate Traffic Moving at 25 mph	110

TABLES

1	Variation of z_o	14
2	Wind Profile Structure in the Adiabatic Surface Layer	16
3	Wind/Turbulence Profile Comparison for Lapse (Unstable) and Inversion (Stable) Conditions	21
4	Peak Drag-Flow Speeds, U(m s^{-1})	32
5	Instructions for Completing Worksheet 1	49
6	Cold-start Temperature Correction Factor (Csf) for Light Duty Vehicles	54
7	Calendar Year Correction Factors (Base Year 1975) for Light Duty Vehicles (Yf)	55
8	CO Grade Emission Correction Factor (Gf)	56
9	Instructions for Completing Worksheet 2	65
10	Inputs for Dispersion Computation	66
11	CO Emission Flux Factor (F) for Slow-Moving Vehicles	105
12	Comparison of ROADMAP Computations of $\chi U/Q(m^{-1})$ for an At-Grade Roadway, Illustrating the Variation with Stability, Height, Cross-Roadway Distance, and Wind-Roadway Orientation	114
13	Comparison of ROADMAP Computations of $\chi U/Q(m^{-1})$ for an At-Grade Roadway, Illustrating the Variation with Surface Roughness, Height, Cross-Roadway Distance, and Wind-Roadway Orientation During Neutral Atmospheric Stability	115
14	Comparison of ROADMAP Concentration Estimates for Five Roadway Configurations	119

METRIC CONVERSION FACTORS

Approximate Conversions to Metric Measures

Symbol	When You Know	Multiply by	To Find	Symbol
	LENGTH			
in	inches	*2.5	centimeters	cm
ft	feet	30	centimeters	cm
yd	yards	0.9	meters	m
mi	miles	1.6	kilometers	km
	AREA			
in^2	square inches	6.5	square centimeters	cm^2
ft^2	square feet	0.09	square meters	m^2
yd^2	square yards	0.8	square meters	m^2
mi^2	square miles	2.6	square kilometers	km^2
	acres	0.4	hectares	ha
	MASS (weight)			
oz	ounces	28	grams	g
lb	pounds	0.45	kilograms	kg
	short tons (2000 lb)	0.9	tonnes	t
	VOLUME			
tsp	teaspoons	5	milliliters	ml
Tbsp	tablespoons	15	milliliters	ml
fl oz	fluid ounces	30	milliliters	ml
c	cups	0.24	liters	l
pt	pints	0.47	liters	l
qt	quarts	0.95	liters	l
gal	gallons	3.8	liters	l
ft^3	cubic feet	0.03	cubic meters	m^3
yd^3	cubic yards	0.76	cubic meters	m^3
	TEMPERATURE (exact)			
°F	Fahrenheit temperature	5/9 (after subtracting 32)	Celsius temperature	°C

*1 in = 2.54 (exactly). For other exact conversions and more detailed tables, see NBS Misc. Publ. 286, Units of Weights and Measures, Price $2.25, SD Catalog No. C13.10:286.

Approximate Conversions from Metric Measures

Symbol	When You Know	Multiply by	To Find	Symbol
	LENGTH			
mm	millimeters	0.04	inches	in
cm	centimeters	0.4	inches	in
m	meters	3.3	feet	ft
m	meters	1.1	yards	yd
km	kilometers	0.6	miles	mi
	AREA			
cm^2	square centimeters	0.16	square inches	in^2
m^2	square meters	1.2	square yards	yd^2
km^2	square kilometers	0.4	square miles	mi^2
ha	hectares (10,000 m^2)	2.5	acres	
	MASS (weight)			
g	grams	0.035	ounces	oz
kg	kilograms	2.2	pounds	lb
t	tonnes (1000 kg)	1.1	short tons	
	VOLUME			
ml	milliliters	0.03	fluid ounces	fl oz
l	liters	2.1	pints	pt
l	liters	1.06	quarts	qt
l	liters	0.26	gallons	gal
m^3	cubic meters	35	cubic feet	ft^3
m^3	cubic meters	1.3	cubic yards	yd^3
	TEMPERATURE (exact)			
°C	Celsius temperature	9/5 (then add 32)	Fahrenheit temperature	°F

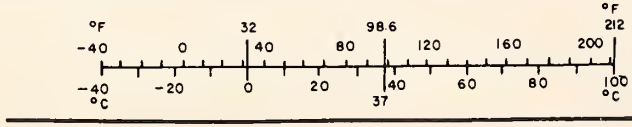

I INTRODUCTION

A. Scope of the Study

The basic objective of the overall study is the development of principles and guidelines for the description of dispersion and air quality conditions on and near roadways. Specifically, the research has been directed toward:

- Understanding how traffic, meteorology, and the geometry of the roadway and nearby buildings interact to influence the transport and diffusion of pollutants on the local- or micro-scale (i.e., within the roadway right-of-way).
- Developing a simulation procedure for predicting ambient pollutant concentrations that result from roadway emissions.

This simulation procedure would give planners a technique with which to assess the probable atmospheric impacts within the corridor of proposed roadways; where adverse impacts are projected, the methodology could be used to evaluate alternative roadway designs.

Because of the aerodynamically complex nature of major roadways, particularly in urban areas, and the impact on atmospheric turbulence and pollutant dispersion, it was proposed that a theoretical/experimental/empirical approach would (1) provide a firm basis for understanding the problem and (2) offer the best chance of developing a generic methodology that would effectively describe the impacts of traffic, meteorology, and geometry.

The conceptual approach of the study is summarized in Figure 1. At the outset, previous work related to microscale pollution-dispersion from highways and the influences of roadway geometry, meteorology, surface roughness, and traffic and vehicle motion was reviewed. The earlier theoretical and experimental investigations at that time (1973) did not adequately treat the combined effects of these four factors; even the effects of individual factors had, for the most part, not been properly addressed on the microscale. As a consequence, we undertook several

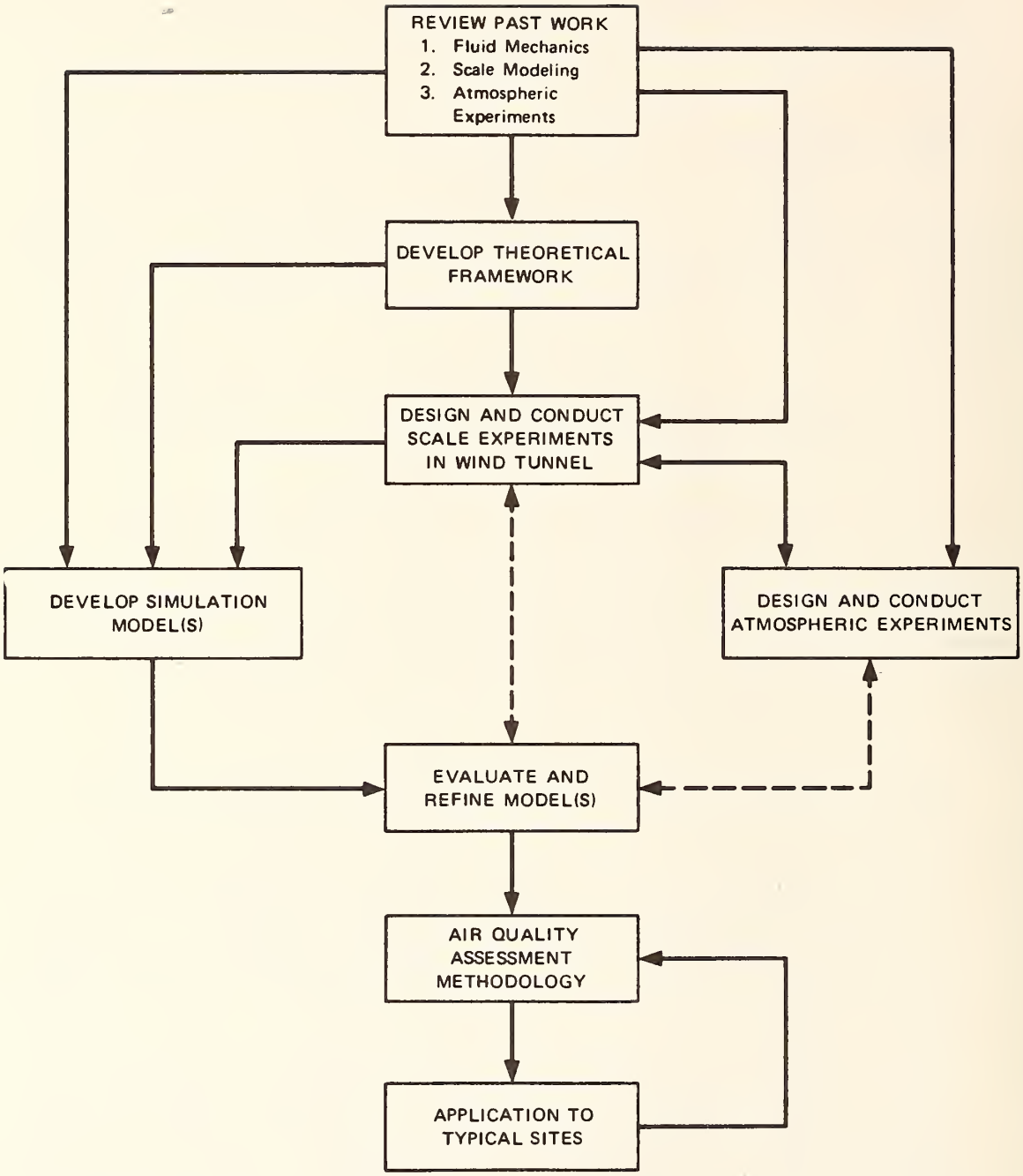

FIGURE 1 CONCEPTUAL FRAMEWORK FOR A PROGRAM TO DEVELOP A RATIONALE FOR THE ASSESSMENT OF THE IMPACT OF VEHICLE, METEOROLOGICAL, ROADWAY, AND ADJACENT BUILDING CHARACTERISTICS ON MICROSALE AIR QUALITY

preliminary theoretical investigations and data analyses to develop a framework for the subsequent atmospheric and wind tunnel tests that were to fill in many of the voids in the area of microscale dispersion processes and the nature of air quality conditions on and near roadways. These preliminary investigations (Dabberdt, 1974) included analytical modeling of the principle features of wake-induced turbulence and drag flow and the use of statistical methods to relate near-roadway pollutant concentrations (measured during several earlier studies in Los Angeles) to meteorological and site characteristics.

Using the results of these preliminary efforts, an extensive number of aerometric experiments was designed and conducted. In all, 16 different roadway configurations were investigated, including various types of at-grade, elevated, and depressed sections with both rough and smooth adjacent terrain. Three tests were conducted at existing roadway locations, and the remaining 13 were conducted in the controlled environment of an environmental wind tunnel. These scale model tests had the advantage of flexibility in that wind, traffic, and geometric variables could be easily varied at will. On the other hand, the atmospheric tests permitted the analysis of impacts due to diabatic stability conditions and vehicular thermal emissions. The design and scope of the wind tunnel and atmospheric tests are thoroughly described in Volume I of the final report. The air quality, meteorological, and traffic data collected in these tests is available to the public. The data have been archived on magnetic tape and a user's manual has been prepared. Inquiries regarding acquisition of the data should be made to: U.S. Department of Transportation, Federal Highway Administration, Office of Research, Environmental Control Group, Washington, D.C. 20590.

The experimental data were first analyzed to investigate the interrelationships among effects from traffic, meteorology, and ground roughness. This proceeded in two phases: First, the data from the atmospheric test at the grade-level roadway section were analyzed to understand dispersion effects due to variations in traffic and meteorology. Next, statistical analyses using factor analysis and multiple regression were

made of the grade-level, cut and elevated roadway data to further identify individual and combined effects resulting from variations in wind, traffic, ground roughness, and roadway configurations.

In addition to providing new and useful insights into the dispersion process, these analyses also helped to identify the framework of a simulation model that could both accurately simulate air quality conditions downwind of a range of roadway configurations and be rapidly and easily applied by nonresearch users. An empirical model called ROADMAP (Roadway Dispersion Model for Air Pollution) was subsequently developed. One feature of the model is that it seeks to characterize dispersion from a line source as the vector sum of two components--one from transport and diffusion along the horizontal wind component that is perpendicular to the line source, and the other along the wind component parallel to the roadway. A second feature of the model is that it implicitly describes aerodynamic and thermal vehicular effects on dispersion.

ROADMAP also forms the basis for the evaluation methodology discussed in this report. The evaluation methodology consists of a fully self-contained set of guidelines for estimating air quality for alternative roadway configurations. To promote the proper assessment of air quality, the guidelines consist of four levels of analysis. First, there is a discussion of theoretical and empirical considerations in quantifying the dispersion process (i.e., transport, diffusion, and terrain and traffic effects). Second, the assessment methodology gives an introduction to the basis and formulation of ROADMAP, followed by a series of worksheets, tables, and graphs to systematize the calculations. Third, the applications section addresses the use of ROADMAP and other considerations in evaluating thirty alternative roadway configurations and environments. A final section discusses the philosophy of the proper use and application of the guidelines as well as providing some insights into possibilities for air quality management and control.

The theoretical, analytical, and experimental aspects of the study are summarized in Volume I of the final report (FHWA-RD-78-179). The user's guide and application notes are presented in this volume. A user's manual for the experimental data collected in the field and wind tunnel

tests is also available (FHWA-RD-78-128)*. A 16-mm color movie entitled "Highway Pollution Dispersion: Air Quality in the Right-of-Way" was also prepared during the research study and is available. This 20-min sound movie uses animation, sketches, and film sequences to present a comprehensive introduction to the causes and characteristics of micro-scale pollution dispersion near highways. The movie is directed toward a wide audience ranging from interested nonspecialists to highway engineers to researchers.

B. Description of the User's Guide and Application Notes

Comprehensive guidelines are presented in the remaining sections of this report to aid in the practical application of the ROADMAP dispersion model and to provide guidance on the potential for application of various pollution reduction measures. The guidelines are presented in three parts:

- A background section (Section II) discusses aspects of emission generation and the physics of pollution dispersion.
- The assessment methodology (Section III) provides a format for implementing the model.
- Applications notes discuss both the direct and indirect use of the dispersion model at 30 different roadway situations (Section IV).

Lastly, application of the methodology for air quality management is discussed in Section V from two aspects: the use of ROADMAP in assessing the pollution potential of alternative roadway designs and guidelines regarding the potential application and efficacy of active and passive pollution control measures.

The background section to the user's guide reviews the dependence of vehicular emission rates of carbon monoxide--the principal pollutant of interest on the local scale. The review covers the dependence of emissions on the pattern of vehicle operation, i.e., acceleration, deceleration, idling, and cruise. Also considered are atmospheric dispersion concepts, including wind transport, diffusion over homogeneous terrain and effects from surface roughness and atmospheric stability, the impacts of mesoscale and microscale terrain features on dispersion and mechanical and thermal effects of traffic on pollutant dispersion.

---

*The data are available on six magnetic tapes.

The assessment methodology is presented in two parts. First, roadway and traffic features are used to estimate the emission flux density from the vehicles. The procedure considers the effects of a wide range of parameters: speed, demand volume, capacity, grade, temperature, location, altitude, and the percentage of cold-start vehicles. A step-by-step worksheet procedure is provided, with corresponding instructions, tables, and graphs. The second part of the assessment methodology treats the atmospheric dispersion. A brief summary introduces the rationale for and the format of the ROADMAP model. Again, a worksheet with instructions and all required inputs are provided to implement the dispersion procedure. Eleven independent parameters must be specified to compute the pollutant concentration: receptor height, road/receptor separation, roadway type (design), roadway height, roadway width, roadway heading, emission flux density (from first worksheet), surface roughness, wind speed, wind direction, and atmospheric stability.

Various types of potential air quality management techniques are discussed: Passive controls include the selection of roadway pavements that will enchance atmospheric instability over the roadway, and median-belts (i.e., shelterbelts in the median strip of the roadway) to increase mechanically the extent of both vertical and horizontal mixing over the roadway. Two types of active controls are also considered: One, ventilation, is not recommended, while the other, filtering, may be effective for certain specific, localized problem areas. Other air quality management aspects considered include the roughness of the nearby terrain, vehicle speed, roadway design, and roadway slope.

C. Caveats

The user should bear in mind the purposes for which the model can properly be applied (i.e., when and where ROADMAP should be used).

Perhaps the most important feature is the scale over which it may be used. ROADMAP is by design a microscale model and its use is most appropriate out to distances of 50-100 m from the roadway edges. Accordingly, it would be inappropriate to assess the larger-scale effects.

Errata Sheet

Text of report contains erroneous or superceded report numbers:

These are:

Report FHWA/RD-81/051 wrongly identified as Report FHWA/RD-78-179

Report FHWA/RD-81/052 wrongly identified as Report FHWA/RD-78-180

Report FHWA/RD-81/053 wrongly identified as Report FHWA/RD-78-181

Report FWWA/RD-81/054 wrongly identified as Report FHWA/RD-78-182

or Report FHWA/RD-78-128

In analyzing local air pollution aspects of any highway project (existing or proposed), it is essential that the user identify and address both the background and the local components of the total air pollution concentration at the site. ROADMAP addresses only the local component.

There are two similar yet distinct ways in which ROADMAP methodology may usefully be applied. In the first application, ROADMAP may be used to estimate the absolute magnitude of the concentration of inert pollutants emitted from an existing or proposed project. If the highway project is already completed and the (total) pollution concentration is known, then this will provide useful information on the relative magnitudes of the local and background components. In this way, it is possible to address the degree of local control necessary to improve existing air-quality conditions to the point where they may, for example, comply with the National Ambient Air Quality Standards (NAAQS). Or alternatively, such analysis could also be used to address proportional controls of both local and background emission sources.

The second use of ROADMAP involves the assessment of the local air pollution impacts of alternative designs or locations of proposed or existing roadways. Such air pollution "benefits" can then be evaluated in conjunction with their corresponding costs against other environmental, engineering, and aesthetic considerations to assess the optimal project design.

II BACKGROUND

Prior to presenting the ROADMAP-based assessment methodology (Section III), background material is given on the fundamentals of pollutant emissions on highways and the principles of their dispersion in the atmosphere.

A. Emissions

In determining near-roadway pollutant concentrations, the rate at which emissions are released from the individual traffic lanes must first be estimated. The dispersion methodology presented later (Section III) provides two alternatives for the spatial resolution required to adequately represent the emission sources: If the two traffic streams are adjacent to each other and the respective traffic flow conditions are similar, then the entire roadway may be treated as a single, homogeneous line source of finite width (W). If there is significant separation between the two traffic streams or if their flow characteristics are dissimilar, however, then each stream (i.e., direction of travel) should be treated as a separate independent roadway.

The rate at which pollutants are emitted from roadway vehicles depends on the corresponding pattern or cycle of operating modes: acceleration, cruise, deceleration, and idle. The cycle will be different for different roadway types (e.g., arterial vs. freeway), environmental conditions, and demand volumes. The Environmental Protection Agency has developed a hypothetical driving cycle (i.e., the Federal Test Procedure (FTP)) that typifies average driving conditions over a lengthy route. A corresponding emission rate is also provided by EPA. This rate corresponds to an average vehicle speed of about 22 mph and "standard" atmospheric and vehicle conditions. The actual emission rate must then be adjusted to correspond to vehicle age, air temperature, engine temperature, altitude, state of residence (California or other), and average vehicle speed. Lastly, this

must be extended to represent the mix of all vehicles using the roadway under study. Other complications and complexities arise when the FTP is not particularly representative of driving conditions on the roadway, as might be the case near a signalized intersection or toll booth. Dabberdt and Sandys (1976) have developed a technique to evaluate emissions for such cases. In the present context we have restricted the approach to cover only limited access roadways and have assumed that the FTP is representative of the local driving pattern. As such, the method may not strictly be appropriate to estimating emissions when the traffic flow is congested.

Congestion occurs when demand volume exceeds the capacity of a roadway or intersection. The demand volume is the number of vehicles that desire to use a roadway or intersection during a period of time, usually one hour. The volume actually using a roadway or intersection is less than the demand volume during congested flow. Congestion with regard to freeway flow can be due to the effects of merging, weaving, or too few lanes. The section causing the congestion is called a bottleneck. The effect of a bottleneck is to:

- Limit vehicle flow to the capacity of the bottleneck
- Reduce vehicle speed over the congested section
- Extend the congestion upstream of the bottleneck
- Extend the duration of the period of peak emissions.

Intuitively, congestion should have the effect of greatly increasing the average vehicle emission rate per mile. Some freeway data supplied by Prof. Adolf May at the University of California, Berkeley, were analyzed to determine whether the average vehicle emission rate during congested flow (average speed of 20 mph*) is much greater than the average emission rate at a similar speed from a vehicle driving the FTP driving cycle. The freeway data indicate ten full stops over a 10-mile length of roadway in which congestion occurred. The FTP driving cycle shows 19 full stops in 7.5 miles. This seems to indicate that driving in an uncoordinated street network is as bad or worse than driving over a congested section

---

*1 mph = 1.6 kmph

of a freeway.* The average vehicle emits more pollutants driving in congestion simply because the vehicle is traveling at a lower speed and at a smaller spacing interval (i.e., headway) than normal and thus emits more pollutants per mile. An offsetting effect on vehicle emissions occurs because less vehicles (i.e., less than the roadway capacity) use the section of roadway during periods of congested flow. Although there is an increase in emissions on a macroscale (since excess demand is effectively being queued upstream), peak microscale emissions may not be increased significantly because of congestion. The effect of extending congestion upstream from the bottleneck has the effect of prolonging the period of congestion and causing congestion at offramps, onramps, and intersections that feed the freeway. Thus, a thorough analysis must account for all the upstream effects of congestion and the duration of these effects as volume demand increases to greater than capacity levels and then decreases to less than capacity.

B. Pollutant Dispersion

The dispersion of the pollutants emitted from roadway traffic is affected both by the velocity and turbulence characteristics of the ambient wind flow and by the thermal and mechanical turbulence generated by the vehicles themselves. The ambient conditions, in turn, are influenced by the mechanical and thermal properties of the terrain as well as the geometric configuration of the roadway.

In the following discussion we present background information on the individual "elements" that affect the intensity and extent of the dispersion of the traffic emissions and subsequently determine the magnitude of the ambient pollutant concentrations near the roadway. These elements include:

(1) The transport of pollutants by the ambient wind (speed and direction) and the influence of local topography

---

*The emission rate is largest when vehicles are in the acceleration mode (the deceleration emission rate is similar to steady-state driving).

(2) The corresponding turbulence characteristics of the ambient wind and their effect on diffusion

(3) Traffic influences on the initial diffusion of the emissions.

In following sections the quantitative methodology is first presented (Section III) and then applied (Section IV) to some of the many different roadway settings that occur [these are made up of various combinations of atmospheric stability, terrain roughness, traffic effects, and roadway design (or geometric configuration)].

1. Wind Transport

Transport of roadway emissions by the ambient wind has two direct effects on the distribution and magnitude of pollutant levels near the roadway. First, the direction of the wind has the obvious impact of determining where the pollutants will be transported. Second, the wind speed determines the volume of air that is available to dilute the emissions.

As discussed in more detail later, wind direction also has an influence on the nature or type of diffusion that results. Briefly, the diffusion that occurs when the wind is perpendicular to the roadway axis is different from when the wind is parallel to the roadway. With a perpendicular wind and a quasi-infinite roadway length, horizontal diffusion along and normal to the mean wind vector does not contribute to the dilution of the pollutant concentration. This is due to: (1) the continuous nature of the emission source which causes the upwind and downwind diffusion (i.e., parallel to the mean wind vector) to compensate for each other, and (2) the quasi-infinite roadway length which has a similar compensating effect, but on the cross-wind horizontal diffusion. As a result, only the vertical diffusion contributes to the reduction (i.e., by diffusion as distinct from transport) in concentration levels. When the wind parallels the road, a similar compensating effect occurs with the along-wind horizontal diffusion. If the road segment is sufficiently long (on the order of 1 km), Dabberdt et al. (1976) have shown that the vertical diffusion along the wind vector is not an important control of the concentration levels; the explanation apparently is that

a pseudo-equilibrium is reached between the rates of pollutant emission from the roadway and the vertical diffusion. The variation of concentration levels with distance away from the road is controlled by the rate of cross-wind horizontal diffusion. In summary, with a roadway-perpendicular wind it is the magnitude and variation of the vertical diffusion that is important, while the horizontal cross-wind diffusion is most important for the roadway-parallel wind case.

The speed of the wind is important as it determines the volume of air available to dilute the emissions. For example, a moderately heavily traveled roadway might have carbon monoxide (CO) emissions on the order of a few centigrams per meter of roadway length per second of time (e.g., 0.03 g m^{-1} s^{-1}). At the same time, the emissions may be mixed from the pavement up to a height of, for example, three meters. Considering a one-meter long segment of pavement and a wind blowing perpendicular to the roadway axis at a speed of one meter per second, then every minute a total volume of air equal to 180 m^3 would be available to dilute the 1.8 g of CO emitted; the resulting average concentration within the air volume would therefore be 0.01 g m^{-3} or about ten parts per million (ppm). Doubling the wind speed to 2 m s^{-1} would also double the available volume of air, while the emission rate does not change. This would then have the effect of halving the average concentration to 5 ppm in this hypothetical example. From this qualitative analysis, we see that a first order effect of wind speed (U, m s^{-1}) is to directly "control" the concentration levels (χ, g m^{-3}) in an inverse manner:

$$\chi \propto \frac{Q_\ell}{U} \quad , \tag{1}$$

where Q_ℓ is the line source emission flux density (g m^{-1} s^{-1}). As will be seen later, wind speed can also have significant indirect or secondary effects on the vertical extent or magnitude of the turbulent mixing and therefore also on the pollution concentration.

2. Diffusion by Ambient Wind

The discussion in the preceding subsection emphasized the importance of wind speed and turbulent diffusion in controlling pollutant

concentrations. Recapitulating, the wind speed determines the horizontal length of a hypothetical box of air into which pollutants are mixed, whereas the vertical diffusion (σ_z,m) determines the height of the box and, for a roadway-parallel wind, the cross-wind horizontal diffusion (σ_y,m) determines its width, where:

$$\chi \propto \frac{Q_\ell}{U\sigma_z\sigma_y} \quad . \tag{2}$$

In the absence of mechanical and thermal effects of the traffic on diffusion, the turbulence in the ambient wind varies with height above ground (z), surface roughness, and atmospheric stability. Many equations have been given to describe the structure of the vertical wind profile; in this discussion the profile formulation described by Lettau (1962) for diabatic conditions will be used. However, before considering diabatic effects from atmospheric heating or cooling, the adiabatic or neutral situation will be discussed first.

In the absence of atmospheric heating or cooling, the temperature in the atmosphere decreases at a rate of 1°C per 100 m; this vertical gradient is equal to the warming that would occur from compression if a parcel of air were subjected to a decrease in altitude (with the corresponding increase in pressure). During neutral conditions, the vertical profile of the wind above the earth's surface (to a height of approximately 50-100 m) is given by the so-called logarithmic wind profile:

$$\overline{U}_a = \frac{U_a^*}{k} \ln\left(\frac{z + z_o}{z_o}\right) \tag{3}$$

where k is the von Karman constant (0.428), z_o is the aerodynamic surface roughness, U^* is the friction velocity, and the subscript a refers to adiabatic conditions. As illustrated below, z_o is essentially the height above ground where the mean wind speed goes to zero owing to the aerodynamic effect of the surface roughness elements. Height (z) is then measured above this level. The height z_o can be computed for a particular location by measuring the wind speed at various levels during neutral

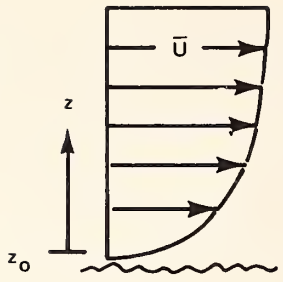

conditions and applying Eq. (3). The surface roughness may also be estimated empirically; Lettau (1969) has suggested a simple relationship:

$$z_o = 0.5 \frac{h^* s}{S} \tag{4}$$

where h^* is the average vertical extent or effective height of the obstacles, s is the average frontal or silhouette area that each obstacle presents to the wind, and S is the specific ground area "occupied" by each obstruction (e.g., a 1000 m^2 lot with 50 trees--obstacles--would have S = 20 m^2). Table 1 summarizes the variation of z_o with different surface types, using Eq. (4).

Table 1

VARIATION OF z_o^*

Obstacle Type	h^*(cm)	s/S	z_o(cm)
Forest trees, houses	1000	5.	214.
Field crops, tall grasses	100	7.	13.8
Lower grasses, weeds	10	11.	0.80
Bare soils	1	17.	0.058

*Estimated from Eq. (4), after Lettau (1969).

The friction velocity (U^*) is equal to the square root of the quotiant of shearing stress, τ (caused by the change in wind speed with

height), and atmospheric density, ρ. The parameter that relates stress to shear is the eddy diffusivity K ($m^2\ s^{-1}$), where:

$$U^{*2} = \frac{\tau_o}{\rho} = K \frac{\partial \overline{U}}{\partial z} \quad . \tag{5}$$

The subscript zero refers to the surface value of the shearing stress. But near the ground, the height-change in τ is small compared to the magnitude of τ and so the shearing stress may be considered relatively invariant up to heights of 25-50 m; this layer is often called the constant-stress or surface layer. Within this layer the eddy diffusivity is easily determined for neutral conditions by combining Eqs. (3) and (5), where:

$$K_a = U_a^* \, k \, (z + z_o) \quad . \tag{6}$$

The diffusivity in turn may be related to the mixing length, ℓ (m), which can be thought of as the distance over which the mixing process occurs at a rate equal to U^*, such that

$$K = \ell \, U^* \quad , \text{ and} \tag{7a}$$

$$\ell_a = k(z + z_o) \tag{7b}$$

Table 2 summarizes the impacts in the wind and turbulence structure that result from variations in the surface roughness and the ambient wind speed (given at some reference height, for example 10 m). Several things are readily depicted in the table: increasing surface roughness decreases wind speed near the surface while at the same time, the mixing length and eddy diffusivity are increased. When the reference wind speed is changed, the shape of the wind and diffusivity profiles are unchanged, while their magnitudes vary in direct proportion to the wind speed change.

The effect that these changes have on the transport and diffusion of pollutants can more easily be understood by examining the form of the dispersion coefficient (i.e., σ_z) used in Eq. (2). The eddy diffusivity

Table 2

WIND PROFILE STRUCTURE IN THE ADIABATIC SURFACE LAYER

z_o(m)	$\bar{U}$ (m s^{-1}) 10m	U (m s^{-1})	z = 1 m			z = 2 m			z = 3 m			z = 5 m			z = 8 m		
			$\bar{U}$	K	ℓ	$\bar{U}$	K	ℓ	$\bar{U}$	K	ℓ	$\bar{U}$	K	ℓ	$\bar{U}$	K	ℓ
0.1	1.0	.0927	0.52	0.04	0.47	0.66	0.08	0.90	0.74	0.12	1.33	0.85	0.20	2.18	0.95	0.32	3.47
0.5	1.0	.141	0.36	0.09	0.64	0.53	0.15	1.07	0.64	0.21	1.50	0.70	0.33	2.35	0.93	0.51	3.64
1.5	1.0	.210	0.25	0.22	1.07	0.42	0.32	1.50	0.54	0.41	1.93	0.72	0.58	3.78	0.91	0.85	4.07
0.1	3.0	.278	1.56	0.13	0.47	1.98	0.25	0.90	2.22	0.37	1.33	2.55	0.61	2.18	2.85	0.96	3.47
0.5	3.0	.422	1.08	0.27	0.64	1.59	0.45	1.07	1.92	0.63	1.50	2.37	0.99	2.35	2.79	1.54	3.64
1.5	3.0	.630	0.75	0.67	1.07	1.26	0.94	1.50	1.62	1.21	1.93	2.16	1.75	2.78	2.72	2.56	4.07
0.1	5.0	.464	2.60	0.22	0.47	3.30	0.42	0.90	3.70	0.62	1.33	4.25	1.01	2.18	4.75	1.61	3.47
0.5	5.0	.703	1.80	0.45	0.64	2.65	0.75	1.07	3.20	1.05	1.50	3.95	1.65	2.35	4.65	2.56	3.64
1.5	5.0	1.051	1.25	1.12	1.07	2.10	1.58	1.50	2.70	2.03	1.93	3.60	2.92	2.78	4.53	4.28	4.07

$\bar{U}$ (m s^{-1}) - mean wind speed

K (m^2 s^{-1}) - eddy diffusivity

ℓ (m) - mixing length

K and the dispersion coefficient σ_z (or σ_y) cannot be directly compared insofar as σ_z represents a characteristic length over which pollutants have been diffused after being transported a given distance from the source of the pollutants, while K can be thought of as the rate at which the pollutants are diffused. Figure 2 illustrates the relationship between σ_z and the shape of the profile of pollution concentration. (In effect, σ_z is the standard deviation of the Gaussian or normal distribution.) The general relationship between σ_z and K is:

$$\sigma_z = \sqrt{\frac{2 \times K}{\bar{U}}} = \sqrt{\frac{2 \times \ell \, U^*}{\bar{U}}} \tag{8a}$$

while for neutral conditions it can be restated using Eqs. (7b) and (3):

$$\sigma_{z-a} = \sqrt{\frac{2 \times (z + z_o) \, k \, U_a^*}{\bar{U}_a}} = \sqrt{\frac{2 \times k^2 (z + z_o)}{\ln\left(\frac{z + z_o}{z_o}\right)}} \tag{8b}$$

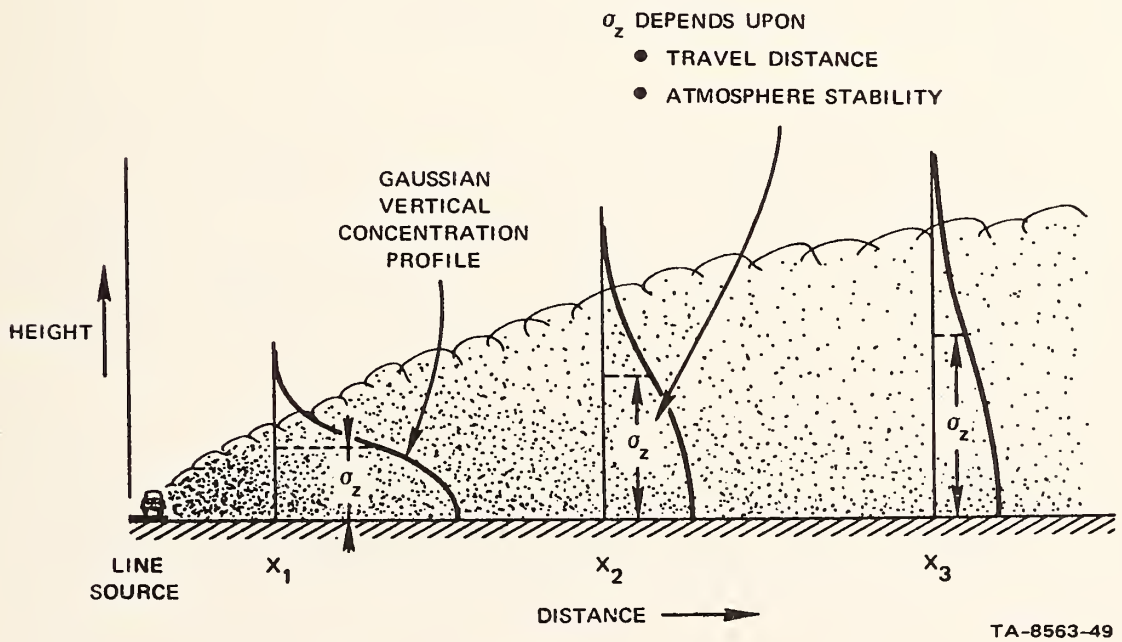

FIGURE 2 VERTICAL DIFFUSION ACCORDING TO GAUSSIAN FORMULATION

Figure 3 plots the relationship between σ_z and K up to x = 50 for four values of the term $K/\overline{U}$: 0.1, 0.2, 0.5, and 1.0 m. In turn, Table 2 can be used to examine the adiabatic variation of $K/\overline{U}$ with z, z_o, and $\overline{U}_{ref}$.

The structure of the vertical profiles of wind, stress, and diffusivity can be quite different when the surface layer is diabatic. The stability of a layer of air can be expressed quantitatively by the Richardson number (Ri)--the ratio of the heat and momentum fluxes. For neutral conditions the heat flux is zero by definition and so must be Ri;

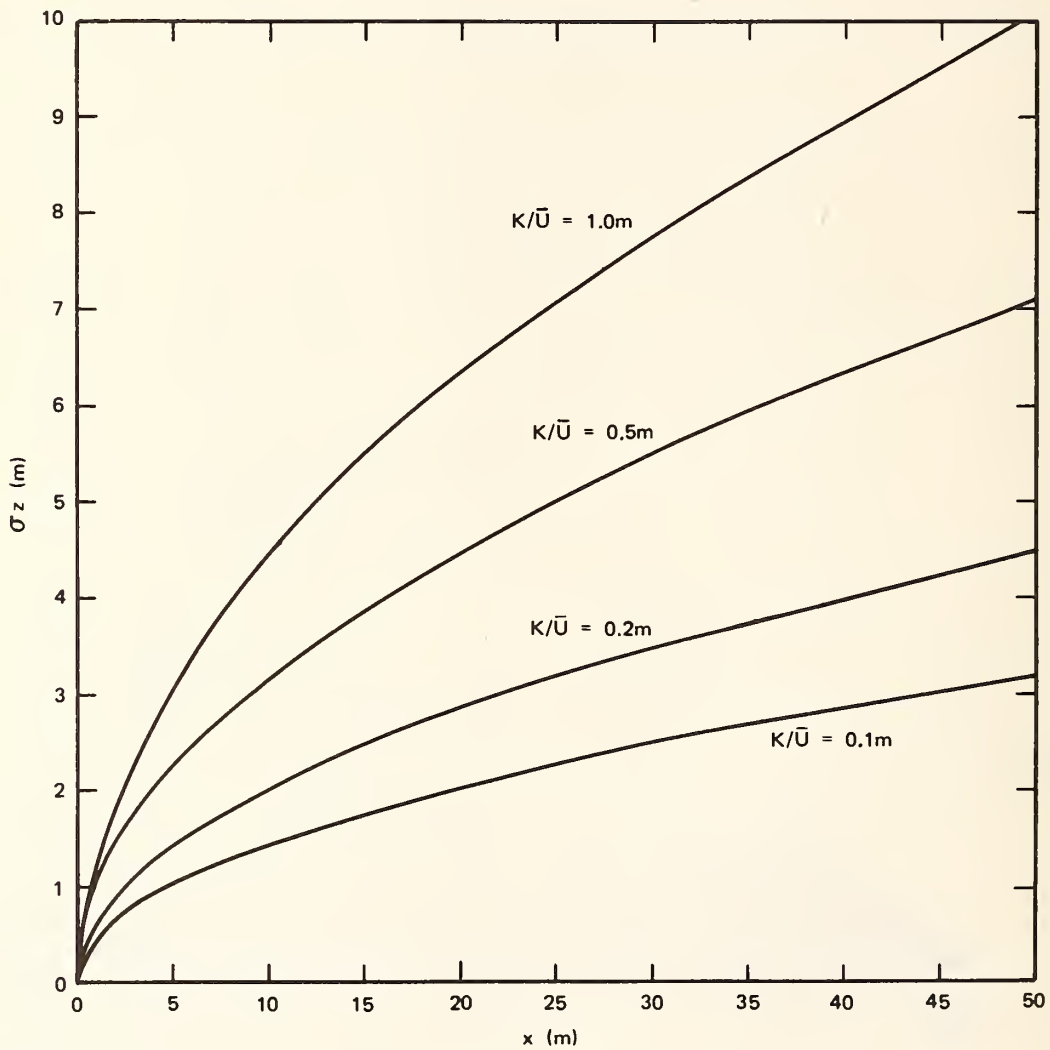

FIGURE 3 RELATIONSHIP BETWEEN σ_z AND K

for lapse (unstable) conditions the heat flux is from the ground to the air and Ri < 0, while the atmospheric heat flux is from air to ground during inversion (stable) conditions and Ri > 0. The equation for calculating Ri is:

$$Ri = \frac{g}{\overline{T}} \frac{\partial\theta/\partial z}{(\partial\overline{U}/\partial z)^2} \tag{9}$$

where g is the gravitational acceleration (9.8 $m^2\ s^{-1}$), $\overline{T}$ is the average air temperature (°K) and θ is the potential temperature (°K). Ri is a height-dependent parameter whose ground value is always zero*. To illustrate stability effects, we will use two assumed vertical profiles of Ri:

$$Ri_u = -0.1z \qquad \text{(lapse profile) , and} \tag{10a}$$

$$Ri_s = 0.005z \qquad \text{(inversion profile) .} \tag{10b}$$

The wind profile equation given earlier for neutral conditions (Eq. (3)) can be modified to reflect the effect of diabatic conditions,

$$\overline{U} = \frac{\phi^* U_a^*}{k} \left\{ \ln\left(\frac{z + z_o}{z_o}\right) + \Phi \right\} . \tag{11}$$

The term ϕ^* is called the diabatic influence function by Lettau (1962) and is independent of height. The so-called integral influence function Φ varies both with height (z) and Richardson number (Ri). For the purposes of illustration, we introduce two further a priori assumptions to supplement Eqs. (10a) and (10b):

$$\phi_u^* = 0.75 \ ; \qquad \text{(unstable case),} \tag{10c}$$

$$\phi_s^* = 1.25 \ ; \qquad \text{(stable case) .} \tag{10d}$$

$$\Phi_u = -0.7\ (Ri^2)^{0.25} \ ; \qquad \text{(unstable case) .} \tag{10e}$$

$$\Phi_s = 0.5\ (Ri)^{0.5} \ ; \qquad \text{(stable case) .} \tag{10f}$$

*For details, see the discussion by Dalrymple, Lettau, and Wollaston (1966).

Substituting these assumptions into Eqs. (11), (5), and (6), a sample table of diabatic $\bar{U}$, K, and ℓ-values is derived, comparable to the adiabatic values listed previously in Table 2. These exemplary wind and turbulence profiles are given in Table 3. Several interesting features are illustrated by the profiles. As expected, the turbulent length scale is increased from its neutral values during lapse conditions and decreased during inversion conditions. However, the corresponding changes in the vertical shear of the wind cause the friction velocity ($U^* = \phi^* U_a^*$) to decrease with lapse conditions and to increase with inversion conditions. Recalling the friction velocity/eddy diffusivity relationship (Eq. (7a)), Table 3 shows that K_u can actually be smaller than K_a in the lower layers over smooth to moderately rough terrain. In the stable cases, the friction-velocity increase (over the neutral case) is sufficient to cause an overall increase in K_s despite the smaller ℓ-values. Perhaps the most significant aspect of Table 3 is that it serves to demonstrate some of the complexities of eddy dispersion and turbulent transfer during diabatic conditions. An excellent in-depth review of diabatic surface-layer structure given by Lettau (1962) provides a review of a methodology to evaluate ϕ^* and Φ and discusses their dependence on Ri and the flux of sensible heat in the surface layer.

3. Terrain Effects

On the small scale, terrain roughness influences wind and turbulence structure in the surface layer as discussed previously. Terrain roughness also has a larger-scale effect on wind in the way in which the retarding force of surface friction influences the synoptic-scale wind direction. For example, the frictional drag of the oceans on the wind is normally quite small. As a consequence, the friction-induced change in wind direction between the free atmosphere (usually 500-1000 m, or the height where the geostrophic wind direction is first attained) and the surface is quite small--about 15°. But over forested regions, the increased drag causes wind changes of 25° and more. This effect is illustrated schematically in Figure 4.

Table 3

WIND/TURBULENCE PROFILE COMPARISON FOR LAPSE (UNSTABLE) AND INVERSION (STABLE) CONDITIONS

Parameter	z(m)	Lapse Conditions			Inversion Conditions		
		z_o = 0.1m	z_o = 0.5 m	z_o = 1.5m	z_o = 0.1m	z_o = 0.5m	z_o = 1.5 m
U^* (m s^{-1})	all	0.209	0.316	0.473	0.348	0.528	0.788
U (m s^{-1})	1	1.68	1.13	0.65	1.54	1.08	0.76
	2	2.10	1.67	1.21	1.96	1.58	1.26
	3	2.34	2.01	1.61	2.21	1.92	1.62
	5	2.64	2.45	2.19	2.54	2.36	2.16
	8	2.88	2.82	2.73	2.85	2.79	2.72
	10	3.00	3.00	3.00	3.00	3.00	3.00
K (m^2 s^{-1})	1	0.11	0.24	0.70	0.16	0.33	0.81
	2	0.23	0.42	0.98	0.30	0.55	1.13
	3	0.34	0.60	1.42	0.45	0.76	1.45
	5	0.61	1.03	1.95	0.73	1.19	2.09
	8	1.07	1.74	3.10	1.15	1.82	3.02
ℓ (m)	1	0.53	0.76	1.48	0.46	0.63	1.03
	2	1.10	1.33	2.07	0.86	1.04	1.43
	3	1.63	1.90	3.00	1.29	1.44	1.84
	5	2.92	3.26	4.12	2.10	2.26	2.65
	8	5.12	5.51	6.55	3.30	3.45	3.83

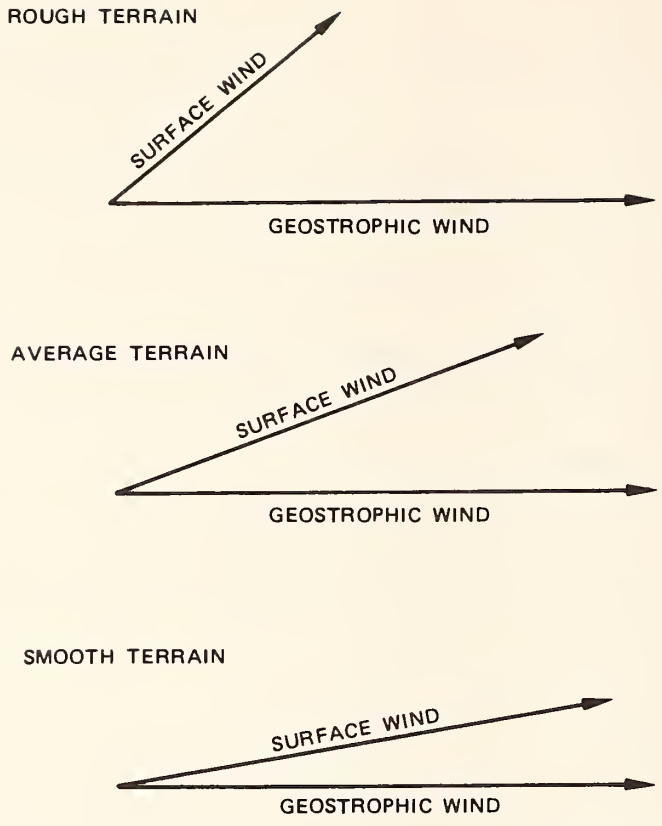

FIGURE 4 INFLUENCE OF TERRAIN UPON VARIATION OF WIND WITH HEIGHT (N. HEMISPHERE)

Other significant terrain effects fall between these two scale limits. These are the effects of natural or man-made topography on the direction and speed of the wind and sometimes also on the turbulence characteristics. Perhaps the most comprehensive review and discussion of these effects is that given by Geiger (1965); Edinger (1967) also gives a good semi-qualitative overview, while Slade (1968) provides a good introduction to the subject in the context of pollutant transport and diffusion. The discussion given here follows Slade (1968) and is intended only to introduce the reader to the magnitude and types of effects that can occur with two of the more common topographic features that affect highway pollutant dispersion: (1) hills and valleys, and (2) depressed or cut roadway sections.

Hills and mountains frequently have their own local wind patterns known as mountain-valley winds. When the prevailing wind is light and the sky clear, the nighttime winds usually flow down into the valley and along the valley floor, as schematically illustrated in Figure 5. This pattern is due to the cooling of the air adjacent to the hillsides; the air there subsequently becomes more dense than the air at the same height over the valley center. The cold air then drains down the hillside into the valley where it continues to flow downslope along the valley axis. There are several consequences from a pollution point of view; the mountain-valley wind transports pollutants from an area that might otherwise be stagnant. For roads aligned on the hillside or across the valley, drainage winds will transport pollutants away from the roadway source. Roads running along the valley axis, on the other hand, may receive little or no benefit due to the roadway-parallel wind direction at that location.

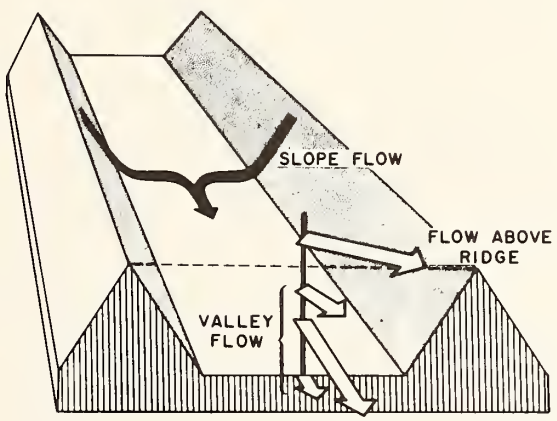

FIGURE 5 IDEALIZED REPRESENTATION OF THE CIRCULATION THAT MIGHT BE EXPECTED IN A TYPICAL VALLEY ON A CLEAR NIGHT (Slade, 1968)

Essentially the opposite situation occurs during the daytime when the air in the valley and along the hillsides rises as its density decreases due to solar heating. The daytime mountain-valley circulation

is usually less pronounced. Whereas at night the lower atmosphere is usually "decoupled" from the upper level winds, the daytime heating causes a transfer of momentum down toward the lower layers such that the daytime synoptic-scale wind overshadows most local effects.

Apart from the idealized situation above, there is a wide variety of local circulation patterns generated by the obstruction hills present to the prevailing wind flow. Figure 6 illustrates five flow patterns that can result from three different topographic configurations. Figure 6(a) shows two flow patterns that can follow from the flow of air over a ridge line oriented perpendicular to the ambient wind. During stable or neutral conditions, the wind flow is generally parallel to the terrain at all levels, whereas a counter-rotating eddy can persist in the lee of the obstruction during unstable conditions. Similar patterns can result when the wind flows perpendicular to the axis of a valley, as seen in Figure 6(b). In both situations, the location of the pollution source is crucial. If located in the recirculation area, the vertical mixing will be enhanced but the horizontal transport may be minimal with the result that pollution

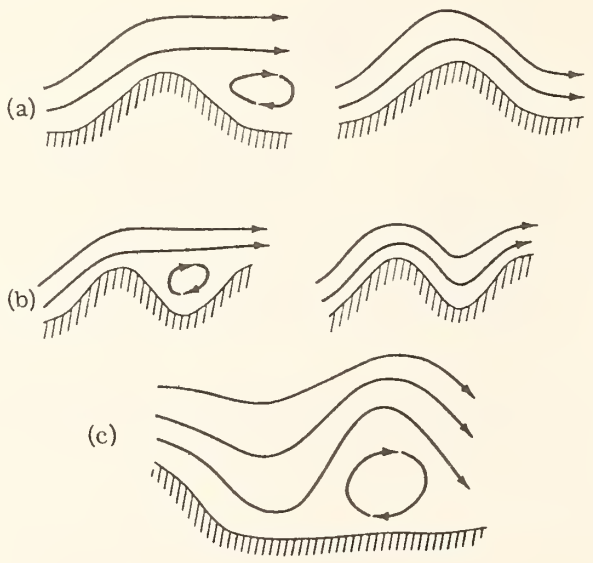

FIGURE 6 VARIOUS FLOW PATTERNS OVER TOPOGRAPHIC OBSTACLES. (a) OVER HILLS, (b) OVER VALLEYS, (c) A ROTOR IN THE LEE OF A MOUNTAIN (Slade, 1968)

concentrations could become large. Locating the source further downwind could improve the dispersion potential. Sometimes stable air can circulate rotor-fashion about a horizontal axis downwind of an obstruction (Figure 6(c)).

In addition to flow over hills and mountains, there are significant effects on the horizontal air flow around these obstructions. Figure 7 (Halitsky, 1961) illustrates the pattern of wind vectors in the immediate lee of an idealized circular hill where the streamlines tend to become curved as they parallel the shape of the obstruction. The data were observed in a wind tunnel simulation and show the marked divergence in wind speeds that occur. Note that winds are nearly calm along the centerline in the immediate lee of the hill while a jet-effect is present about one hill-radius in both cross-wind directions.

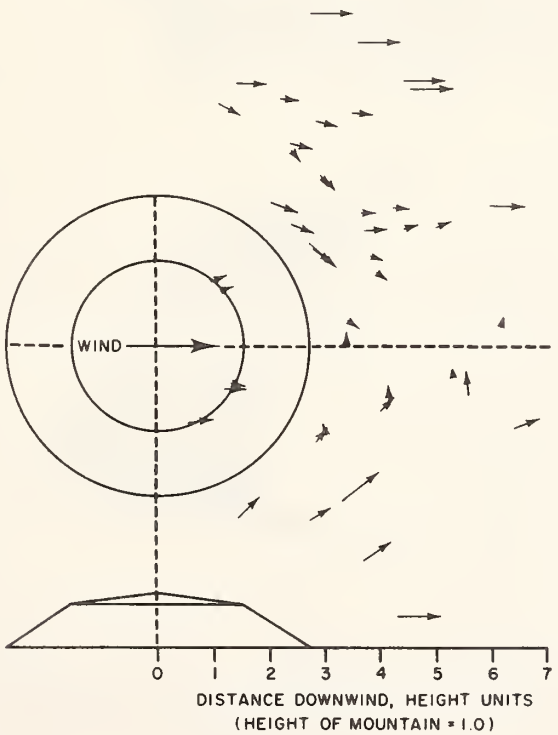

FIGURE 7 THE AIRFLOW IN THE VICINITY OF AN IDEALIZED HILL. THE SMALL ARROWS INDICATE HORIZONTAL WIND DIRECTIONS ABOUT THE PLAN VIEW OF THE HILL. (Halitsky, 1961)

Lastly, multiple terrain effects result when the wind blows at some angle to the obstruction; two examples are given in Figure 8. In Figure 8(a), the "thermal" wind component that flows up or down the valley sides and along the valley floor is present along with a prevailing cross-valley wind. The result is a bifurcation in the flow representing the influence of both wind components. Often there may be a gap in the obstruction, as depicted in Figure 8(b). In this case, the air is channeled through the opening with a proportional increase in speed (and pollutant transport).

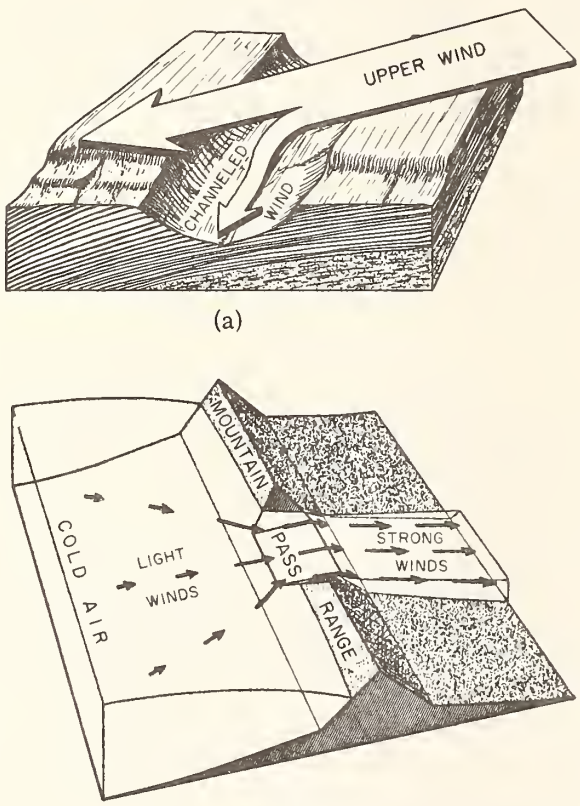

FIGURE 8 DISTORTIONS OF THE WIND FLOW BY TOPOGRAPHIC OBSTACLES. (a) CHANNELING OF THE WIND BY A VALLEY, (b) THE EFFECT OF A MOUNTAIN PASS ON THE WIND FLOW (Slade, 1968)

In addition to natural topographic features, man-made obstructions on and near various roadway configurations can also have a pronounced effect on wind flow and dispersion. Elevated roads on fill sections can have leeward wind circulations similar to those illustrated in Figure 6; tall viaduct sections with minimal frontal areas, on the other hand, may do relatively little to the wind flow (Dabberdt, 1977). However the rectangular "notch" formed (in cross-section) by a vertical-walled cut section or an urban street canyon can have pronounced effects on pollutant concentrations. A number of investigators have studied the urban street canyon; two of the earliest definitive studies were reported by Georgii et al. (1967) for conditions in Frankfurt, Germany and Johnson et al. (1971) for San Jose, California.

Figure 9 is a schematic of the mean circulation pattern in a typical street canyon as suggested by Johnson and later supported by additional

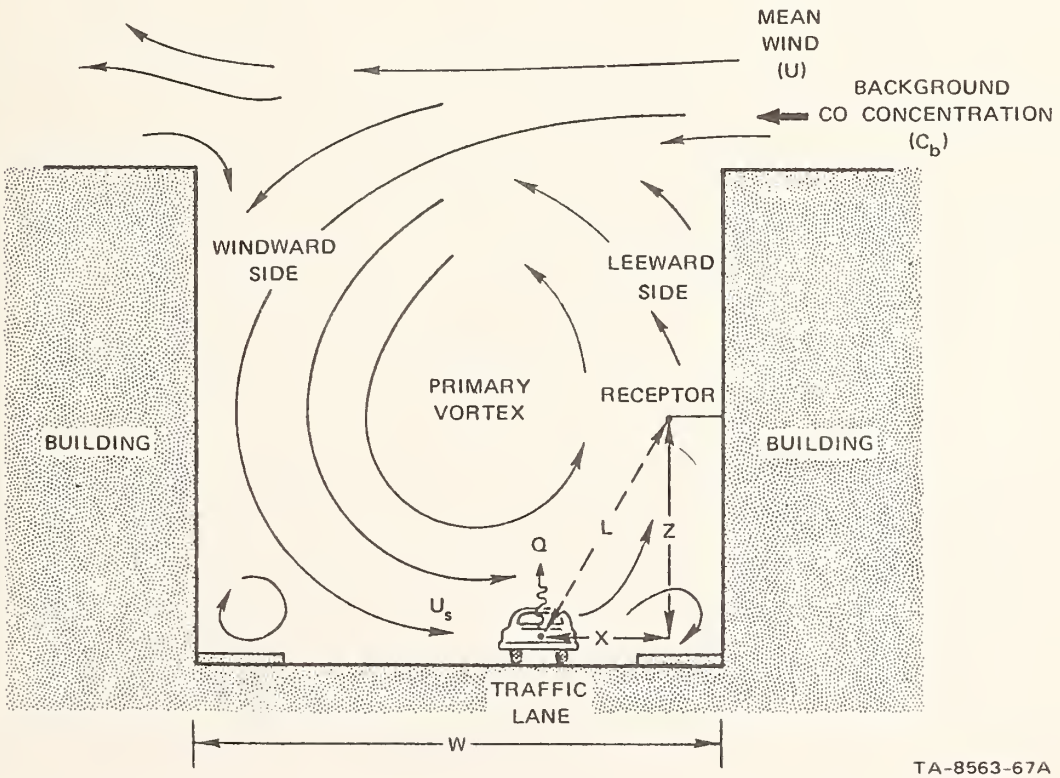

FIGURE 9 SCHEMATIC OF CROSS-STREET CIRCULATION BETWEEN BUILDINGS

work reported by Ludwig and Dabberdt (1972) for St. Louis, Missouri. It is important to note that the circulation pattern has been inferred from extensive pollutant measurements and not from the limited number (i.e., four) of anemometers located in each of the four "corners" of the notch. Wind structure can vary dramatically over a few meters and a few spot wind measurements can be misleading. This was confirmed by smoke releases made during the St. Louis study. Period-averaged pollutant measurements, on the other hand, serve to filter out the turbulent fluctuations and provide a good picture of the net transport and dilution of the street-level emissions. (In the St. Louis study, air samples were obtained continuously in each of two street canyons at 15 locations up the sides of the buildings and at two heights over the middle of the street.)

Figure 9 illustrates the flow pattern when the ambient, roof-level wind is oriented perpendicular to the notch. As the ambient air passes over the notch, part of it is diverted downwards in the downwind half of the notch. At street level, this descending flow becomes curved and moves across the street in a direction opposite to the roof-level wind. Upon reaching the other (vertical) side of the notch, the flow curves upward to complete the primary vortex pattern within the notch. As a consequence, pollutant emissions from the street are transported horizontally against the ambient wind at the base of the notch. Experimental measurements have shown that this can result in upwind, street-level concentrations that are two-to-three times greater than the downwind values.

Figure 10 shows the average concentrations patterns measured by Ludwig and Dabberdt (1972) for each of 12 wind direction sectors and each of three wind speed categories. The street-canyon recirculation pattern was generally observed to occur with wind/roadway angles greater than 30°, although variations in building heights and design can cause this to change. The wind tunnel studies reported by Dabberdt (1977) for a roadway in a vertical-walled cut also revealed the recirculation regime at 30°-angles, but not at 15°-angles.

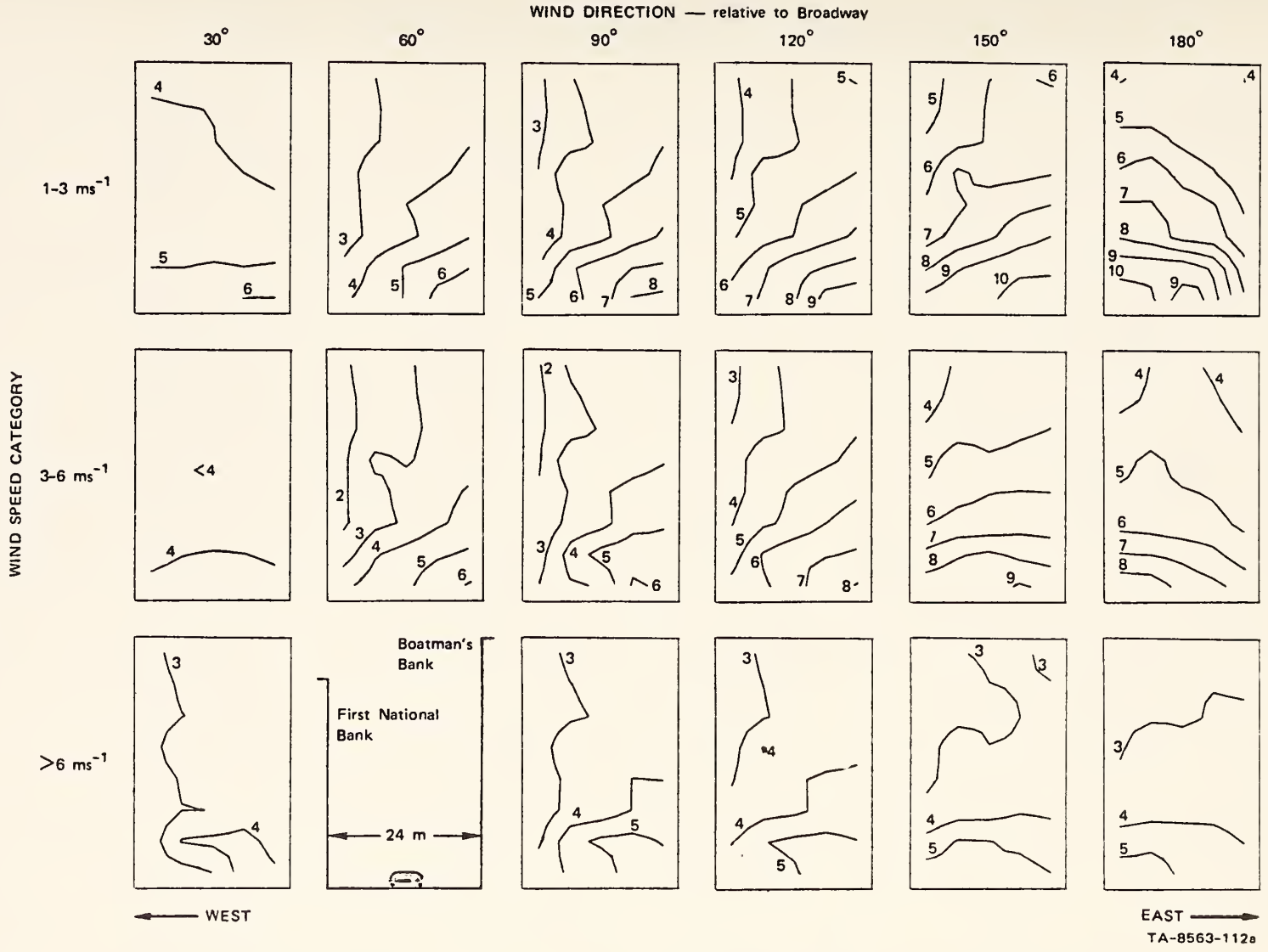

FIGURE 10 DISTRIBUTION OF CO CONCENTRATION IN BROADWAY STREET CANYON (Ludwig and Dabberdt, 1972)

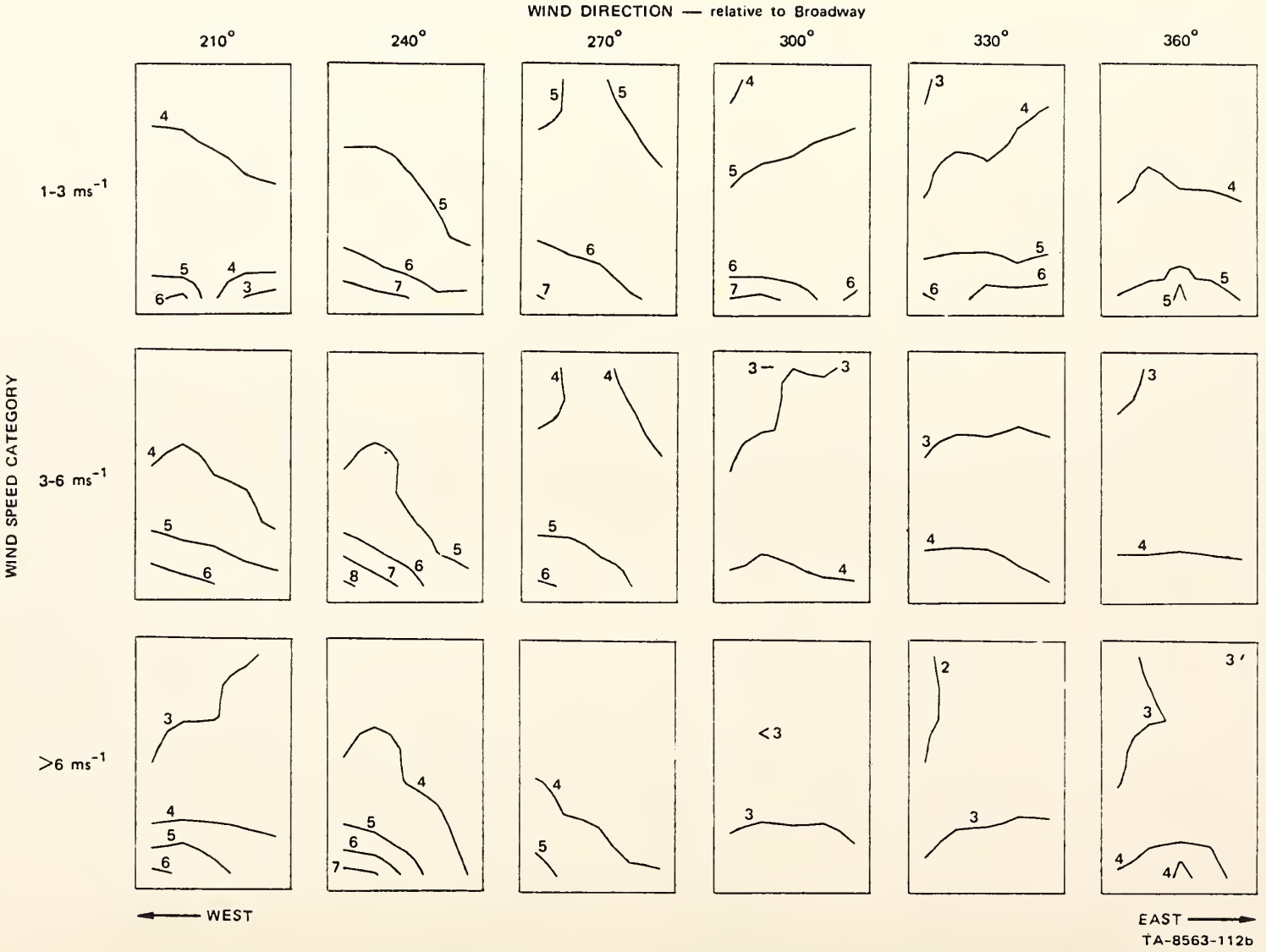

FIGURE 10 DISTRIBUTION OF CO CONCENTRATION IN BROADWAY STREET CANYON (Ludwig and Dabberdt, 1972) (Concluded)

As indicated at the very beginning of this discussion of topographic effects, they are as varied as the range in topographic configurations. Only the surface has been scratched in these discussions, but they should be viewed as an insight into the causes and types of effects that can be expected in terms of wind speed, wind direction, turbulence, and ultimately pollutant dispersion and concentration. In the following subsection traffic effects will be reviewed, followed by a series of representative scenarios that may shed further light on the nature of pollutant dispersion near highways. These scenarios combine atmospheric, topographic, and traffic influences.

4. Traffic Effects

The influence of traffic on wind, turbulence, and dispersion is a combination of three individual processes: (1) aerodynamic drag of moving vehicles, (2) aerodynamic displacement of the wind flow caused by a wall of vehicles, and (3) buoyancy from vehicular thermal emissions.

a. Drag

The surface of a vehicle is aerodynamically rough, and as the vehicle moves it drags with it the adjacent layers of air. The speed of the air (U_d) next to each individual vehicle is proportional to the average vehicle speed (v) and the vehicle drag coefficient (C_d), where

$$U_d = C_d V \quad . \tag{11a}$$

The estimate of the average drag flow ($\bar{U}_d$) for the traffic stream is further refined by multiplying U from Eq. (11a) by the percentage (R) of the roadway actually occupied by vehicles (R = total vehicle overhead area ÷ total roadway area):

$$\bar{U}_d = RC_d V \quad . \tag{11b}$$

The range of C_d is typically 0.5-0.6 for all roadway vehicles; an average value of 0.55 will be used in this discussion. Table 4 provides drag-flow

Table 4

PEAK TIME-AVERAGED DRAG-FLOW SPEEDS, $\bar{U}_d$(m s^{-1})

Vehicle Spacing (car lengths)	Aerodynamic Roughness (z_o, m)	Vehicle Speed (mph)*		
		20	30	45
2	0.038	1.64†	2.46	3.70
3	0.028	1.22	1.84†	2.76
4	0.023	0.98	1.48	2.22
5	0.019	0.82	1.22	1.84†
6	0.016	0.70	1.04	1.58

*1 mph = 1.6 kmph

†Recommended safe spacing.

estimates for several vehicle speeds/spacings and the following assumptions: (1) average lane width = 4 m; (2) average vehicle width = 2 m; and (3) the vehicle drag-effect extends one car length behind each vehicle. These estimates should be considered peak values since they represent the maximum drag speed adjacent and averaged over the entire roadway area. The drag speed will decrease with horizontal and vertical distance (i.e., L) from the roadway in much the same way that the velocity deficit of the ambient wind profile ($\bar{U}_{ref}$-$\bar{U}$) decreases with height above ground. If we assume (as a first approximation) that the drag flow profile resembles a neutral constant-stress layer, we can hypothesize the following formulation as analogy to Eq. (3):

$$\bar{U}_{d-o} - \bar{U}_d = \frac{U^*}{k} \ln\left[\frac{L + z_o}{z_o}\right] . \qquad (12)$$

Experimental data from Dabberdt (1975) suggest that $\bar{U}_d \approx 0$ at z (or L) $\approx$ 6m. Recalling Eq. (4), z_o can be estimated as summarized in Table 4. Figure 11 illustrates profiles of the drag wind speed and diffusivity computed from Eq. (12) with an assumed two car-length vehicle spacing and a 45-mph vehicle speed. The speed of the drag flow is significant close to the

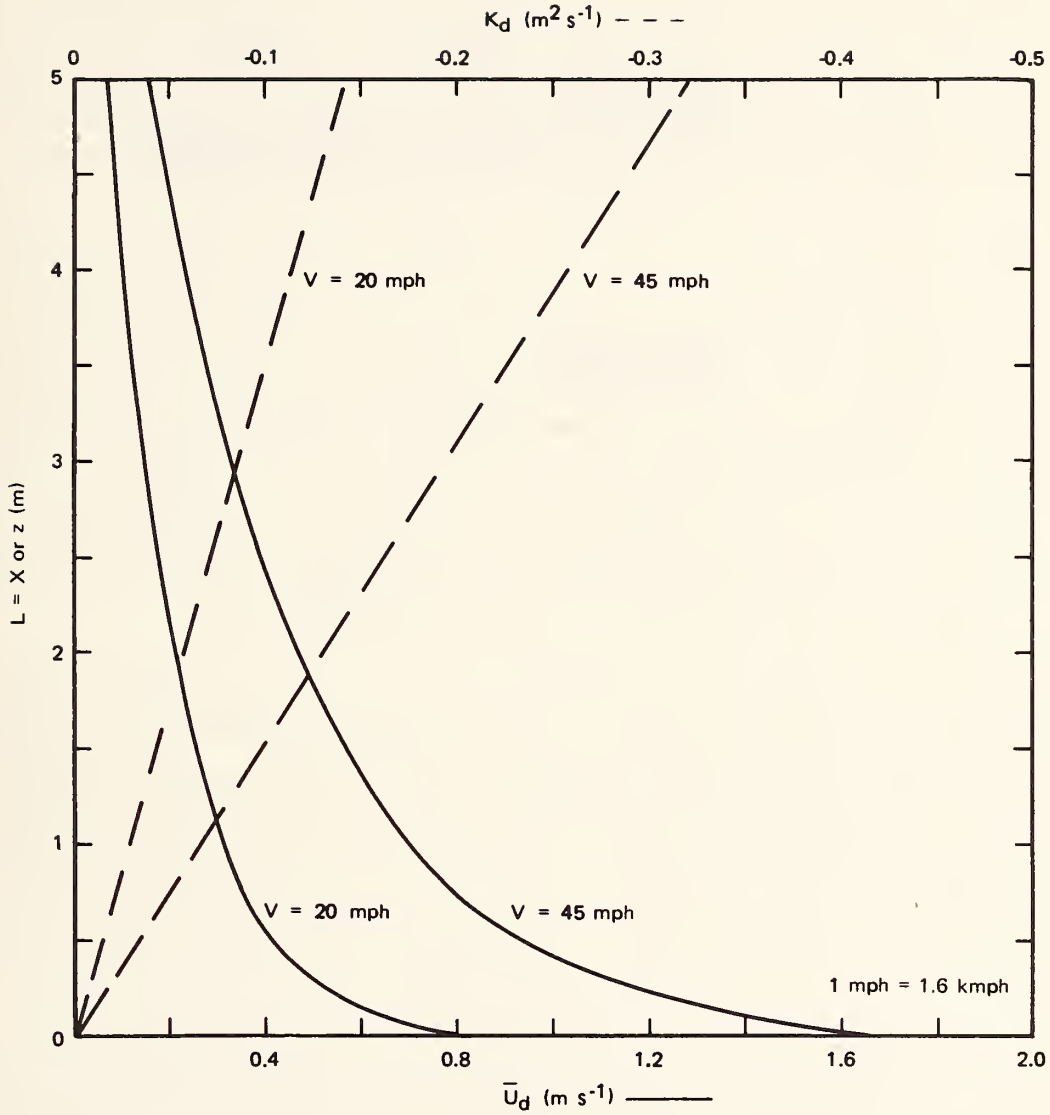

FIGURE 11 VARIATION OF EDDY DIFFUSIVITY (K_d) AND WIND SPEED (U_d) WITH DISTANCE FROM VEHICLES FOR DRAG FLOW CORRESPONDING TO DIFFERENT VEHICLE SPEEDS (V)

vehicles, dropping off sharply with height and cross-roadway distance. The corresponding values of the eddy diffusivity are equivalent to those computed earlier for a neutral atmosphere with moderately rough terrain (z_o = 0.5m) and a 1-m s^{-1} ambient wind (at z = 10m). When the vehicle speed or density decreases, the drag flow decreases proportionately. Moreover, when the ambient wind speed is more than a few meters per second, the ambient K-values are significantly larger than the peak drag-induced values.

Because it has no mean vertical or cross-roadway component to transport pollutants, drag flow should not be considered a major factor in controlling off-roadway pollutant levels. Rather, it is an effective factor in diffusing pollutants over the roadway. One way this occurs is through the horizontal transport of the drag flow that aids in producing a uniformly mixed layer along the roadway axis. Vertical mixing over the roadway occurs in two ways: One is through vertical diffusion from the shear in the vertical profile of drag flow; more significant is the turbulent mixing that occurs above and behind the moving vehicles.

Figure 12* illustrates the turbulent eddies that are formed in both the horizontal and vertical planes. Having lateral dimensions of 1-2 car widths and longitudinal scales of perhaps 1-2 car lengths, these eddies effectively mix the exhaust gases in the horizontal plane (over the roadway) and up to a height on the order of two or three car heights above the road surface (Dabberdt, 1975). This vertical mixing is further enhanced by the local instability generated by vehicular waste heat emissions, in addition to the turbulent diffusion of the ambient wind and the aerodynamic effects from the obstruction the wall of vehicles presents to the ambient flow. These effects are discussed in the following subsections.

b. Displacement

In an analysis of an extensive set of meteorological, traffic, and pollution data obtained at a major at-grade freeway, Dabberdt (1975) proposed the importance of another aerodynamic effect of roadway vehicles--the so-called "shelterbelt" effect. The term was used because individual

*Figure 12 is the pseudo steady-state pattern an observer would "see" when moving with the vehicle.

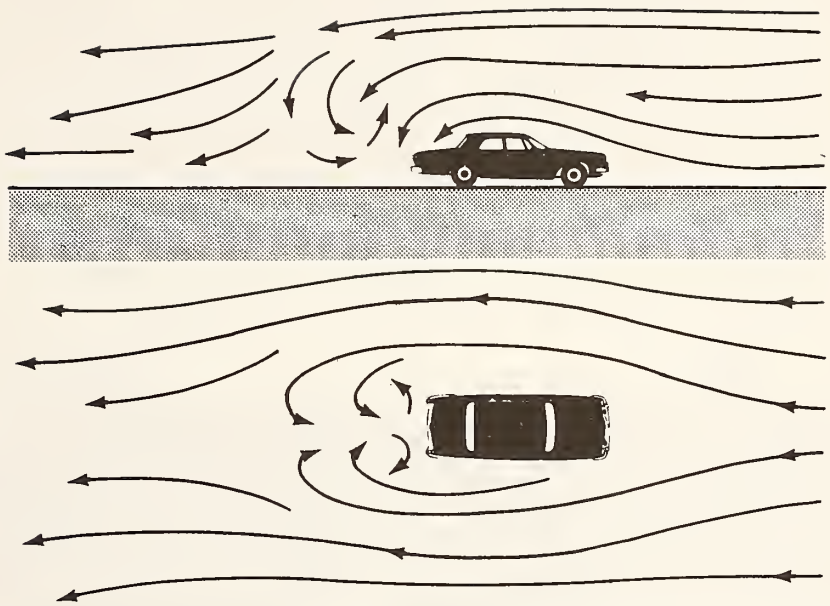

FIGURE 12 SCHEMATIC OF AIR FLOW OVER AND AROUND A VEHICLE UNDER STEADY-STATE FLOW CONDITIONS

vehicles, as well as the composite stream of vehicles on the roadway, present a barrier to the wind in much the same way as a row of trees or a fence used as an agricultural windbreak (or shelterbelt). Individual vehicles may act as much like a classical windbreak as a stream of vehicles because: (1) they are also the source of the pollutants, and (2) the drag flow and turbulent wake-vortices that they generate help to initially keep the pollutant plume near the obstruction.

The major effects of the roadway shelterbelt are illustrated schematically in Figure 13(a), which is adapted from classical wind tunnel studies reported by Plate and Lin (1965). As the ambient flow approaches the wall of vehicles at an oblique angle, the flow in the lower layers is lifted up and over the roadway. The upper part of this lifted air increases in speed and flows over the roadway in the "displaced zone." Closer to the roadway, the air becomes very turbulent as it come in contact with the rough surface of the roadway vehicles. There is also a tendency for the air to flow upwind near the ground at the leeward edge of the roadway. Further downwind, this very turbulent

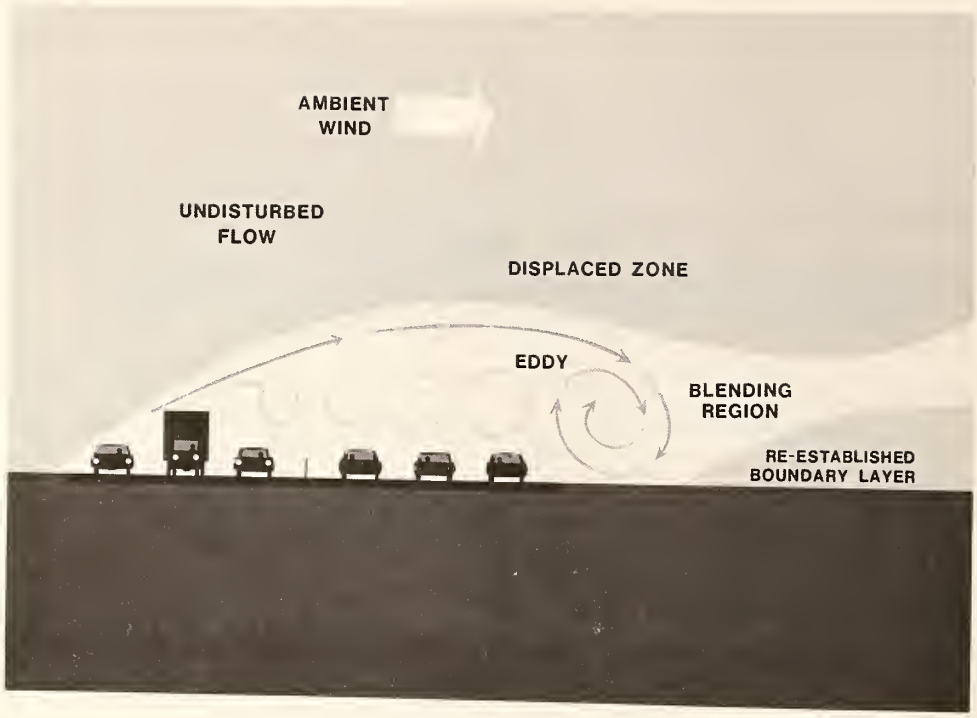

(a)

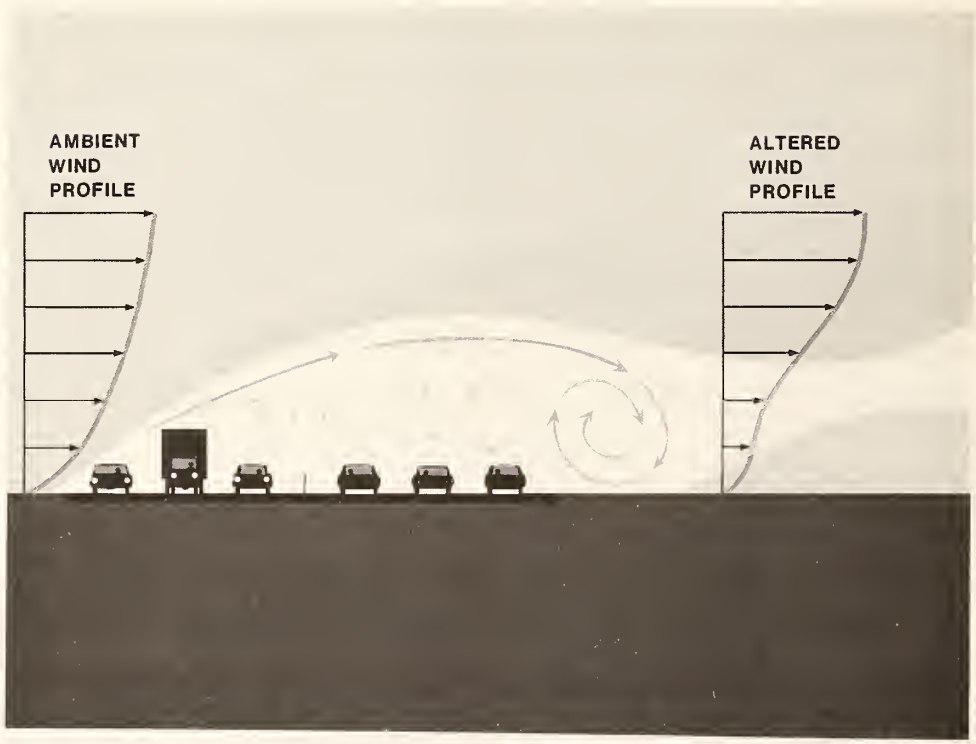

(b)

FIGURE 13 SCHEMATIC ILLUSTRATION OF ROADWAY-SHELTERBELT EFFECT ON WIND FLOW AND TURBULENCE

layer entrains with the adjacent layers in the "blending region" as it begins to return to its ambient (pre-roadway) state. Figure 13(b) illustrates the effect of the roadway shelterbelt on the vertical wind profile; of particular note is the velocity deficit in the blending region where the increased turbulent energy has reduced the mean wind speed. Close to the ground surface, the ambient wind profile structure is re-established downwind at a slope (height to downwind distance) of 1:20 to 1:50 according to the roughness of the surface.

Stearns and Lettau (1963) have conducted atmospheric experimental studies of the effect of a 36-m diameter circular stand of Christmas trees planted in the frozen surface of Lake Mendota, in Madison, Wisconsin. Each tree was trimmed to a height of 1.75 m, had an average frontal area of 0.3 m^2, and occupied an average ice area of 4 m^2. Figures 14(a) and (b) show the variation in the profiles of the horizontal and vertical wind components upwind, within, and downwind of the shelter. Most striking is the strong upward vertical motion (0.60 m s^{-1}) at the upwind edge of the shelter and the moderate downflow (-0.15 m s^{-1}) at the downwind edge.

Several studies (e.g., Nägeli, 1941) have been made of the effects of the porosity* of the shelterbelt (i.e., the vehicle density) on the wind speed reduction downwind. Some of these findings are shown in Figure 15. The maximum speed reduction occurs with a near-solid obstruction (low porosity), where the speed just behind the obstruction drops to 15 percent of the ambient value but again increases quite rapidly further downwind. When the porosity is moderate (30-50 percent), the wind speed is still reduced to 30 percent of the ambient speed, but the speed deficit persists further downwind than with the low porosity shelter such that the sheltering (integral speed deficit) is a maximum.

Figure 13(b) showed how the vertical velocity gradients are enhanced in the blending region. This, in turn, leads to larger diffusivity

---

*Porosity is defined as the percentage open area in the total cross-sectional area of the shelterbelt.

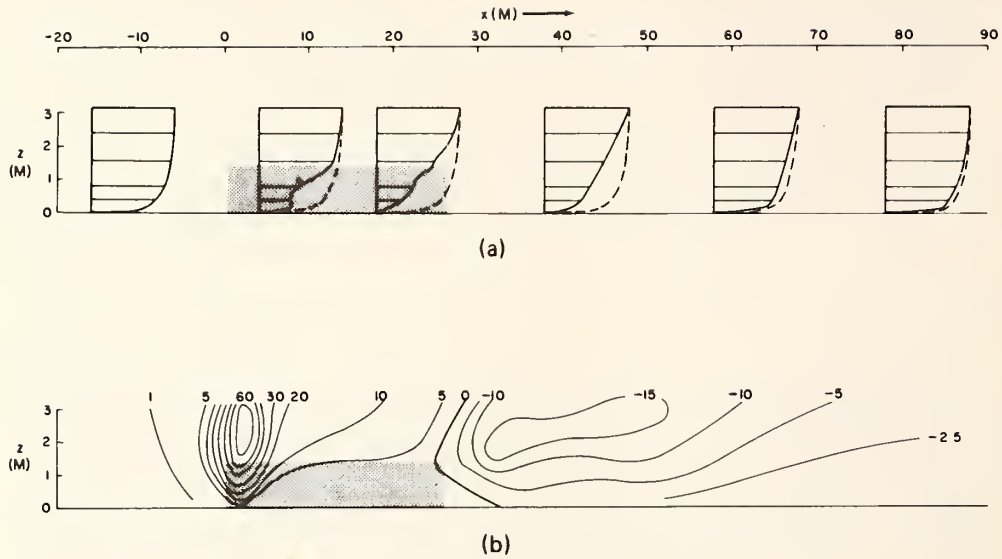

SOURCE: Sterns and Lettau, 1963

FIGURE 14 WIND STRUCTURE ABOUT A SMALL SHELTER CONSISTING OF SHORT CHRISTMAS TREES

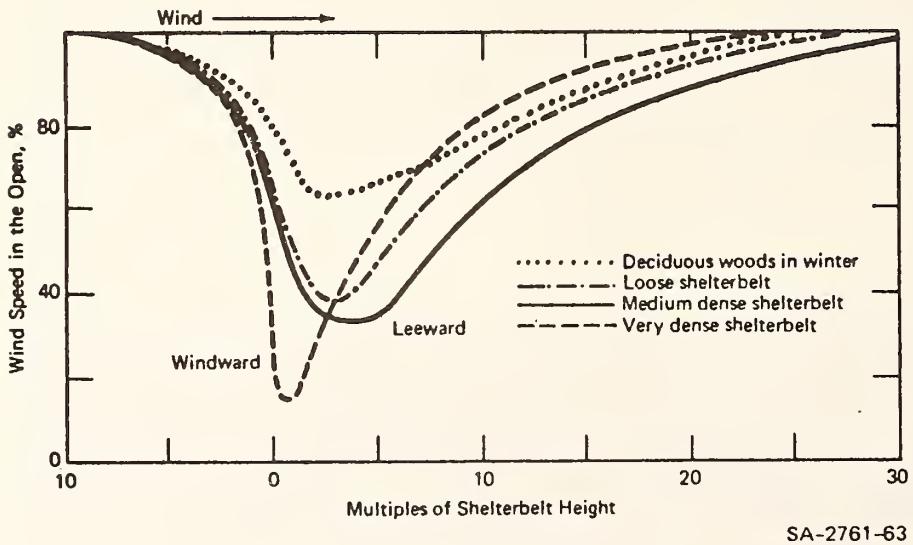

FIGURE 15 SHELTERING AT DIFFERENT POROSITIES
(According to Nägeli, 1941)

values and an increase in the rate of transfer of momentum and mass (i.e., emissions). Plate (1971) suggests that the turbulence intensity in the blending region is proportional to $(U_\infty^2 - U_b^2)(U_\infty - U_b)$, where U_∞ is the ambient cross-shelter wind component and U_b is the wind speed in the lee of the shelter. Using the speed profiles from Figure 15, the following peak turbulence increments (relative) are likely to result:

Shelter Type	U_b/U_∞	Relative Added Turbulence Intensity*
No obstruction	1.00	0%
Low density	0.40	50%
Medium density	0.30	64%
High density	0.15	83%

These estimates are consistent with the magnitude of the added turbulence levels measured in atmospheric studies. Dabberdt (1975) reported on the turbulence gradient across a six-lane divided grade-level freeway located in smooth terrain. Turbulence intensities measured 10 m downwind of the roadway at various heights were enhanced up to: (1) 150 percent of the upwind levels at a height of 2 m above ground; (2) 200 percent at 4 m height; (3) 150 percent at 7.5 m height; and (4) 75 percent at 14 m height.

c. Waste Heat

Vehicular emissions of waste heat also affect the dispersion of pollutants near the roadway, and when the pavement is a dark asphalt, the waste heat flux can be enhanced by the release of sensible heat from the roadway surface. (Conversely, dark asphalt can subtract from the vehicular heat emissions during the late evening to midmorning period when the asphalt can cool off more rapidly than the adjacent ground surface of concrete pavement and thus act as a heat sink.)

---

*$(U_\infty^2 - U_b^2)(U_\infty - U_b)/U_\infty^3$.

Waste heat emissions can be estimated from: (1) the automotive fuel consumption rate; (2) the energy capacity of gasoline--about 3.1×10^7 cal gal^{-1}; and (3) the mechanical efficiency of the automobile--about 15 percent. Figure 16 shows a typical speed-fuel consumption relationship for standard-size 1970-71 automobiles. For the traffic data reported by Dabberdt (1975) for a major six-lane suburban freeway, waste heat flux-densities ranged from 0.15 cal cm^{-2} min^{-1} for typical midday traffic to 0.35 cal cm^{-2} min^{-1} for rush-hour traffic. By way of contrast, peak summer daytime heat fluxes from grass fields would be around 0.30 cal cm^{-2} min^{-1} in the mid-latitudes of the United States, while nighttime minima would typically be about -0.10 cal cm^{-2} min^{-1}. Thus the vehicular waste heat emissions are sufficiently large to modify the atmospheric

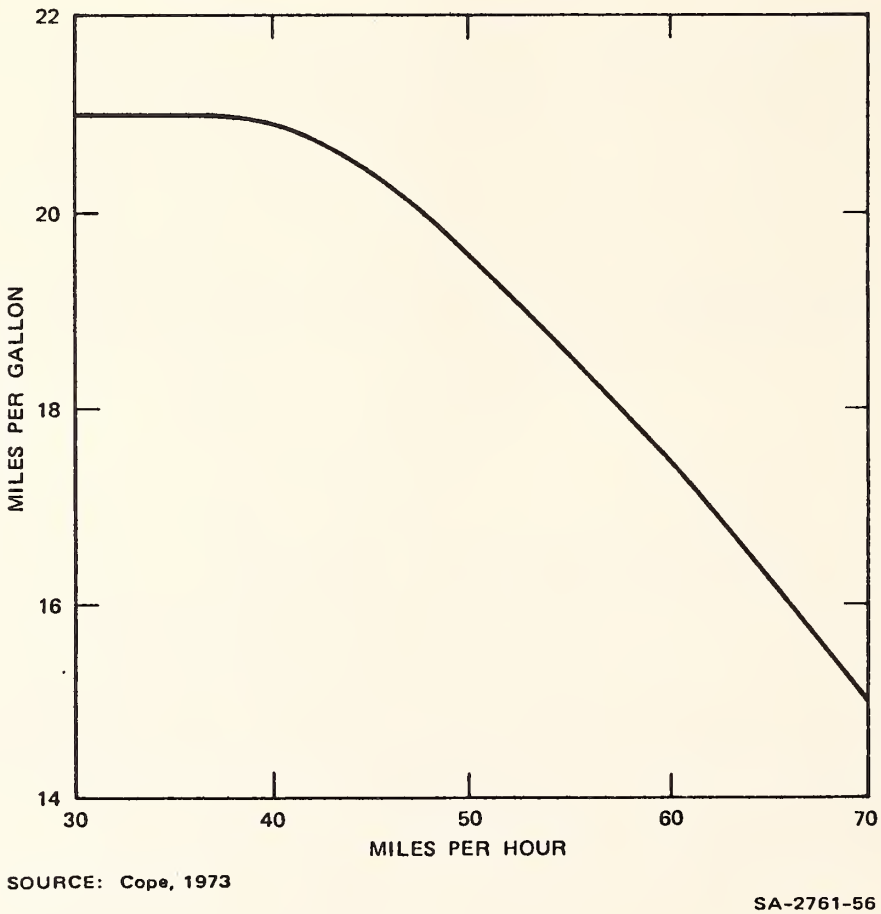

FIGURE 16 AVERAGE EFFECT OF SPEED ON AUTOMOBILE FUEL CONSUMPTION—1970/71 MODELS (4500 pounds)

stability over the roadway. During moderate to heavy traffic periods, the waste heat flux will maintain neutral or unstable conditions over the roadway, thereby enhancing the dispersion process.

The effect of the vehicular heat emissions is reflected in the temperature distribution near the roadway (Figure 17). On the upwind side of the roadway, about 65 percent of all observations of the vertical temperature gradient indicate unstable (lapse) conditions, while the 97^{th} percentile value is a strong inversion of $0.4°C\ m^{-1}$. Downwind of the roadway, 85 percent of all profiles are unstable, while the 97^{th} percentile value is only $0.08°C\ m^{-1}$. In summary, vehicular waste heat emissions increase the frequency of unstable conditions near the roadway while significantly decreasing the intensity of the inversion conditions downwind.

The effect of waste heat in vertically dispersing exhaust emissions can often be visualized during cold weather when low atmospheric temperatures condense the water vapor in the exhaust. Figure 18 is an example of the rise of the exhaust plume as photographed on an overcast day (near-neutral stability) with very low wind speeds and a temperature around -23°C (-10°F). In Figure 18(b), the elevated plume can be seen from a vehicle that just passed out of the photo to the left; in Figure 18(a), the rise of an idling vehicle is depicted.

d. Summary

The preceding discussions have provided relatively isolated overviews of the three physical processes by which motor vehicles influence the dispersion of their exhaust emissions on and near the roadway. It should be understood that the drag flow, shelterbelt, and waste heat effects will usually occur in combination, although each contributes differently to the overall effect. The drag phenomena serve two primary functions: (1) to uniformly mix the emissions along the roadway axis, and (2) to vertically diffuse the emissions by the induced eddy diffusivity and the vortex generation in the lee of the individual vehicles. The shelterbelt effect caused by the wind obstruction of the vehicles causes the air flow and the pollutants to be both vertically transported and diffused over

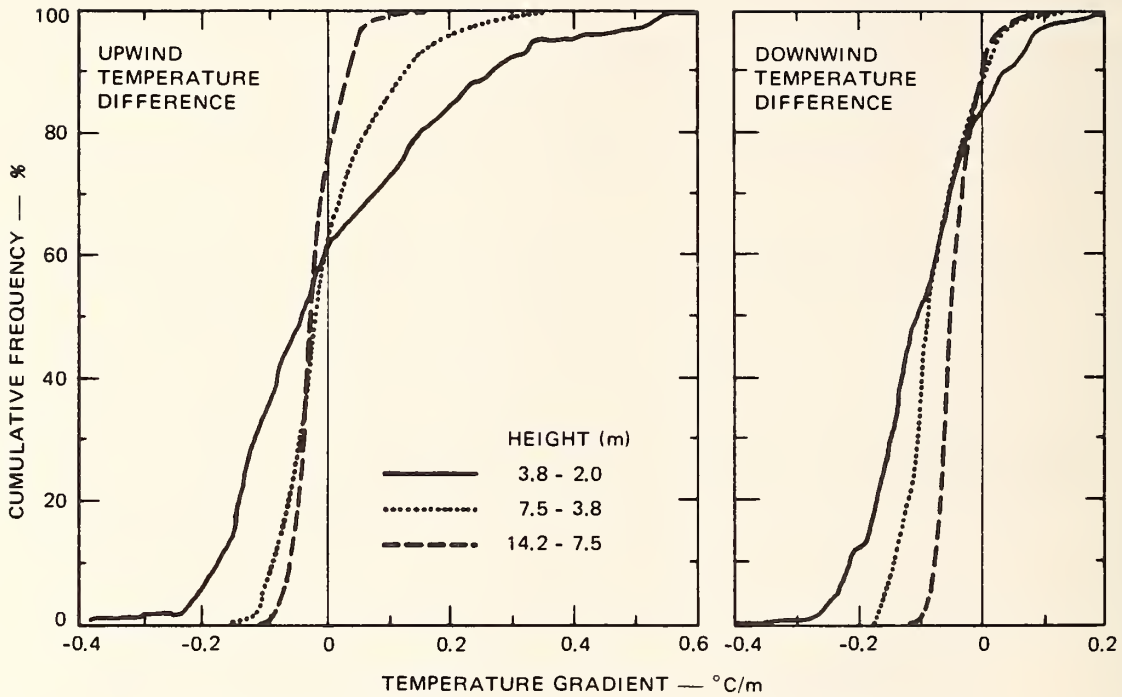

FIGURE 17 CUMULATIVE FREQUENCY DISTRIBUTIONS
OF VERTICAL TEMPERATURE GRADIENTS

(a)

(b)

FIGURE 18 EXAMPLES OF VERTICAL DISPERSION OF VEHICLE EXHAUST PLUME DUE TO WASTE HEAT EMISSION

Stability: Near Neutral; Winds: Very Light; Temperature: -23°C

the roadway. The shelterbelt effect is suspected to have the most significant effect on the initial vertical dispersion over the roadway. This initial mixing and the subsequent dispersion downwind are augmented by the effects of waste heat emissions on atmospheric stability which can maintain unstable roadway conditions, even when ambient conditions upwind are stable. Even though subsequent entrainment will re-establish the ambient temperatures profile further downwind, the waste heat (as well as the drag and shelterbelt) effect on the initial mixing will still result in a net decrease in pollutant concentrations at all downwind locations. This is shown schematically in Figure 19.

oo Cooperating Organizations: SRI: Dr. Ronald Ruff, Dr. Randall Pozdena, Mr. Hisao Shigeishi, Mr. Albert Smith, Mr. Lu Salas, and Mr. Charles Flohr. Design and construction of the mechanical highway model and the wind tunnel dispersion tests were conducted at Calspan Corporation, Buffalo, New York, under subcontract to SRI: Dr. George Skinner, Dr. Gary Ludwig, and Dr. Al Ritter. Atmospheric tests and installation of traffic sensors: Mr. James Collins and District 04 of the California Department of Transportation and Mr. Earl Shirley, Transportation Research Laboratory. Meteorological Instruction: Mr. Lawrence Niemeyer and the Meteorology Laboratory of the U.S. Environmental Protection Agency, Research Triangle Park, North Carolina.

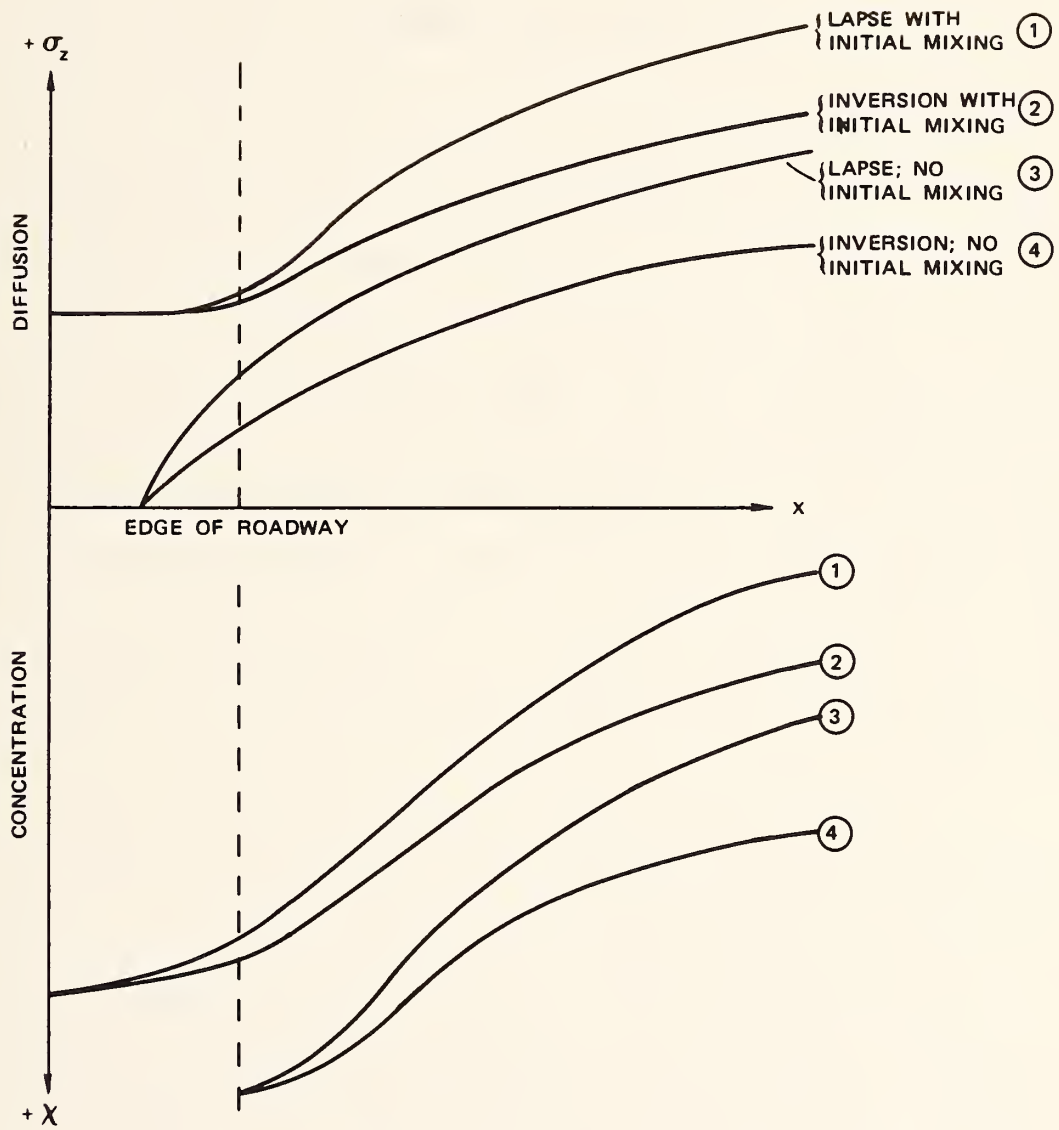

FIGURE 19 SCHEMATIC ILLUSTRATION OF THE EFFECTS OF STABILITY AND INITIAL MIXING ON DIFFUSION AND CONCENTRATION

III ASSESSMENT METHODOLOGY

A. Introduction

The preceding section discussed the individual physical elements that combine to determine the concentration of vehicle-generated pollutants on and close to highways. Although these elements were described quantitatively where possible, it would be impossible to develop from first principles a holistic model that described both the individual and synergistic effects of each element. That this cannot be done is apparent from the various elemental discussions and will be further discussed in part C of this section. The approach used to quantify the dispersion is adapted from the results given in Volume I of this report (Dabberdt et al., 1979); the methodology for estimating vehicular emissions is extracted from a report by Dabberdt and Sandys (1976) entitled "Guidelines for Evaluating Indirect Sources," prepared for the United States Environmental Protection Agency.*

The discussions on emissions estimation is restricted to a short introduction followed by a worksheet and accompanying set of instructions that relate traffic and roadway characteristics to carbon monoxide emissions for limited access highways. If the user wishes to apply the dispersion methodology to emissions at or near signalized or signed intersections (for example), then the emissions estimation procedures given by Dabberdt and Sandys (1976) or EPA (1978) should be followed. The dispersion subsection begins with a discussion of the rationale for the approach used, followed by a summary of the methodology and a worksheet with instructions. The methodology is then applied in Section IV, and

*While the methodology is quite rigorous, the emission estimates that result should not be considered official EPA values since recent changes in estimating procedures by EPA have caused minor differences between the results of the two methods. Current EPA methodology is provided in EPA Report 450/4-78-001.

user notes are given that highlight the air pollution impacts and causal physical process(es) for each of a wide variety of roadway configurations.

B. Emissions from Uninterrupted Flow

This methodology is used to determine the emission flux-density on roadway sections having uninterrupted or freely flowing traffic, e.g., freeway, expressway, midblock section of a public roadway, or well-defined roadway within a parking lot. Worksheet 1 summarizes all steps in the emissions calculation procedure. The first step in the methodology is to determine the demand volume (V) and free-flow capacity (C) of the road segment. The demand volume is a required input traffic parameter; free-flow capacity can be estimated, for example, using the Highway Capacity Manual (1965) or Dabberdt and Sandys (1976). The ratio V/C is then determined and used to enter Figures 20-23 to find average vehicle speed (S) on each road segment. The figures associated with each road type are as follows:

- Freeways (Figure 20)
- Multilane rural highways (Figure 21)
- Two-lane rural highways (Figure 22)
- Urban arterial streets (Figure 23).

The user enters each figure with a V/C ratio intersected with the appropriate curve for the road type to determine average speed. The user should also note that the three curves of Figure 23 are for typical signal progressions but that the figure does not include curves for every possible arterial speed. The user should interpolate a "cruise" speed by adding the speed limit differential between the subject arterial and the appropriate curve to the graphically determined speed. (For example, an uncoordinated arterial with a speed limit of 40 mph and a V/C ratio of 0.5 requires that a 15-mph differential be added to the 20-mph average speed read from "Curve III," to give an interpolated average speed of 35 mph.)

Figure 24 illustrates the variation of the emission density (EF, g veh m^{-1}) for a single vehicle as a function of vehicle speed. The

Worksheet 1

LINE SOURCE CARBON MONOXIDE EMISSION FLUX-DENSITY COMPUTATION
(see following set of instructions)

Project Location:_____ Analyst:_____

Project Review Year: 19___ Date:_____

Step	Symbol	Input/Units	Traffic Stream	
1.	θ_i^*	Direction (deg)	1	2
2.	i	Identifier		
3.	G_i	Roadway grade		
4.	V_i	Demand Volume (veh hr^{-1})		
5.	C_i	Free-flow capacity (veh hr^{-1})		
6.	S_i	Cruise speed (mi hr^{-1})		
7.	Ef_i	Free-flow unit emission density (g veh^{-1} m^{-1})		
8.	Csp_i	Cold-start percentage		
9.	T	Ambient temperature (°F)		
10.	H	Altitude (m, msl)		
11.	Csf_i	Cold-start adjustment factor		
12.	Yf_i	Year/location adjustment factor		
13.	Gf_i	Grade correction factor		
14.	Ef_i	Free-flow unit emission density (g veh^{-1} m^{-1})		
15.	Qfc_i	Free-flow emission flux-density (g m^{-1} hr^{-1})		
16.	--	Seconds per hour (s hr^{-1})	3600	3600
17.	Qfc_i	Free-flow emission flux-density (g m^{-1} s^{-1})		

Table 5

INSTRUCTIONS FOR COMPLETING WORKSHEET 1

Step*	Instructions
1	Enter the compass direction vehicles are heading on each traffic stream (e.g., 090° for vehicles heading east).
3	Enter roadway grade: The number of meters (feet) of vertical rise per 100m (100 ft) of horizontal distance.
4	Enter demand volume (veh hr^{-1}).
5	Enter free-flow capacity (veh hr^{-1}) as given in the project description, or as computed from the Highway Capacity Manual (1965) or Dabberdt and Sandys (1976).
6	First, divide line 5 by line 4 to obtain the V/C ratio; then, obtain the cruise speed (S, mi hr^{-1}) using V/C and the appropriate roadway type in either Figure 19, 20, 21 or 22.
7	Obtain the unit free-flow emission density (Ef, g veh^{-1} m^{-1}) from Figure 23 using S from line 6.
8	Enter the percentage of vehicles which were started within 8.5 minutes of passing the project site.
9	Enter the ambient temperature (T, °F).
10	Enter the elevation in feet above mean sea level.
11	Obtain the cold-start adjustment factor from Table 6 using Csp (line 8) and T (line 9).
12	Obtain the year/location adjustment factor from Table 7 using H (line 10) and the year for which the project is being reviewed.
13	Obtain the grade correction factor from Table 8 using H (line 10) and G (line 3).
14	Obtain the adjusted unit free-flow emission density by multiplying: Ef (line 7), Csf (line 11), Yf (line 12), and Gf (line 13).
15	Calculate the total (per hour) free-flow emission flux density (Qfc, g m^{-1} hr^{-1}) by multiplying Ef (line 14) and demand volume V (line 4).
16	Calculate the total (per second) carbon monoxide free-flow emission flux density (Qfc, g m^{-1} s^{-1}) by dividing Qfc (line 15) by 3600.

*Refers to Worksheet 1.

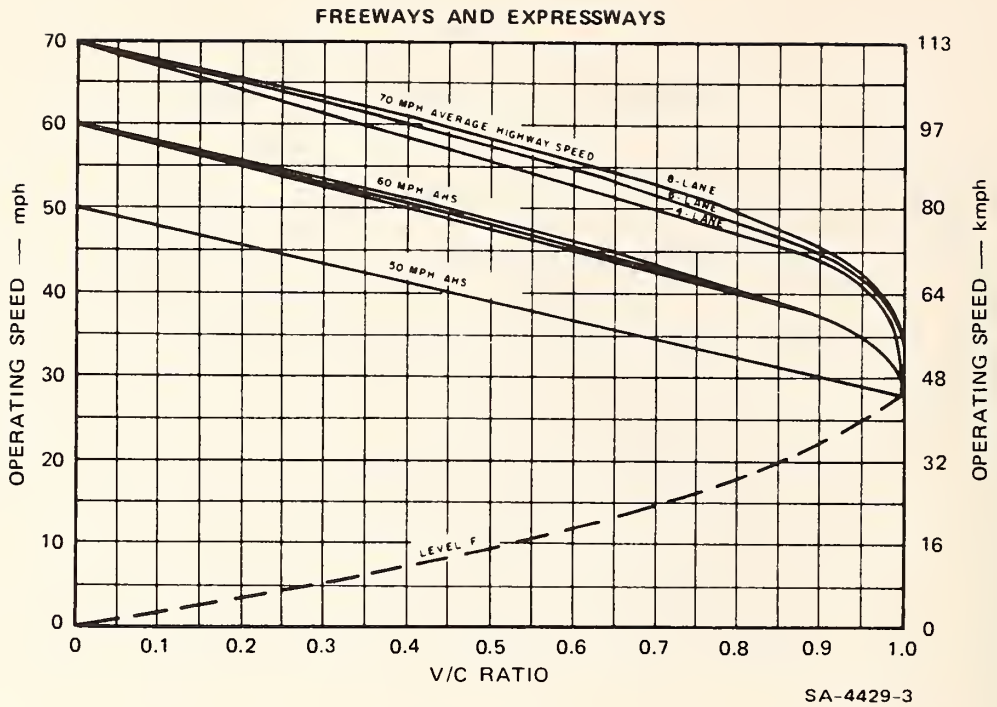

FIGURE 20 RELATIONSHIPS BETWEEN V/C RATIO AND OPERATING SPEED, IN ONE DIRECTION OF TRAVEL, ON FREEWAYS AND EXPRESSWAYS, UNDER UNINTERRUPTED FLOW CONDITIONS (SOURCE: Highway Capacity Manual, 1965)

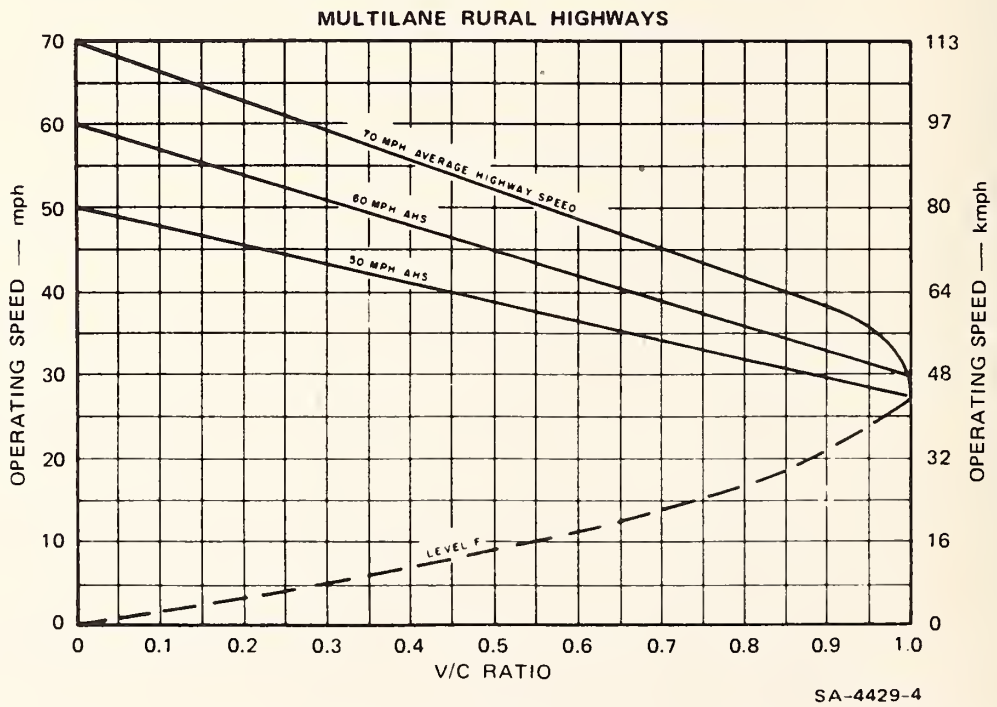

FIGURE 21 RELATIONSHIPS BETWEEN V/C RATIO AND OPERATING SPEED, IN ONE DIRECTION OF TRAVEL, ON MULTILANE RURAL HIGHWAYS, UNDER UNINTERRUPTED FLOW CONDITIONS (SOURCE: Highway Capacity Manual, 1965)

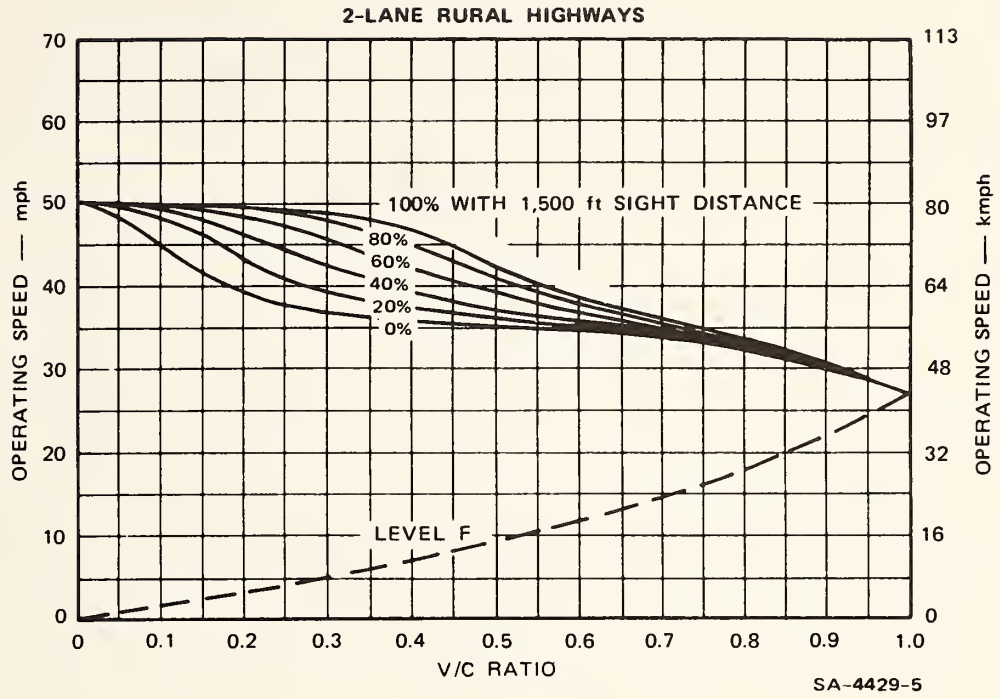

FIGURE 22 RELATIONSHIPS BETWEEN V/C RATIO AND OPERATING SPEED, OVERALL FOR BOTH DIRECTIONS OF TRAVEL, ON TWO-LANE RURAL HIGHWAYS WITH AVERAGE HIGHWAY SPEED OF 50 MPH, UNDER UNINTERRUPTED FLOW CONDITIONS (SOURCE: Highway Capacity Manual, 1965)

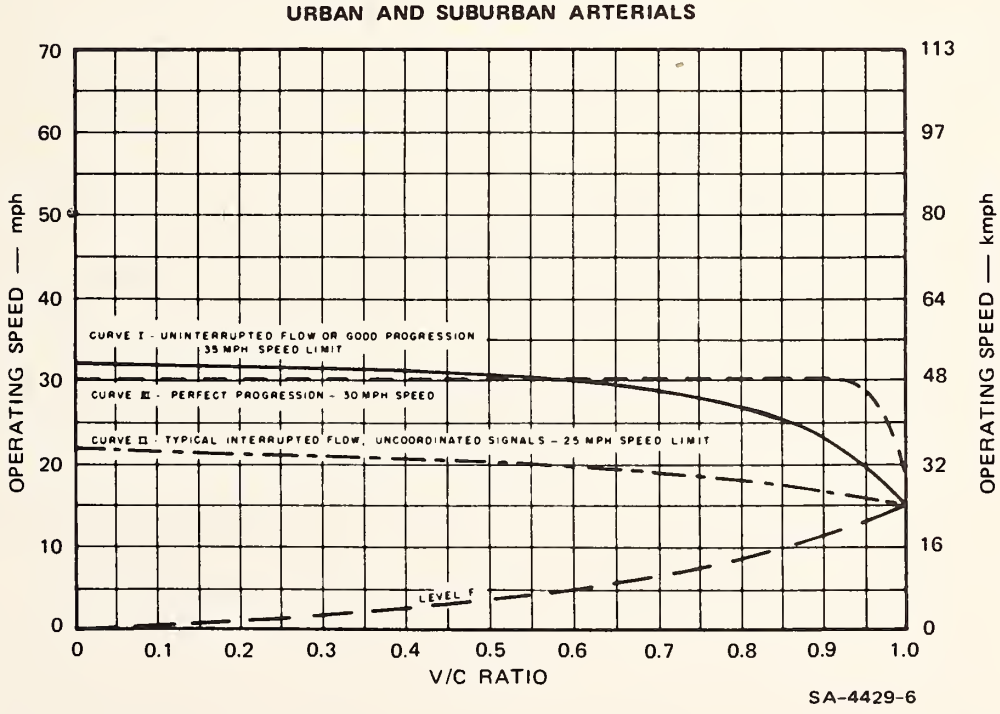

FIGURE 23 TYPICAL RELATIONSHIPS BETWEEN V/C RATIO AND AVERAGE OVERALL TRAVEL SPEED, IN ONE DIRECTION OF TRAVEL, ON URBAN AND SUBURBAN ARTERIAL STREETS (SOURCE: Highway Capacity Manual, 1965)

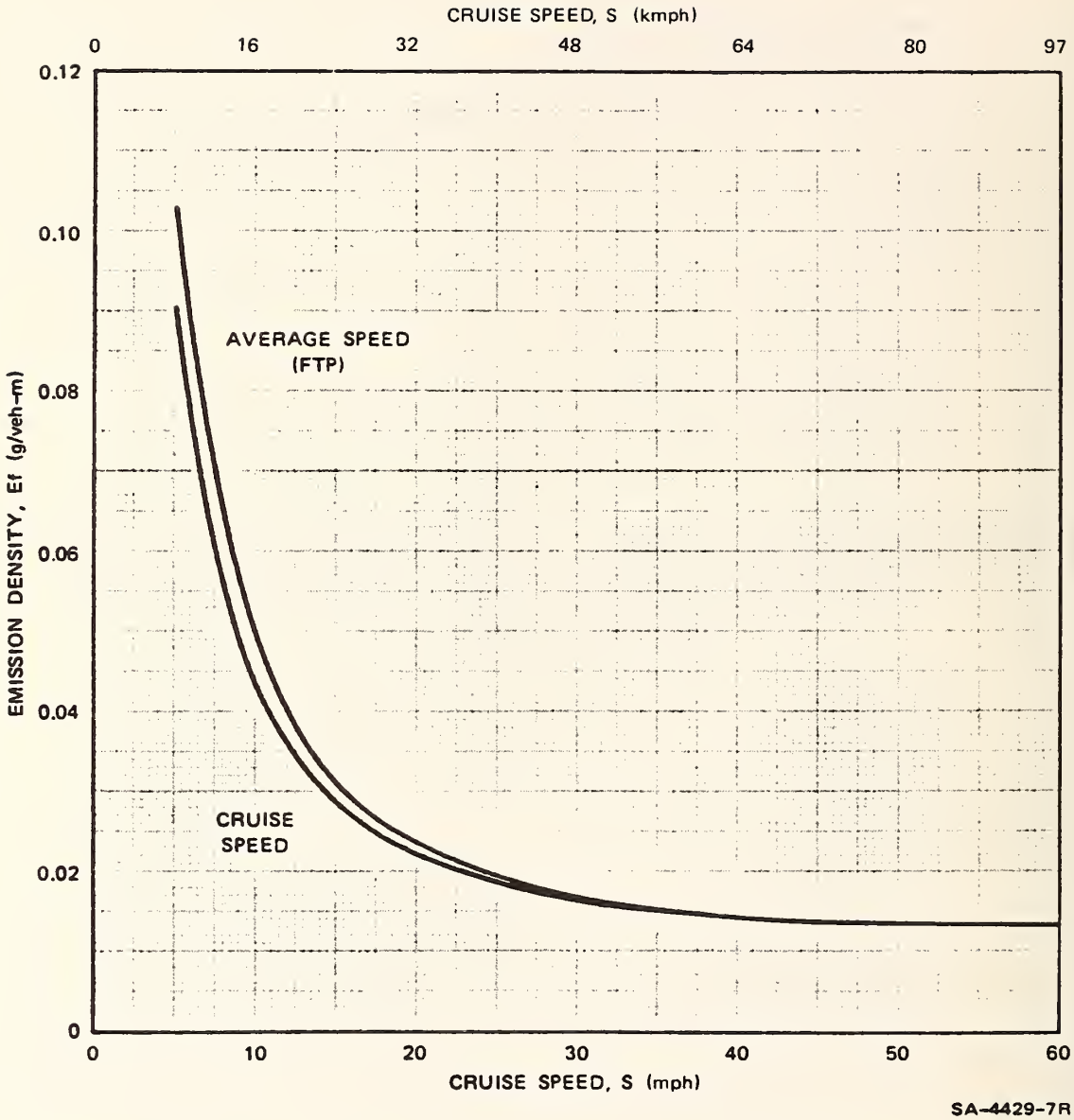

FIGURE 24 EMISSION DENSITY AS A FUNCTION OF SPEED FOR 1975 BASE YEAR

"Average speed (FTP)" curve should be used to determine uninterrupted flow emissions while the "Cruise" curve should be used for signalized intersection approaches. This value (i.e., Ef) multiplied by the vehicle flow rate (veh s^{-1}) determines the roadway emission flux-density (Qf):

$$Qf = \frac{Ef \cdot V}{3600} \qquad (13)$$

The emission flux-density calculated in Eq. (13) is a reference value appropriate to vehicle emission rates for: (1) a given reference year and (2) specified ambient characteristics (e.g., temperature). Thus, the actual emission factors vary depending on calendar year, altitude, state of residence (California or elsewhere), ambient temperature, and the percentage of cold-start vehicles. Tables 6 and 7 summarize the dependence of an emissions correction factor on these five parameters. To determine the composite emissions correction factor, multiply the correction factor obtained from Table 6 by the factors obtained from Tables 7 and 8. The actual emission flux-density is then determined as the product of Qf [Eq. (13)] and the composite emission correction factor:

$$Qfc = (Qf)(Csf)(Yf)(Gf) \quad . \qquad (14)$$

Emission flux-density values must be calculated for each roadway analyzed. Freeways and expressways require no further emission calculations. Signalized and signed intersection approaches require the additional computation of "excess" emissions due to the acceleration, deceleration and idling of vehicles that stop at the intersection; see details and procedures given by Dabberdt and Sandys (1976).

C. Dispersion Methodology

1. Background

Volume I of this report provided an overview and analysis of the atmospheric and experimental data obtained during the course of this study. One of the principal objectives of the data analysis was the

Table 6

COLD-START TEMPERATURE CORRECTION FACTOR
(Csf) FOR LIGHT DUTY VEHICLES*

% Cold Start	Temperature (°F)						
	20	30	40	50	60	70	80
0	1.0	1.0	1.0	1.0	1.0	1.0	1.0
10	1.81	1.55	1.40	1.31	1.24	1.20	1.16
20	2.62	2.09	1.80	1.62	1.49	1.40	1.33
30	3.43	2.64	2.20	1.92	1.73	1.60	1.49
40	4.24	3.18	2.60	2.23	1.98	1.77	1.65
50	5.05	3.73	3.00	2.54	2.22	1.99	1.82
60	5.85	4.27	3.40	2.85	2.47	2.19	1.98
70	6.66	4.82	3.80	3.16	2.71	2.39	2.14
80	7.47	5.36	4.20	3.47	2.96	2.59	2.31
90	8.28	5.91	4.60	3.77	3.20	2.79	2.47
100	9.09	6.45	5.00	4.08	3.45	2.99	2.63

*These correction factors are appropriate for cold start-cold temperature emissions for vehicles that are not equipped with catalysts. Emission factors for catalytically equipped vehicles may be estimated using the appropriate table in Supplement 5 to AP-42.

Note: T(°C) = 0.555 [T(°F) - 32°F]

Table 7

CALENDAR YEAR CORRECTION FACTORS (BASE YEAR 1975)
FOR LIGHT DUTY VEHICLES (Yf)*

Year	Altitude			
	Low (Non-California)	High (Non-California)	Low (California)	High (California)
1975	1.00	1.75	0.99	1.75
1976	0.87	1.55	0.86	1.54
1977	0.76	1.36	0.73	1.33
1978	0.63	1.15	0.61	1.11
1979	0.53	0.96	0.50	0.91
1980	0.42	0.76	0.40	0.73
1985	0.15	0.23	0.33	0.20
1990	0.07	0.07	0.07	0.07

*These correction factors reflect the imposition of interim federal CO emission standards (for the low altitude and high altitude areas) through model year 1977 and the statutory standard thereafter. For California, the CO correction factors reflect the California interim standards through the 1977 model year and the statutory standards thereafter. Should amendments to the Clean Air Act proposed in March 1975 become law, correction factors for 1978 and later years may be altered. In the event Congress amends the Clean Air Act, this table should be altered accordingly. This may be done using Supplement 5 to AP-42.

Table 8

CO GRADE EMISSION CORRECTION FACTOR (Gf)

Average Grade (%)*	Correction Factor (Gf)
10	1.48†
8	1.38†
6	1.28†
4	1.18
3	1.13
2	1.08
1	1.04
0	1.00
-1	0.95
-2	0.90
-3	0.85
-4	0.80
-6	0.70†
-8	0.60†
-10	0.50†

*Grade (%) is the number of feet (0.305m) of vertical rise per 100 ft (30.5m) of horizontal distance.

†Extrapolated values.

Source: Permanent International Association of Road Congresses (1975)

development of a simulation model that would both: (1) represent the interrelationship among the independent atmospheric and geometric variables and the dependent variable--pollutant concentration near the roadway; and (2) be readily applicable, flexible, and accurate. In considering the framework for such a model, four alternative approaches were considered: (1) gradient transfer, (2) Gaussian, (3) statistical, and (4) empirical. The first three methods were eventually rejected for a variety of reasons (discussed below), and a semi-empirical approach relying on some Gaussain dispersion concepts was adopted.

The gradient transfer or K-theory approach is based on a numerical solution of the Fickian equation for mass diffusion in analogy to similar equations for other transport phenomena: Darcy's Law for groundwater flow, Fourier's Law for heat conduction, Maxwell's Law for electrostatics, and Ohm's Law for current conduction. The basic one-dimensional equation (for momentum transfer) was given earlier in Eq. (5); when extended to three-dimensional mass ($\bar{q}$) transfer in the presence of sources and sinks (S_q)

$$\frac{d\bar{q}}{dt} = \frac{\partial}{\partial x}\left(K_x \frac{\partial \bar{q}}{\partial x}\right) + \frac{\partial}{\partial y}\left(K_y \frac{\partial \bar{q}}{\partial y}\right) + \frac{\partial}{\partial z}\left(K_z \frac{\partial \bar{q}}{\partial z}\right) \pm S_q \quad . \qquad (15)$$

The applicability of the concept of a meaningful eddy diffusion coefficient (K) in the complex environment of the turbulent vehicle wake or notch flow of the cut section is open to serious question. Furthermore, determination of representative diffusivity patterns is tenuous and the application of the method is difficult, requiring not only a large amount of secondary (derived) inputs but also a sizeable computing facility. In view of these limitations and uncertainties, the gradient transfer approach was not employed.

The continuous Gaussian point-source dispersion equation is a special case of the generalized gradient transfer method, where the turbulence is homogeneous and stationary:

$$\chi(x,y,z) = \left\{ \frac{Q_p}{2\pi\sigma_y\sigma_z\bar{u}} \exp\left[\frac{-1}{2}\left(\frac{y}{\sigma_y}\right)^2\right] \right\}$$

$$\left\{ \exp\left[\frac{-1}{2}\left(\frac{z-h}{\sigma_z}\right)^2\right] + \exp\left[\frac{-1}{2}\left(\frac{z+h}{\sigma_z}\right)^2\right] \right\} , \qquad (16)$$

where

Q_p = point-source emission flux density

χ = pollutant concentration

h = effective height of the pollution source

σ = dispersion function [see Eq. (8)]

$\bar{u}$ = mean transport wind speed

x = along-wind, horizontal distance

y = across-wind, horizontal distance

z = height above ground

The two terms in the second bracketed function describe the effect of the ground surface in "reflecting" the impinging plume from the elevated source; mathematically, it is equivalent to having an imaginary source of comparable strength located an equal distance h below the ground surface. For an infinite roadway aligned in the y-direction, Eq. (16) can be integrated over y (roadway length) to yield the Gaussian line-source equation:

$$\chi(x,z) = \frac{Q_\ell}{\sqrt{2\pi}\ \bar{u}\ \sigma_z} \left\{ \exp\left[\frac{-1}{2}\left(\frac{z-h}{\sigma_z}\right)^2\right] + \exp\left[\frac{-1}{2}\left(\frac{z+h}{\sigma_z}\right)^2\right] \right\} \qquad (17)$$

where Q_ℓ is the line-source emission flux density (g m^{-1} s^{-1}). The Gaussian line-source equation [Eq. (17)] suffers from several inherent limitations: It cannot simulate topographic effects, nor is it strictly applicable for near-parallel winds. Using an approximation, Calder (1973) has shown where a slightly modified version of Eq. (17) agrees very well with a numerical integration (e.g., Zimmerman and Thompson, 1975) of Eq. (16) for wind/roadway angles as small as 15°. However, both Dabberdt et al. (1976) and Chock (1977) have shown that the integrated line-source

equation significantly overpredicts concentrations observed near roadways. In view of these limitations and previous comparisons, the integrated Gaussian line-source model was not used in its classical form in the development of the assessment methodology. As demonstrated later in this subsection, Eq. (17) was incorporated into a new semi-empirical model that avoids the limitations discussed above.

In an earlier interim report Dabberdt et al. (1974) discussed the possible application of a statistical model for the assessment methodology. The early results indicated the method (continuous, piecewise, linear regression) was able to accurately reproduce the significant features of cut sections on the Santa Monica and Harbor Freeways in Los Angeles. However, the method does not provide outputs to help understand the significance of the various dispersion mechanisms and thus cannot be easily applied to other sites with different geometry, surface roughness, and traffic.

In view of the limitations associated with each of the first three methods, a semi-empirical approach was followed in the development of the assessment methodology. Formulation of the roadway atmospheric dispersion model for air pollution (ROADMAP) is based on the treatment of the dispersion as the vector sum of two components. One is the dispersion that occurs along the horizontal wind component oriented perpendicular or normal (n) to the roadway axis; the other is the dispersion along the horizontal wind component that is parallel (p) to the roadway. It is assumed that there is no vertical transport by a non-zero mean vertical wind component. Figure 25 illustrates the coordinate system for a one-way road.

The two-component dispersion formulation can be written as:

$$\frac{\chi_T U}{Q_\ell} = \vec{i}\left(\frac{\chi_n u}{Q_\ell}\right) + \vec{j}\left(\frac{\chi_p v}{Q_\ell}\right) \qquad (18)$$

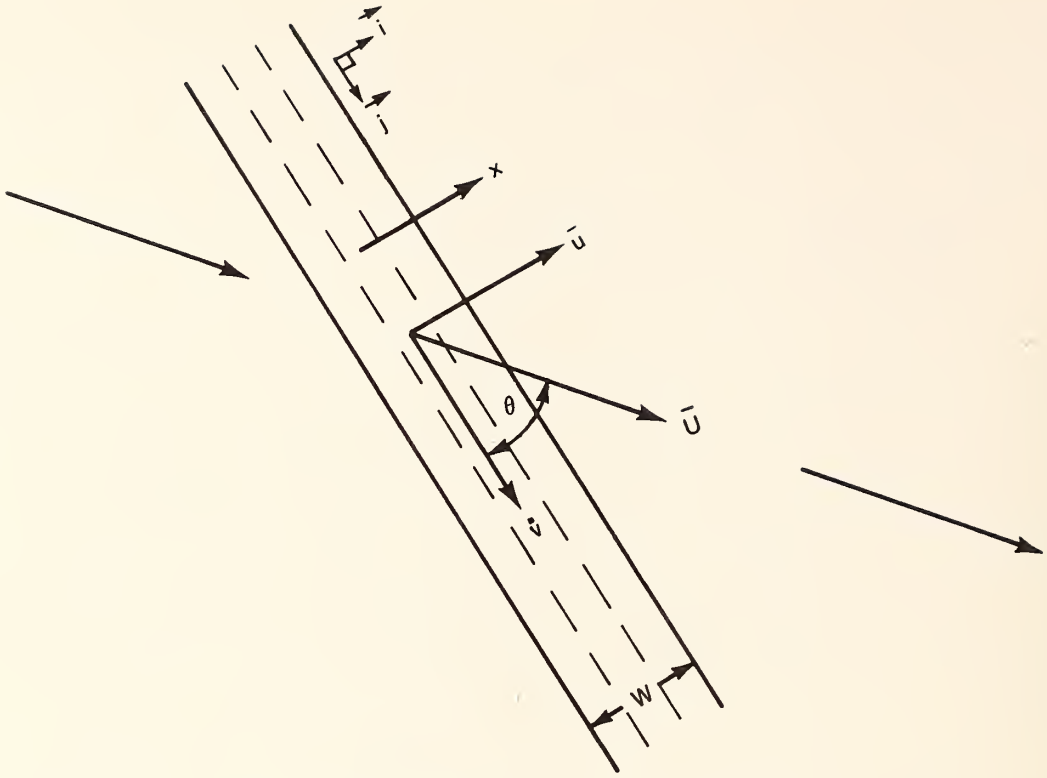

FIGURE 25 COORDINATE SYSTEM FOR ROADMAP

where

$\vec{i}$ = unit vector normal to roadway

$\vec{j}$ = unit vector parallel to roadway

U = vector wind speed (m/s)

u = wind component normal to roadway (m/s)

v = wind component parallel to roadway (m/s)

Q_ℓ = line source emission flux density (g/m-s)

χ_T = total pollutant concentration (g/m^3)

χ_n = concentration from lateral dispersion (g/m^3)

χ_p = concentration from longitudinal dispersion (g/m^3)

When θ is introduced as the angle between the longitudinal axis of the line source and the wind vector, then

$$u = U \sin \theta \quad , \tag{19a}$$

and

$$v = U \cos \theta \quad . \tag{19b}$$

Substituting Eq. (19) into Eq. (18) and squaring both sides,

$$\left[\frac{\chi_T U}{Q_\ell}\right]^2 = \left[\frac{\chi_n U \sin\theta}{Q_\ell}\right]^2 + \left[\frac{\chi_p U \cos\theta}{Q_\ell}\right]^2 \qquad (20)$$

For convenience, the first right-hand term in Eq. (20) is designated the "perpendicular" term and the second, the "parallel" term.

The form of the perpendicular term is specified in analogy to the Gaussian line source equation for a perpendicular wind,

$$\left[\frac{\chi_n U}{Q_\ell}\right] = \frac{\sqrt{2/\pi}}{k\sigma_z}\left\{\exp\left[\frac{-1}{2}\left(\frac{z + z' - H}{\sigma_z}\right)^2\right] + \exp\left[\frac{-1}{2}\left(\frac{z + z' + H}{\sigma_z}\right)^2\right]\right\}, \qquad (21)$$

where

k = constant ($H = 0$, $k = 2$; $H \neq 0$, $k = 1$)

σ_z = vertical Gaussian dispersion function (m)

z = height above grade-level or above roadway (depressed section) (m)

z' = height offset from plume rise (m)

H = roadway height above grade-level (m).

A unique feature of Eq. (21) is the term z' which serves as a height-modifier to represent the possible change in the height of the plume centerline as a function of distance downwind. This offset could result either from the aerodynamic influence (i.e., shelterbelt) of the traffic stream or from the buoyancy effect of vehicular waste heat emissions. In principle, both σ_z and z' may vary with distance (x) away from the roadway and with atmospheric stability, but not with height.

The parallel dispersion term was formulated to represent the general features of the Gaussian point source equation when the latter is integrated for a wind aligned parallel to a semi-infinite line source (see Dabberdt and Sandys, 1976). The resulting formulation may be thought of as a type of expanding-box model where the sides and top of the box are

given as exponential functions of height (z) and cross-roadway distance (x). The form chosen assumes the same functional dependence on height as the perpendicular term, but a different cross-roadway dispersion representation (f),

$$\left[\frac{\chi_p U}{Q_\ell}\right] = \frac{1}{k\sigma_{z-o} f}\left\{\exp\left[\frac{-1}{2}\left(\frac{z + z' - H}{\sigma_z}\right)^2\right] + \exp\left[\frac{-1}{2}\left(\frac{z + z' + H}{\sigma_z}\right)^2\right]\right\}, \quad (22)$$

where $$\sigma_z = \sigma_{z-o} + a_1 x^{b_1} \quad , \quad (23a)$$

$$z' = z'_o + a_2 x^{b_2} \quad , \quad (23b)$$

$$f = a_3\left(c_3 + \frac{2x}{W}\right)^{b_3} \quad (23c)$$

and, W = roadway width (m).

When the model is applied to both traffic streams, W is defined as the total roadway width (i.e., from shoulder-to-shoulder). On the other hand, physical separation of the traffic streams or marked dissimilarities in the traffic volumes (and hence emissions) may warrant application of the model separately for each direction. In this case W would, of course, be redefined accordingly.

2. Application Procedure

The procedure for implementing the ROADMAP model is given in Worksheet 2 and the accompanying instructions (Table 9). Briefly, it entails the following steps. First, identify the roadway configuration as one of the nine discussed in Volume I of this report:

Roadway Configuration	Surface Roughness		Dispersion Functions
	Upwind	Downwind	
Grade-level	rough	rough	Fig. 26
Grade-level	rough	smooth	Fig. 27
Grade-level	smooth	rough	Fig. 28
Grade-level, neutral atmosphere	smooth	smooth	Fig. 29
Street canyon	rough	rough	Fig. 30
Cut section (vertical walls)	smooth	smooth	Fig. 31
Cut section (sloping walls)	smooth	smooth	Fig. 32
Fill section	smooth	smooth	Fig. 33
Viaduct section	smooth	smooth	Fig. 34
Grade-level, stable atmosphere	smooth	smooth	Fig. 35
Grade-level, unstable atmosphere	smooth	smooth	Fig. 36

Next, refer either to Table 10 or Figures 26-36 to obtain the appropriate values of the dispersion functions σ_z, z', and $f\sigma_{z-o}$. Using the worksheet, calculate the normalized concentration ($\chi_t \bar{U}/Q_\ell$), then compute a calibrated estimate of the normalized concentration by applying the slope and intercept-values derived in Volume I in the comparison of experimental observations and model calculations. This calibrated value is called the second-order estimate of normalized concentration. Estimates obtained in this way are representative of neutral atmospheric stability conditions. Since none of the wind tunnel tests had diabatic stability, it is not possible to directly estimate the impact of stability variations on concentration-values appropriate to the roadway configurations tested in the wind tunnel. Of the nine configurations listed above, only the grade-level/smooth-terrain case is based on atmospheric tests. Figures 35 and 36 summarize the three dispersion functions for stable and unstable conditions, respectively, and can be used directly in lieu of the neutral-stability values (Figure 29) to compute concentrations for a grade-level roadway. The three atmospheric tests (i.e., Figures 29, 35, and 36) enable the user to distinguish between emissions from the upwind traffic lanes and those on the downwind side of the median. The total concentration at a given receptor location is therefore calculated as the sum of the contribution from each of the two traffic streams.

WORKSHEET 2

COMPUTATION OF AMBIENT CARBON MONOXIDE CONCENTRATION

Project Location:_____ Analyst:_____

Roadway Configuration:_____ Date:_____

Step	Symbol	Parameter/Units	Traffic Stream	
		Basic Inputs:	1	2
1	H_i	Roadway height (m)		
2	W_i	Roadway width (m)		
3	θ_i^*	Roadway heading (deg)		
4	Qfc_i	Emission flux-density (g m^{-1} s^{-1})		
5	--	Surface roughness		
6	$\bar{U}$	Ambient wind speed (m s^{-1})		
7	θ'	Ambient wind direction (deg)		
8	z	Receptor height (m)		
9	x	Road-receptor distance (m)		
		Derived Inputs:		
10	θ	Wind/roadway angle (deg)		
11	sin θ	Sine θ		
12	cos θ	Cosine θ		
13	σ_z	Vertical dispersion function (m)		
14	z'	Height-offset function (m)		
15	$f\sigma_{z-o}$	Lateral dispersion function (m)		
		Computed Functions:		
16	①	$-0.5[(z + z' - H) \div \sigma_z]^2 \equiv$ ①		
17	-	exp [①]		
18	②	$-0.5[(z + z' + H) \div \sigma_z]^2 \equiv$ ②		
19	-	exp [②]		
20	3	exp [①] + exp [②] ≡ ③		
21	$[\chi_n\bar{U}/Q_1]^2$	$[(0.8 \sin \theta \div k\sigma_z)$③$]^2 \equiv$ ④		
22	$[\chi_p\bar{U}/Q_1]^2$	$[(\cos \theta \div kf\sigma_{z-o})$③$]^2 \equiv$ ⑤		
23	$[\chi_t\bar{U}/Q_1]$	$\sqrt{④ + ⑤} \equiv$ ⑥; normalized concentration		
24	χ_t	First-order CO concentration estimate (mg m^{-3})		
25	α	Slope of linear calibration curve		
26	β	Intercept of linear calibration curve		
27	χ_t^*	Second-order CO concentration estimate (mg m^{-3})		

Table 9

INSTRUCTIONS FOR COMPLETING WORKSHEET 2

Step	Instructions
1	Estimate the height (m) of the roadway surface above ground level. For depressed and grade-level roads, H = 0.
2	Enter the width (m) of the roadway between the outside edges of the two outermost lanes. If the two traffic streams on a two-way road are widely separated or have dissimilar emission values, then treat each as a separate roadway (except for the cut sections and street canyon which should only as one road be considered.)
3,4	Enter from lines 1 and 17 of Worksheet 1.
5	Estimate the surface roughness as either smooth ($z_o \leq 1$ m) or rough ($z_o > 1$ m) using Eq. (4).
6,7	Enter the ambient wind speed (m s^{-1}) and direction (deg) appropriate to $z \approx 3$m.
8,9	Enter the height (z,m) and lateral position (x,m) of the receptor (i.e., the point where concentration estimate will be made); x has its origin at the center of the emission line-source.
10	Calculate θ(deg) as the angle ($\leq 90°$) between the wind vector and roadway axis.
11,12	Calculate the sine and cosine of the angle θ.
13-15	Calculate the three dispersion functions from Eqs. (23a) through (23c) and the coefficient values given in Table 10 appropriate to the configuration of the roadway, or estimate the values from the graphs that comprise Figures 26-36.
16-20	Compute the height-dependence term of the dispersion model using z, z', H, and σ_z.
21	Compute the perpendicular (i.e., normal) dispersion term from Eq. (20); the constant k is listed in Table 10.
22	Compute the parallel dispersion term from Eq. (20).
23	Compute the first-order estimate of the normalized concentration ($\chi_t \bar{U}/Q_\ell$, m^{-1}) as the square root of the sum of the perpendicular (line 21) and parallel (line 22) terms.
24	Compute the first-order estimate of the carbon monoxide concentration (χ_t, mg m^{-3}) from the following equation: $$\chi_t = 1000 \left(\frac{\chi_t \bar{U}}{Q_\ell} \right) \frac{Q_\ell}{\bar{U}}$$ where 1000 is the conversion from g m^{-3} to mg m^{-3}, and Q_ℓ and $\bar{U}$ are given on lines 4 and 6.
25,26	Enter the slope and intercept-values of the calibration curve from Table 10.
27	Compute the second-order estimate of CO concentration (χ_t^*, mg m^{-3}) from the following calibration equation: $$\chi_t^* \alpha + \beta \chi_t \quad .$$

Table 10

INPUTS FOR DISPERSION COMPUTATION

Configuration	Ground Roughness	Stability	a_1	b_1	c_1	a_2	b_2	c_2	a_3	b_3	c_3	k	α	β	Comments
Grade-level	rough	neutral	0.154	0.878	2.15	-18.4	0.003	19.1	0.007	3.49	4.09	2	.023	.90	
Grade-level	rough upwind, smooth downwind	neutral	0.028	1.41	2.89	-8.09	0.026	7.77	0.094	2.78	1.50	2	.066	.32	
Grade-level	smooth upwind, rough downwind	neutral	0.096	0.957	0.642	-0.017	1.46	-1.10	0.006	3.84	3.94	2	.088	.76	
"Porous" street canyon	rough	neutral	1.07	0.731	-3.25	36.8	-17.5	-1.49	-0.810	2.01	0.196	2	.064	.45	
Cut section (vertical side walls)	smooth	neutral	0.0006	2.53	2.24	-0.016	1.47	-3.65	0.010	3.19	4.33	2	.071	.83	z = 0 at road surface
Cut section (sloping side walls)	smooth	neutral	0.00004	3.22	2.53	-0.734	0.496	-0.522	0.0036	3.37	3.97	2	.057	.56	z = 0 at road surface
Fill section	smooth	neutral	0.390	0.810	0.185	0.127	1.07	-1.78	0.259	4.29	2.64	1	.037	1.08	z = 0 at ground surface
Viaduct section	smooth	neutral	0.00005	3.14	3.07	-0.0018	2.20	1.44	0.040	3.78	4.93	1	.028	1.07	z = 0 at ground surface
Grade-level (upwind lanes)	smooth	neutral	-6.94	-0.078	6.78	-0.0006	1.58	-1.82	0.053	0.914	1.02	2	0	1	
Grade-level (downwind lanes)	smooth	neutral	0.003	1.54	0.765	-0.150	0.621	-0.729	0.054	1.95	4.50	2	0	1	
Grade-level (upwind lanes)	smooth	stable	0.295	0.775	0.236	-33.4	-1.74	-1.23	0.053*	0.914*	1.02*	2	0	1	
Grade-level (downwind lanes)	smooth	stable	0.739	0.534	0.993	1.79	0.038	-1.90	0.054*	1.95*	4.50*	2	0	1	
Grade-level (upwind lanes)	smooth	unstable	-217.	-1.92	2.60	-0.021	0.992	-1.63	0.0061	2.37	4.99	2	0	1	
Grade-level (downwind lanes)	smooth	unstable	0.154	0.242	1.15	-0.360	0.830	2.90	1.37	0.096	-1.51	2	0	1	

*Coefficients a_3, b_3, and c_3 for the stable cases have been set equal to the neutral counterparts due to a lack of sufficient experimental, stable-case data for winds nearly parallel to the roadway.

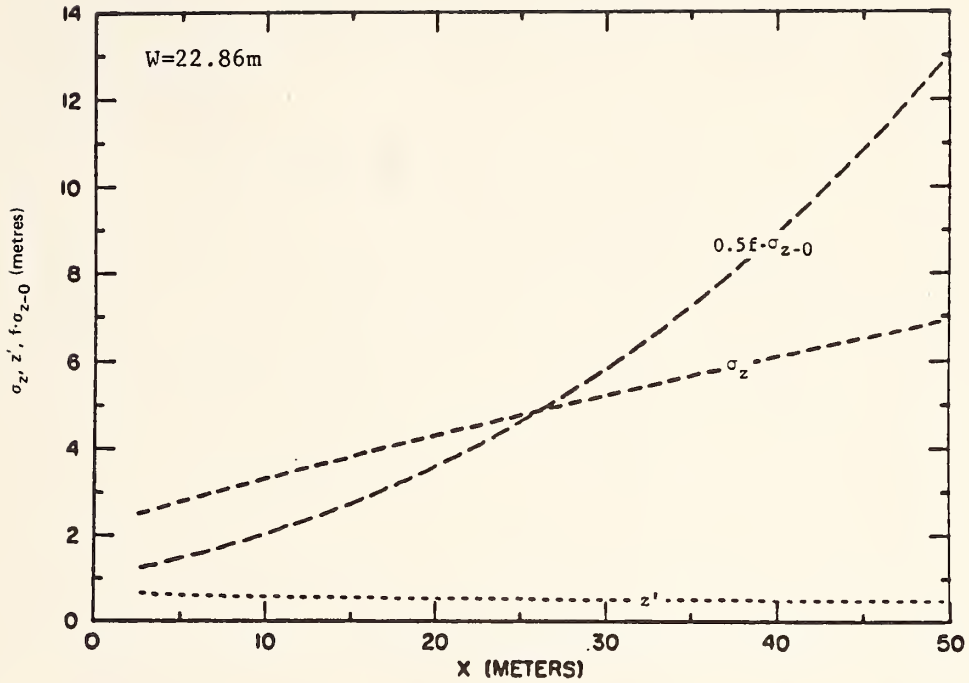

FIGURE 26 VARIATION OF DISPERSION PARAMETERS WITH CROSS-ROADWAY DISTANCE FOR GRADE-LEVEL ROADWAY AND ROUGH TERRAIN

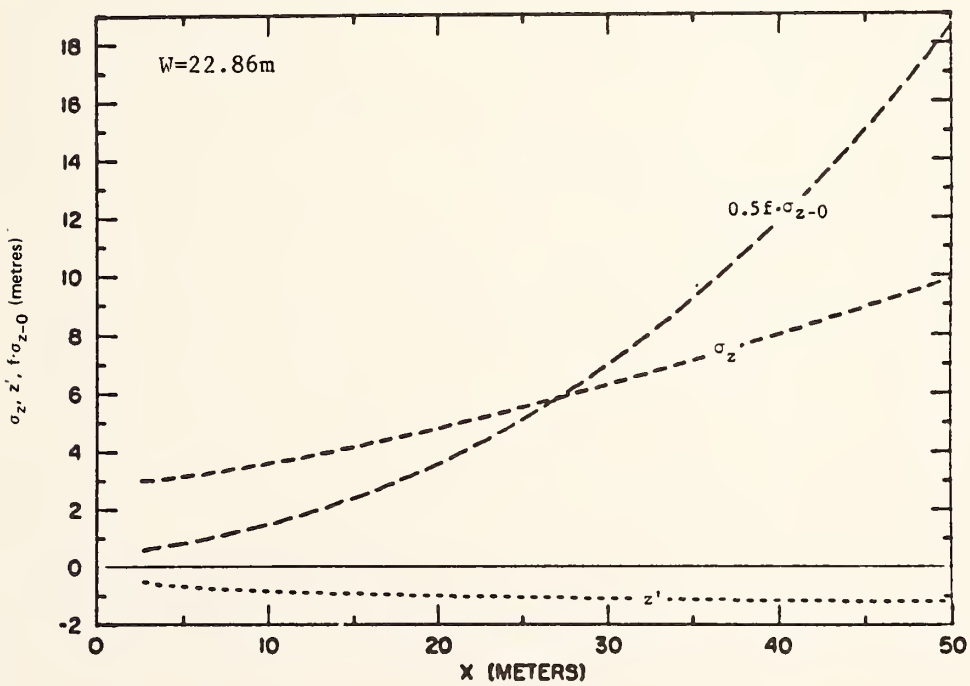

FIGURE 27 VARIATION OF DISPERSION PARAMETERS WITH CROSS-ROADWAY DISTANCE FOR GRADE-LEVEL ROADWAY AND SMOOTH TERRAIN DOWNWIND/ROUGH UPWIND

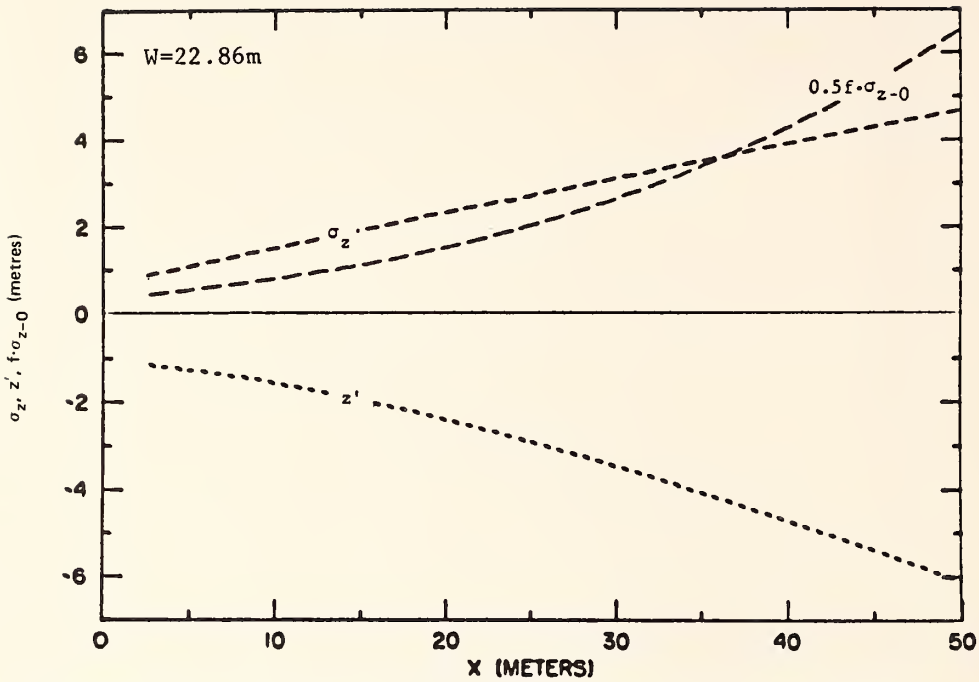

FIGURE 28 VARIATION OF DISPERSION PARAMETERS WITH CROSS-ROADWAY DISTANCE FOR GRADE-LEVEL ROADWAY AND ROUGH TERRAIN DOWNWIND/SMOOTH UPWIND

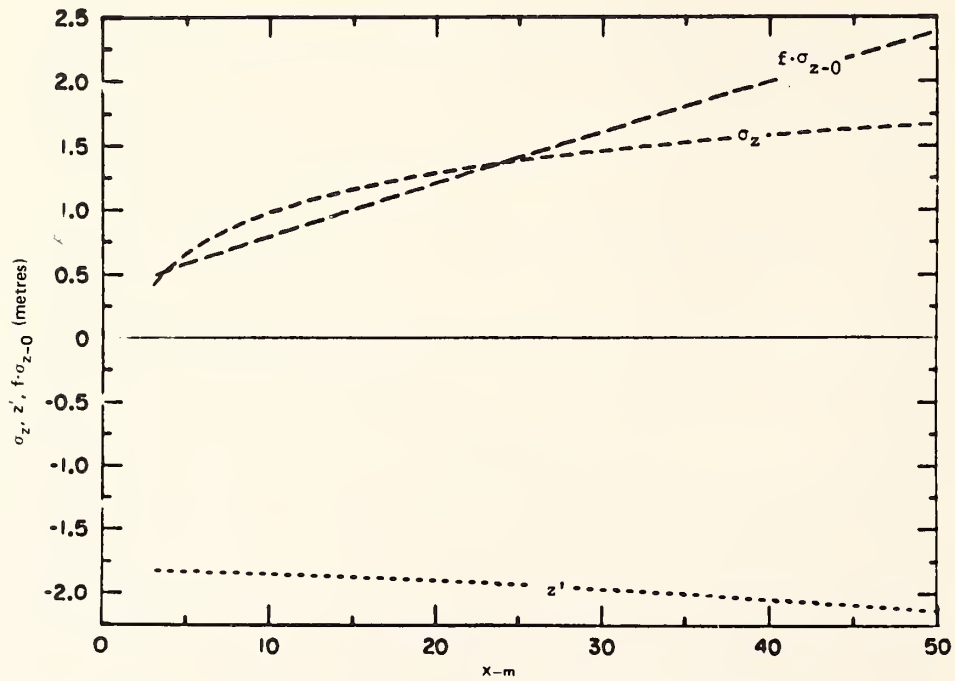

FIGURE 29a VARIATION OF ROADMAP DISPERSION PARAMETERS WITH CROSS-ROADWAY DISTANCE FOR UPWIND TRAFFIC LANES ON HIGHWAY 101; NEUTRAL ATMOSPHERIC CONDITIONS

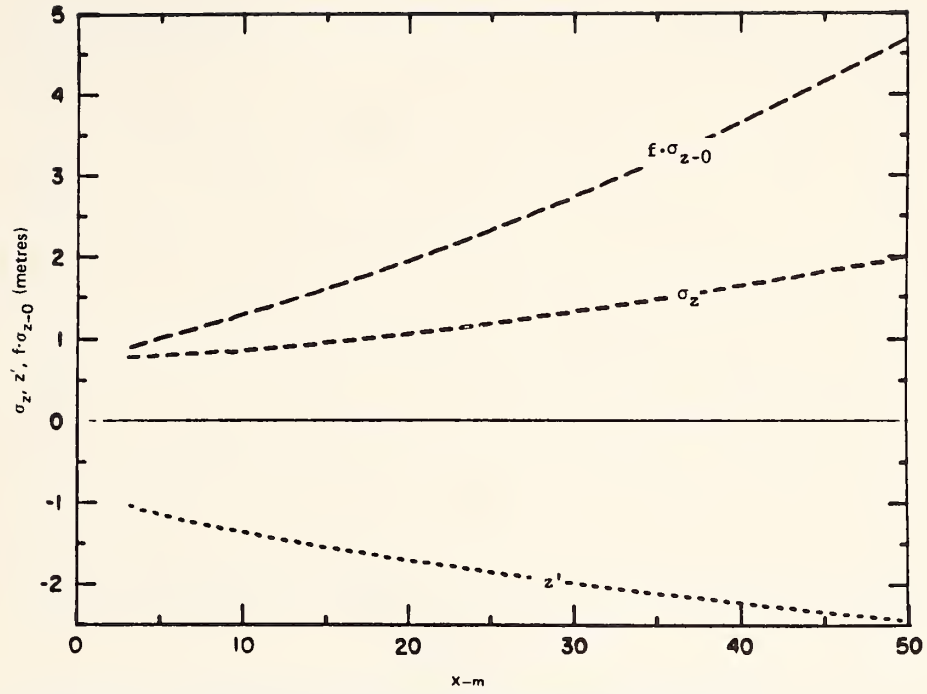

FIGURE 29b VARIATION OF ROADMAP DISPERSION PARAMETERS WITH CROSS-ROADWAY DISTANCE FOR DOWNWIND TRAFFIC LANES ON HIGHWAY 101; NEUTRAL ATMOSPHERIC CONDITIONS

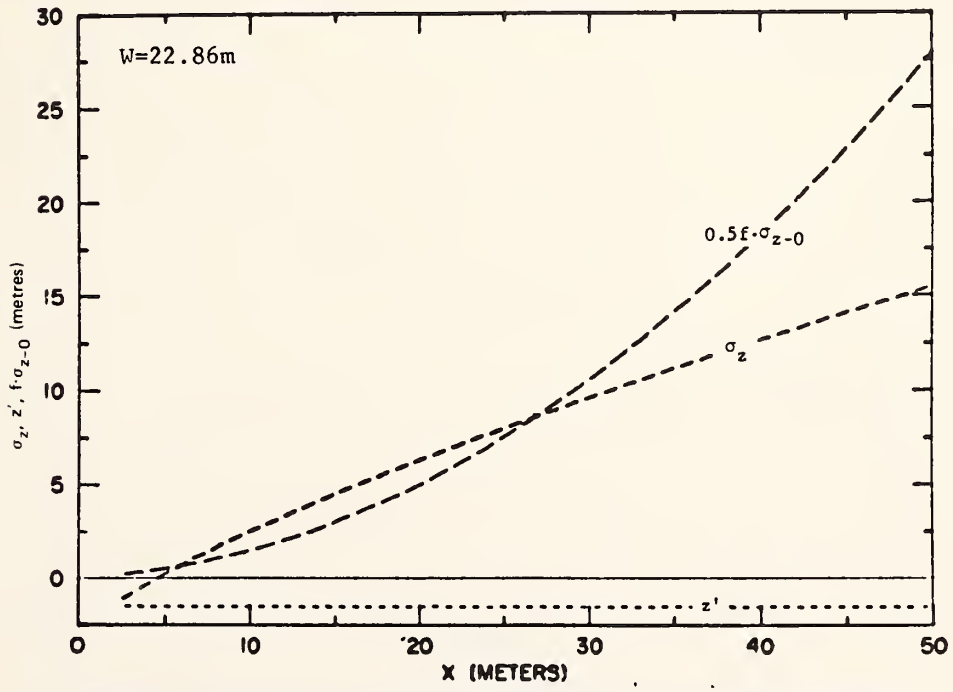

FIGURE 30 VARIATION OF DISPERSION PARAMETERS WITH CROSS-ROADWAY DISTANCE FOR ROUGH TERRAIN AND STREET CANYON (i.e., narrow right-of-way)

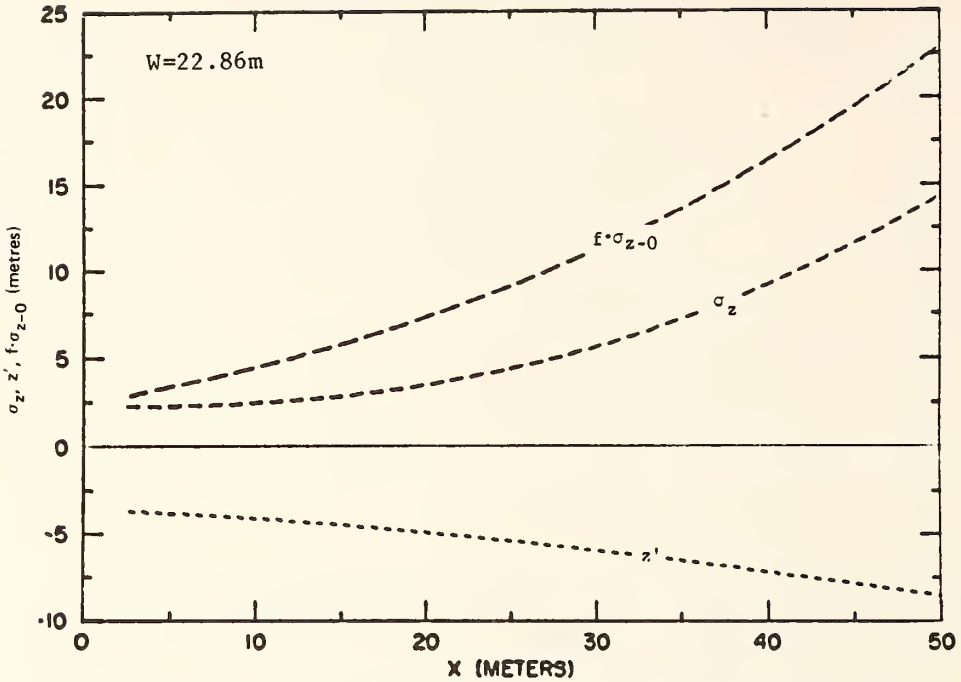

FIGURE 31 VARIATION OF DISPERSION PARAMETERS WITH CROSS-ROADWAY DISTANCE FOR CUT SECTION WITH VERTICAL WALLS AND SMOOTH TERRAIN

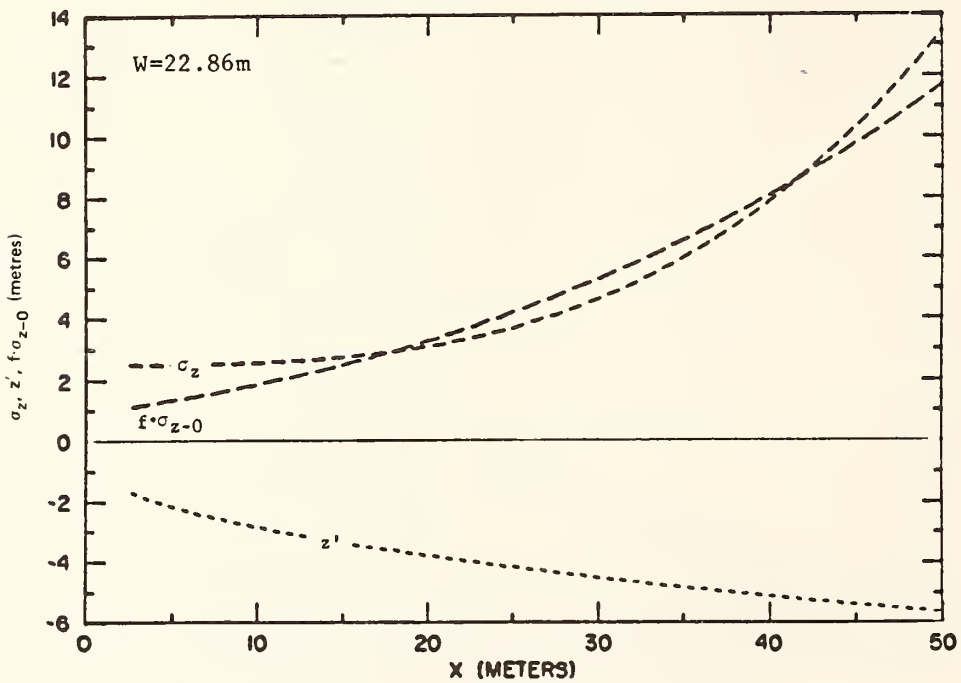

FIGURE 32 VARIATION OF DISPERSION PARAMETERS WITH CROSS-ROADWAY DISTANCE FOR CUT SECTION WITH SLOPING WALLS AND SMOOTH TERRAIN

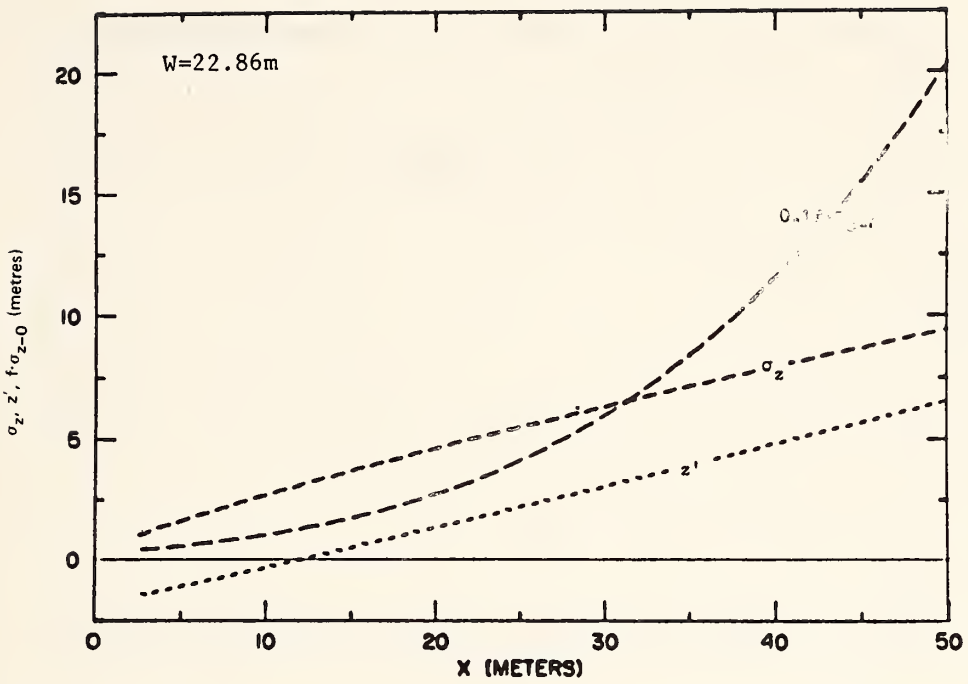

FIGURE 33 VARIATION OF DISPERSION PARAMETERS WITH CROSS-ROADWAY DISTANCE FOR FILL SECTION AND SMOOTH TERRAIN

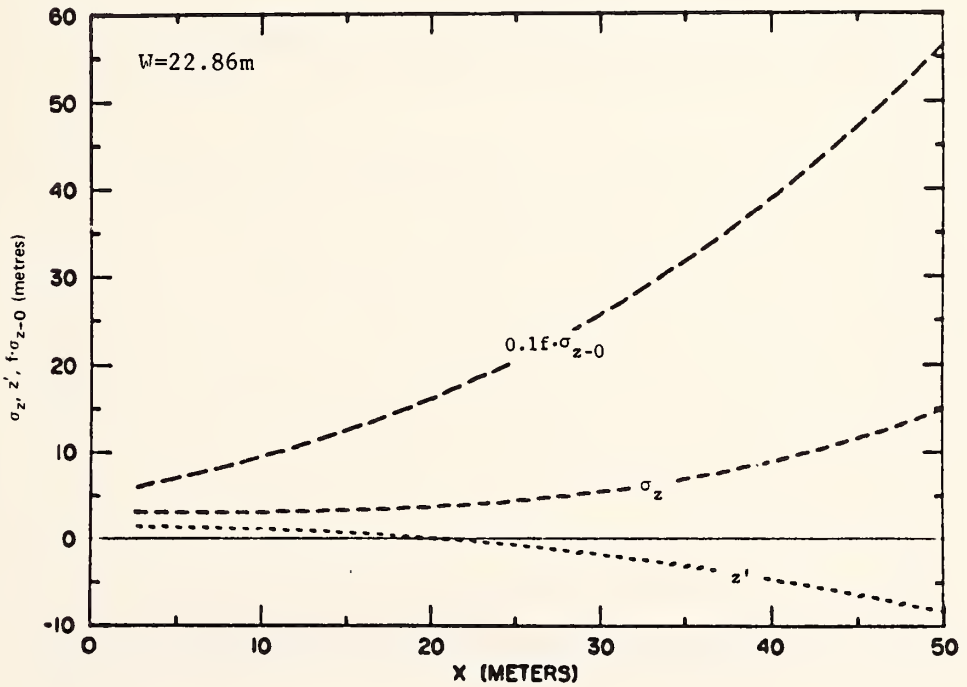

FIGURE 34 VARIATION OF DISPERSION PARAMETERS WITH CROSS-ROADWAY DISTANCE FOR VIADUCT SECTION AND SMOOTH TERRAIN

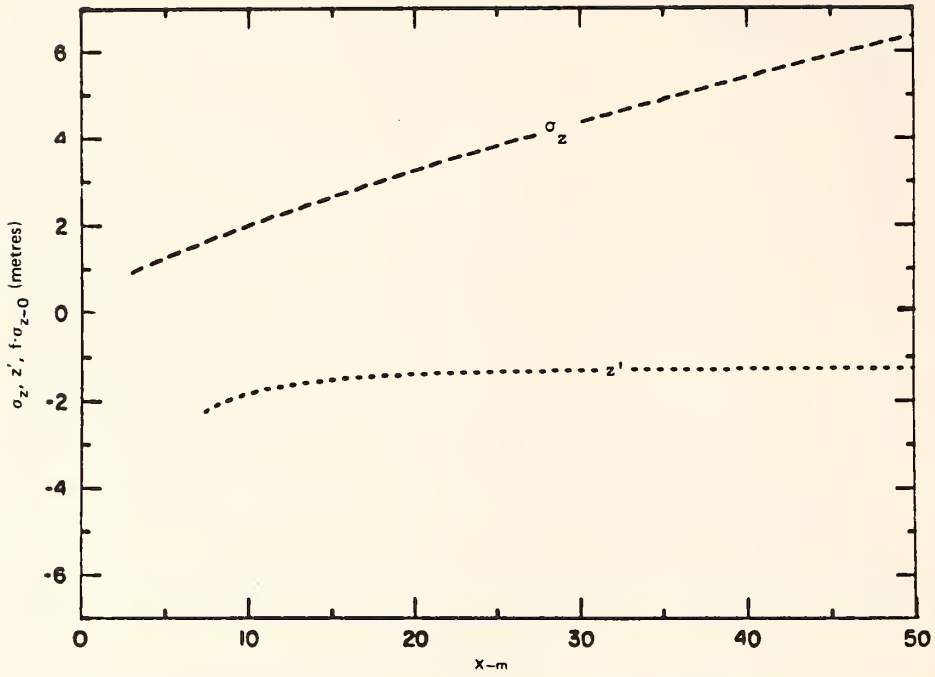

FIGURE 35a VARIATION OF ROADMAP DISPERSION PARAMETERS WITH CROSS-ROADWAY DISTANCE FOR UPWIND TRAFFIC LANES ON HIGHWAY 101; STABLE ATMOSPHERIC CONDITIONS

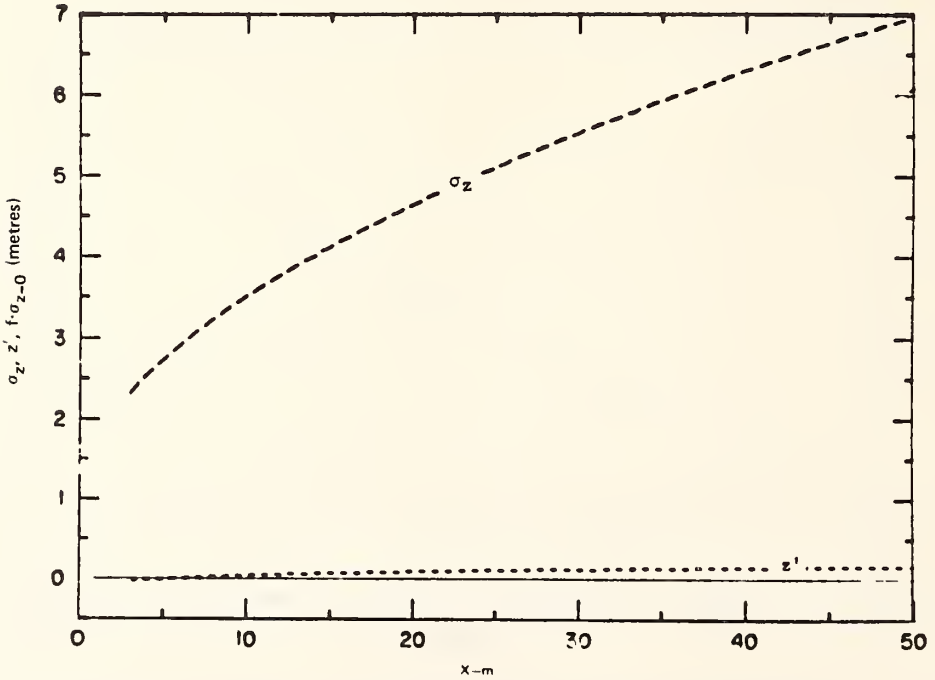

FIGURE 35b VARIATION OF ROADMAP DISPERSION PARAMETERS WITH CROSS-ROADWAY DISTANCE FOR DOWNWIND TRAFFIC LANES ON HIGHWAY 101; STABLE ATMOSPHERIC CONDITIONS

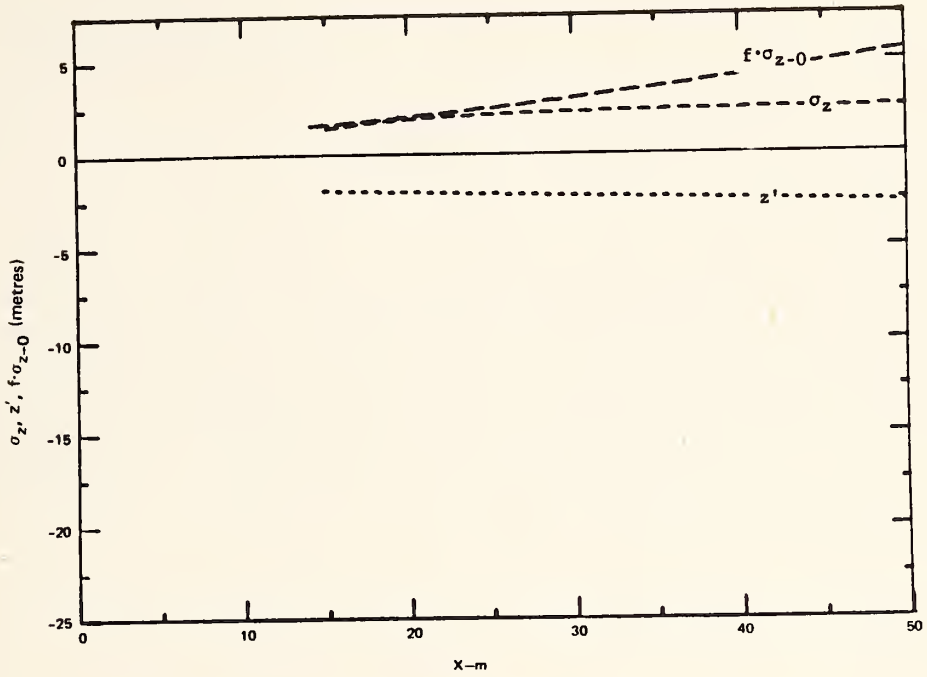

FIGURE 36a VARIATION OF ROADMAP DISPERSION PARAMETERS WITH CROSS-ROADWAY DISTANCE FOR UPWIND TRAFFIC LANES ON HIGHWAY 101; UNSTABLE ATMOSPHERIC CONDITIONS

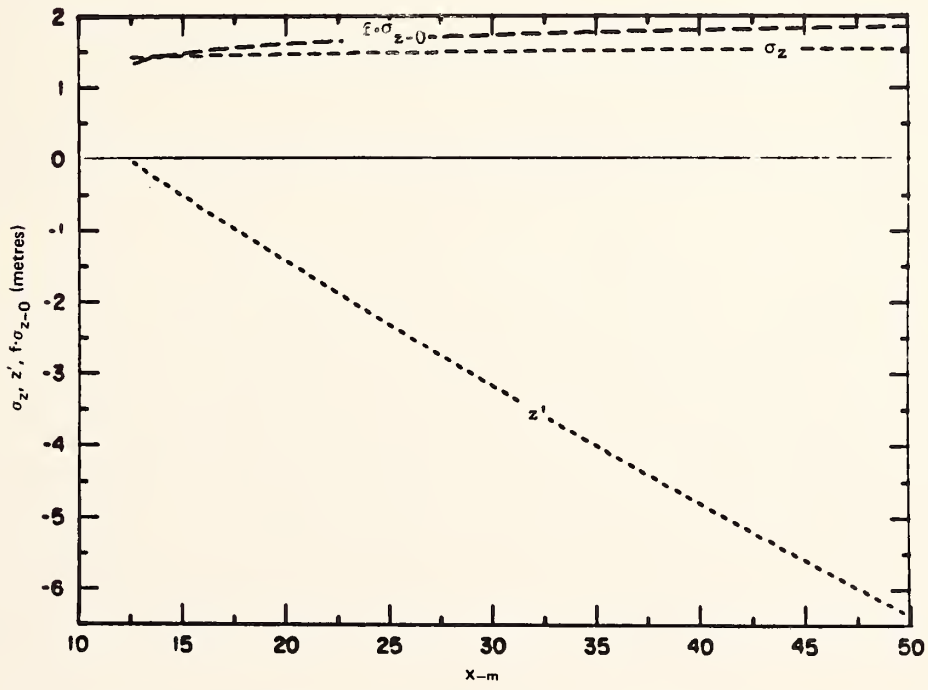

FIGURE 36b VARIATION OF ROADMAP DISPERSION PARAMETERS WITH CROSS-ROADWAY DISTANCE FOR DOWNWIND TRAFFIC LANES ON HIGHWAY 101; UNSTABLE ATMOSPHERIC CONDITIONS

IV APPLICATIONS

A. Introduction

The assessment methodology presented in the preceding section provides quantitative methods for (1) estimating carbon monoxide emissions on freely-flowing, limited access highways, and (2) estimating CO concentrations as a function of wind speed and receptor location and wind direction with respect to the roadway. This dispersion methodology has been developed from experimental data from nine distinct roadway configurations. In the case of the grade-level highway in smooth terrain, the analysis can be done for stable, neutral and unstable atmospheric conditions. The procedure for the other eight configurations is strictly applicable to neutral conditions, although a scaling procedure was suggested to provide estimates for diabatic conditions. With the assessment methodology (summarized in two worksheets), the user can quantitatively estimate concentration levels of CO near a wide range of roadway types. However, there is an even broader range of roadways for which the assessment methodology cannot be applied directly, although in some cases it may be an aid in developing a qualitative evaluation of the air pollution potential.

In this section we explore these two applications. In Subsection B, the methodology is applied directly to each of the nine configurations. Furthermore, the grade-level roadway in smooth terrain (neutral stability) is used as a reference to compare the relative differences among the different configurations. Subsection C then presents a qualitative discussion of the possible application of the mthodology to other roadway configurations and traffic conditions. Subsection D suggests ways in which the ROADMAP procedure may be modified to accommodate variations in roadway and environmental conditions.

B. Direct (Quantitative) Applications

Normalized CO concentrations ($\chi\bar{U}/Q$) for each of the nine "basic" configurations have been evaluated for a prescribed array of 16 receptor locations (ranging in x from 15 to 40 m and z from 1 to 15 m) and five wind/roadway bearings (0, 15, 30, 60, and 90°)*. Values of roadway width and height have been chosen to correspond to the experimental values of the actual wind tunnel and atmospheric tests described in Volume I. Neutral atmospheric conditions are appropriate to each of the nine configurations; additionally, the grade-level/smooth-ground configuration is evaluated for both stable and unstable conditions.

*0^{o} wind "into paper," 90^{o} wind to the right side of paper,
X distances to the right of the roadway centerline.

Case One:

- Grade-level, six-lane divided freeway
- Smooth terrain to both sides of roadway
- Neutral atmospheric stability

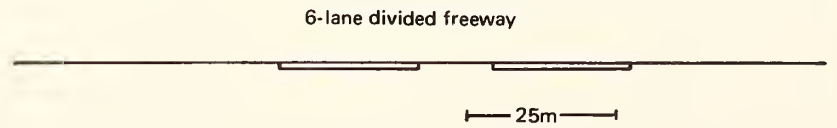

The ROADMAP parameters used in this example (as well as Cases Two and Three) were derived from the atmospheric field test data (i.e., grade-level site, Highway 101), whereas Cases Four through Eleven are based on wind tunnel test data. Cases One through Three are based on a ROADMAP formulation that distinguishes between emissions and dispersion from the traffic lanes on the upwind side of the roadway median and those downwind of the median. Emission rates were assumed equal for the two traffic streams.

Concentrations are highest near the surface and where the wind is parallel to the roadway axis, although the variation for angles between 0 and 30° is less than 15 percent. Between heights of 1 and 3 m, concentrations generally decrease gradually, while there is a marked decrease between 3 and 8 m (the latter are essentially zero). Interesting to note is the increase in concentrations at the 3-m level that occurs with increasing distance from the roadway for wind angles of 60° and 90°.

		$\chi U/Q(m^{-1})$ z(m)			
θ(deg)	x(m)	1	3	8	15
0.	15.	1.712	1.136	.000	.000
0.	20.	1.428	1.072	.000	.000
0.	30.	1.059	.984	.001	.000
0.	40.	.843	.897	.002	.000
15.	15.	1.672	1.100	.000	.000
15.	20.	1.400	1.040	.000	.000
15.	30.	1.041	.961	.001	.000
15.	40.	.830	.882	.002	.000
30.	15.	1.557	.993	.000	.000
30.	20.	1.314	.944	.000	.000
30.	30.	.986	.891	.001	.000
30.	40.	.789	.833	.002	.000
60.	15.	1.142	.609	.000	.000
60.	20.	.993	.600	.000	.000
60.	30.	.759	.626	.001	.000
60.	40.	.611	.628	.001	.000
90.	15.	.738	.234	.000	.000
90.	20.	.667	.270	.000	.000
90.	30.	.524	.370	.000	.000
90.	40.	.431	.427	.001	.000

MODEL INPUTS

Parameter	Upwind Lanes	Downwind Lanes
a_1	-6.94	0.003
b_1	-0.078	1.54
c_1	6.78	0.765
a_2	-0.0006	-0.150
b_2	1.58	0.621
c_2	-1.82	-0.729
a_3	0.053	0.054
b_3	0.914	1.95
c_3	1.02	4.50
W	6.5	6.5
H	0.	0.
k	2	2
α	0	0
β	1	1

Case Two:

- Grade-level, six-lane divided freeway
- Smooth terrain to both sides of roadway
- Stable atmospheric conditions

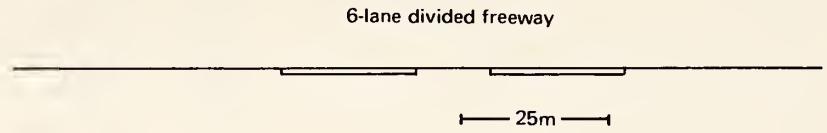

Atmospheric stability is the only change from the conditions appropriate to Case One. Again, ROADMAP simulated the up- and downwind traffic streams separately while the emission rates were assumed equal. The most notable changes from the neutral cases are the overall decrease in concentrations at the 1- and 3-m heights, and the enhanced vertical diffusion reflected in the concentration-levels at the 8-m level. Concentrations are highest for wind directions nearly parallel to the roadway and nearest the ground surface. Comparing Cases One and Two, peak concentrations are consistently about twice as high for neutral conditions than for stable atmospheric conditions. This result is contrary to most other experimental and theoretical work and should be interpreted with caution and reserve as it may reflect a local peculiarity of the test or the small size of the sample containing stable conditions.

		z(m) $\chi U/Q(m^{-1})$			
θ(deg)	x(m)	1	3	8	15
0.	15.	.896	.666	.133	.002
0.	20.	.753	.630	.171	.005
0.	30.	.561	.509	.218	.018
0.	40.	.445	.416	.227	.037
15.	15.	.869	.645	.129	.002
15.	20.	.729	.610	.165	.005
15.	30.	.544	.493	.211	.018
15.	40.	.432	.404	.220	.036
30.	15.	.788	.584	.116	.001
30.	20.	.661	.552	.149	.004
30.	30.	.494	.447	.190	.016
30.	40.	.393	.367	.200	.032
60.	15.	.505	.367	.070	.001
60.	20.	.420	.348	.091	.003
60.	30.	.317	.285	.119	.010
60.	40.	.257	.239	.127	.020
90.	15.	.255	.169	.026	.000
90.	20.	.204	.162	.036	.001
90.	30.	.159	.139	.052	.004
90.	40.	.134	.122	.060	.008

MODEL INPUTS

Parameter	Upwind Lanes	Downwind Lanes
a_1	0.295	0.739
b_1	0.775	0.534
c_1	0.236	0.993
a_2	-33.4	1.79
b_2	-1.74	0.038
c_2	-1.23	-1.90
a_3	0.053	0.054
b_3	0.914	1.95
c_3	1.02	4.50
W	6.5	6.5
k	2	2
α	0.	0.
β	1	1

Case Three:

- Grade-level, six-lane divided roadway
- Smooth terrain both sides of roadway
- Unstable atmospheric conditions

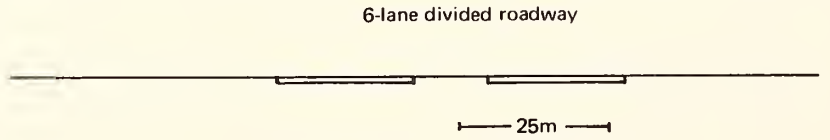

Again, only atmospheric stability has been changed from Case One. Emissions from the up- and downwind traffic streams have been assumed equal and their dispersion simulated separately using ROADMAP.

Concentrations are less than the neutral stability equivalents at virtually all locations; peak values are only about one-fourth the maximum concentrations accompanying neutral stability. Near-ground (i.e., 1-m) concentrations first increase with increasing distance from the roadway before peaking at x = 30 m; 3-m concentrations, on the other hand, increase monotonically to x = 40 m where they are also larger than the corresponding 1-m values. The height and distance dependence is nearly independent of the wind-roadway orientation.

		$\chi U/Q(m^{-1})$			
		z(m)			
θ(deg)	x(m)	1	3	8	15
0.	15.	.176	.157	.005	.000
0.	20.	.261	.140	.007	.000
0.	30.	.390	.229	.007	.000
0.	40.	.191	.358	.008	.000
15.	15.	.177	.158	.005	.000
15.	20.	.262	.142	.007	.000
15.	30.	.393	.234	.008	.000
15.	40.	.197	.366	.009	.000
30.	15.	.178	.160	.005	.000
30.	20.	.264	.148	.007	.000
30.	30.	.399	.245	.009	.000
30.	40.	.212	.382	.011	.000
60.	15.	.183	.166	.005	.000
60.	20.	.268	.164	.008	.000
60.	30.	.408	.269	.012	.000
60.	40.	.241	.414	.015	.000
90.	15.	.184	.169	.006	.000
90.	20.	.270	.171	.008	.000
90.	30.	.410	.278	.013	.000
90.	40.	.252	.426	.017	.000

MODEL INPUTS

Parameter	Upwind Lanes	Downwind Lanes
a_1	-217.	0.154
b_1	-1.92	0.242
c_1	2.60	1.15
a_2	-0.021	-0.360
b_2	0.992	0.830
c_2	-1.63	2.90
a_3	0.0061	1.37
b_3	2.37	0.096
c_3	4.99	-1.51
W	6.5	6.5
H	0.	0.
k	2	2
α	0	0
β	1	1

Case Four:
- Grade-level, four-lane divided roadway
- Rough terrain both sides
- Neutral atmospheric stability

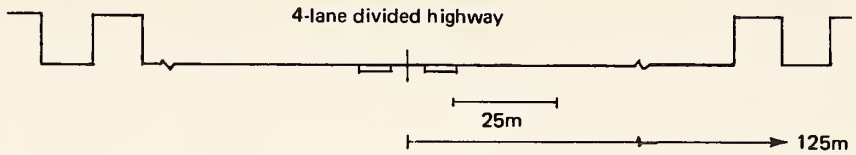

The roughness elements are sufficiently displaced from the roadway edges that there is no recirculation over the roadway. With a parallel wind the concentration decreases rapidly with distance at the lower heights, whereas the rate of decrease is very gradual for perpendicular winds. The increased mixing due to the rough surface causes concentrations to decrease gradually with height for the more-perpendicular wind angles.

		$\chi U/Q(m^{-1})$			
		z(m)			
θ(deg)	x(m)	1	3	8	15
0.	15.	.175	.130	.036	.023
0.	20.	.141	.113	.040	.023
0.	30.	.097	.085	.043	.024
0.	40.	.072	.066	.042	.025
15.	15.	.177	.131	.036	.023
15.	20.	.144	.115	.041	.023
15.	30.	.102	.089	.045	.024
15.	40.	.079	.072	.045	.025
30.	15.	.181	.134	.037	.023
30.	20.	.152	.121	.042	.023
30.	30.	.115	.100	.048	.024
30.	40.	.094	.085	.051	.026
60.	15.	.192	.142	.038	.023
60.	20.	.172	.136	.045	.023
60.	30.	.144	.123	.056	.024
60.	40.	.125	.112	.063	.027
90.	15.	.197	.145	.038	.023
90.	20.	.180	.142	.046	.023
90.	30.	.156	.133	.059	.025
90.	40.	.138	.123	.068	.028

MODEL INPUTS

a_1 = 0.15
b_1 = 0.88
c_1 = 2.15
a_2 = -18.4
b_2 = 0.0029
c_2 = 19.1
a_3 = .007
b_3 = 3.49
c_3 = 4.09
W = 11.4
H = 0.
k = 2.0
α = 0.023
β = 0.90

Case Five:
- "Porous street canyon"
- Four-lane divided roadway
- Rough terrain both sides of roadway
- Neutral atmospheric stability

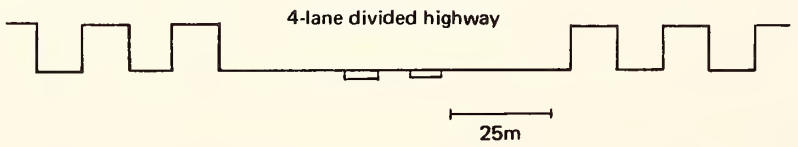

Because of the high aspect ratio (1:7) [compare to Case Four (1:21)], the street-canyon recirculation discussed in Section II is established. The model results do not reflect the high concentrations on the upwind edge of the roadway because the model was only developed for positive x-values (downwind of roadway center). Section IV, Subsection C(7) should be perused for a methodology to estimate upwind concentrations. Downwind of roadway center the concentrations are similar to Case Four, except they are somewhat smaller at the lower levels but greater at the upper levels. As before, the dependence on wind direction is minimal.

$\chi U/Q(m^{-1})$

θ(deg)	x(m)	z(m) = 1	3	8	15
0.	15.	.138	.134	.090	.065
0.	20.	.109	.107	.090	.069
0.	30.	.085	.085	.081	.072
0.	40.	.076	.076	.075	.071
15.	15.	.138	.135	.090	.065
15.	20.	.109	.108	.091	.069
15.	30.	.087	.086	.082	.072
15.	40.	.078	.078	.076	.072
30.	15.	.139	.136	.091	.065
30.	20.	.112	.111	.092	.069
30.	30.	.090	.090	.085	.074
30.	40.	.082	.082	.080	.074
60.	15.	.142	.138	.092	.065
60.	20.	.118	.117	.096	.069
60.	30.	.098	.098	.091	.077
60.	40.	.089	.089	.086	.078
90.	15.	.144	.140	.092	.065
90.	20.	.121	.119	.098	.070
90.	30.	.101	.101	.094	.078
90.	40.	.093	.092	.089	.080

MODEL INPUTS

$a_1 = 1.07$
$b_1 = 0.73$
$c_1 = -3.25$
$a_2 = 36.8$
$b_2 = -17.5$
$c_2 = -1.49$
$a_3 = -0.81$
$b_3 = 2.01$
$c_3 = 0.20$
$W = 11.4$
$H = 0.$
$k = 2.0$
$\alpha = 0.064$
$\beta = 0.45$

Case Six:

- Rough terrain downwind, smooth terrain upwind
- Four-lane divided roadway
- Neutral atmospheric stability

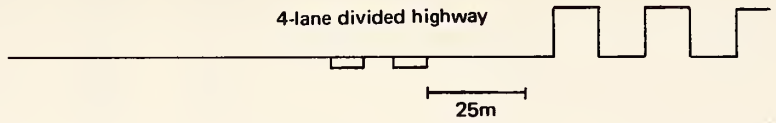

Many of the features of the concentration pattern are similar to those of some of the preceding cases: The dependence on wind direction is again very small, particularly at the lower locations, for all horizontal distances. The concentrations at the 1- and 3-m levels are nearly uniform, with significant decreases observed at the 8-m level at the 15-, 20-, and 30-m separations. One unusual feature is the consistent concentration increase with height between 1 and 3m for all separations except 15m. This feature suggests a convergence in the flow around the 3-m level that likely is caused by the uplifing of the near-surface streamlines as a result of the aerodynamic influence of the downwind roughness field. That this pattern was not observed in Case Five can be attributed to the chaotic flow created near the ground surface by the upwind roughness field that enhances the vertical wind fluctuations at the expense of the horizontal flow.

$\chi U/Q(m^{-1})$

		z(m)			
θ(deg)	x(m)	1	3	8	15
0.	15.	.385	.380	.090	.088
0.	20.	.294	.328	.102	.088
0.	30.	.192	.229	.138	.088
0.	40.	.144	.168	.150	.091
15.	15.	.384	.378	.090	.088
15.	20.	.295	.329	.102	.088
15.	30.	.195	.233	.139	.088
15.	40.	.148	.174	.154	.091
30.	15.	.381	.375	.090	.088
30.	20.	.297	.332	.102	.088
30.	30.	.203	.244	.143	.088
30.	40.	.157	.187	.165	.091
60.	15.	.372	.367	.090	.088
60.	20.	.302	.338	.102	.088
60.	30.	.222	.269	.152	.088
60.	40.	.178	.217	.188	.092
90.	15.	.367	.362	.090	.088
90.	20.	.305	.342	.103	.088
90.	30.	.230	.281	.156	.088
90.	40.	.187	.229	.197	.093

MODEL INPUTS

$a_1 = 0.096$
$b_1 = 0.96$
$c_1 = 0.64$
$a_2 = -0.017$
$b_2 = 1.46$
$c_2 = -1.10$
$a_3 = 0.0060$
$b_3 = 3.84$
$c_3 = 3.94$
$W = 11.4$
$H = 0.$
$k = 2.0$
$\alpha = 0.088$
$\beta = 0.76$

Case Seven:
- Smooth terrain downwind, rough terrain upwind
- Four-lane divided roadway
- Neutral atmospheric stability.

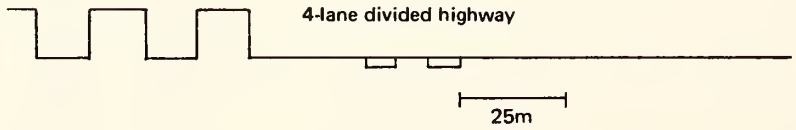

Reversing the location of the large-roughness field to the upwind side of the roadway (vis a vis Case Six) results in the reduction of peak concentrations by nearly a factor of three and the disappearance of a height-increase of concentrations (although 1- and 3-m values are consistently within a few percent). Near-surface values again demonstrate no wind-directional dependence at the close-in locations while the values at 40-m separation are about 25% larger for perpendicular winds than they are for parallel winds.

		$\chi U/Q(m^{-1})$			
		z(m)			
θ(deg)	x(m)	1	3	8	15
0.	15.	.132	.124	.082	.066
0.	20.	.110	.107	.081	.067
0.	30.	.089	.088	.078	.068
0.	40.	.079	.079	.075	.069
15.	15.	.132	.124	.082	.066
15.	20.	.111	.107	.082	.067
15.	30.	.090	.089	.079	.068
15.	40.	.081	.081	.077	.069
30.	15.	.131	.123	.081	.066
30.	20.	.113	.109	.082	.067
30.	30.	.094	.093	.081	.068
30.	40.	.086	.085	.080	.070
60.	15.	.129	.121	.081	.066
60.	20.	.117	.113	.084	.067
60.	30.	.103	.101	.086	.069
60.	40.	.094	.094	.086	.072
90.	15.	.127	.120	.080	.066
90.	20.	.119	.115	.084	.067
90.	30.	.107	.105	.088	.070
90.	40.	.098	.097	.088	.073

MODEL INPUTS

$a_1 = 0.028$
$b_1 = 1.41$
$c_1 = 2.89$
$a_2 = -8.09$
$b_2 = 0.026$
$c_2 = 7.77$
$a_3 = 0.094$
$b_3 = 2.78$
$c_3 = 1.50$
$W = 11.4$
$H = 0.$
$k = 2.0$
$\alpha = 0.066$
$\beta = 0.32$

Case Eight:
- Vertical-walled cut section
- Four-lane divided roadway
- Neutral atmospheric stability

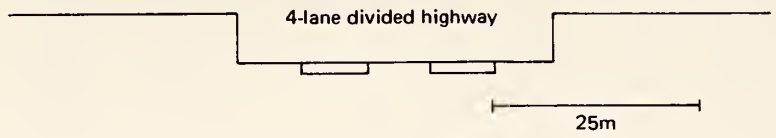

The ROADMAP methodology does not estimate concentrations on the upwind half of the cut section, even though the flow recirculation associated with this case results in significant upwind concentrations. Subsection C(7) later in this section presents an alternative method for estimating upwind effects. Near-surface concentrations (z = 1m) are consistently larger than the "porous" counterpart configuration (Case Five) by up to 30%, while values at the 3-m level are nearly twice as large for roadway-perpendicular winds. Concentrations at 3m are significantly greater than at 1m (up to 50%), while 8-m values are slightly larger than the 1-m concentrations. A strong directional dependence is present at all levels and distances: cross-roadway wind directions yield consistently higher concentrations than roadway-parallel winds.

$\chi U/Q(m^{-1})$

		z(m)			
θ(deg)	x(m)	1	3	8	15
0.	15.	.138	.196	.136	.071
0.	20.	.130	.168	.146	.072
0.	30.			.140	.090
0.	40.			.121	.106
15.	15.	.141	.203	.140	.071
15.	20.	.133	.174	.151	.073
15.	30.			.143	.091
15.	40.			.123	.107
30.	15.	.150	.220	.149	.071
30.	20.	.142	.189	.163	.073
30.	30.			.153	.094
30.	40.			.128	.110
60.	15.	.171	.259	.170	.071
60.	20.	.163	.222	.189	.073
60.	30.			.174	.100
60.	40.			.139	.118
90.	15.	.180	.276	.179	.071
90.	20.	.171	.237	.200	.073
90.	30.			.183	.102
90.	40.			.144	.121

MODEL INPUTS

$a_1 = 0.0006$
$b_1 = 2.53$
$c_1 = 2.24$
$a_2 = -0.016$
$b_2 = 1.47$
$c_2 = -3.65$
$a_3 = 0.010$
$b_3 = 3.19$
$c_3 = 4.33$
$W = 11.4$
$H = 0.$
$k = 2.0$
$\alpha = 0.071$
$\beta = 0.83$

Case Nine:
- Sloping-wall cut section
- Four-lane divided roadway
- Neutral atmospheric stability

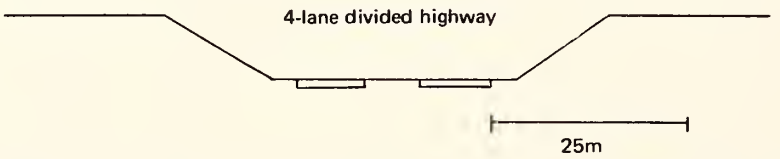

The sloping-wall cut section is seven metres narrower at road level than its vertical-wall counterpart and 18m wider at grade level; the smooth walls slant at an angle of 30° to the horizontal. At the 1- and 3-m levels, peak concentrations are equal to those in the vertical cut except that there is a significant directional dependence: highest concentrations occur with roadway-parallel winds. For all wind angles and horizontal distances (within the cut), peak concentrations occur at the 3-m level and then decrease markedly at the 8-m level.

$\chi U/Q(m^{-1})$

		z(m)			
θ(deg)	x(m)	1	3	8	15
0.	15.	.214	.279	.111	.057
0.	20.		.223	.126	.057
0.	30.			.138	.067
0.	40.			.122	.091
15.	15.	.211	.275	.110	.057
15.	20.		.221	.125	.057
15.	30.			.137	.067
15.	40.			.121	.091
30.	15.	.204	.265	.108	.057
30.	20.		.216	.123	.057
30.	30.			.135	.066
30.	40.			.119	.089
60.	15.	.182	.234	.100	.057
60.	20.		.202	.117	.057
60.	30.			.130	.066
60.	40.			.112	.085
90.	15.	.170	.216	.096	.057
90.	20.		.194	.114	.057
90.	30.			.128	.066
90.	40.			.107	.083

MODEL INPUTS

$a_1 = 0.00004$
$b_1 = 3.22$
$c_1 = 2.53$
$a_2 = -0.73$
$b_2 = 0.50$
$c_2 = -0.52$
$a_3 = 0.0036$
$b_3 = 3.37$
$c_3 = 3.97$
$W = 11.4$
$H = 0.$
$k = 2.0$
$\alpha = 0.057$
$\beta = 0.56$

Case Ten:

- Elevated, Fill Section
- Four-lane divided roadway
- Neutral atmospheric stability

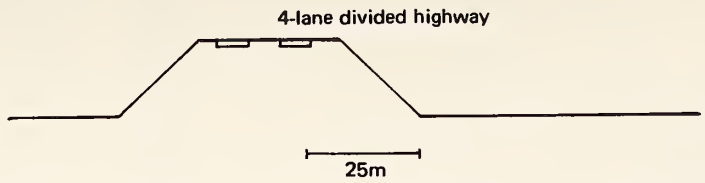

A large number of near-roadway receptors are not depicted in the tabulation as they lie within the fill. At the 40-m separation distance, concentrations are consistently greatest at the uppermost level (15m) for all wind directions. Peak values occur under perpendicular wind conditions and decrease systematically as the parallel component increases. Compared to the cut sections and some of the rough-ground cases, concentrations are relatively low for the receptor locations used. Other, more elevated or more distant receptors would, however, have values greater than those given in the tabulation below.

		$\chi U/Q(m^{-1})$			
		z(m)			
θ(deg)	x(m)	1	3	8	15
0.	15.				
0.	20.				.074
0.	30.			.047	.055
0.	40.	.040	.041	.045	.046
15.	15.				
15.	20.				.095
15.	30.			.059	.076
15.	40.	.046	.050	.061	.066
30.	15.				
30.	20.				.131
30.	30.			.075	.107
30.	40.	.054	.061	.081	.091
60.	15.				
60.	20.				.191
60.	30.			.102	.156
60.	40.	.067	.079	.113	.129
90.	15.				
90.	20.				.213
90.	30.			.112	.174
90.	40.	.072	.085	.125	.143

MODEL INPUTS

$a_1 = 0.39$
$b_1 = 0.81$
$c_1 = 0.19$
$a_2 = 0.13$
$b_2 = 1.07$
$c_2 = -1.78$
$a_3 = 0.26$
$b_3 = 4.29$
$c_3 = 2.64$
$W = 11.4$
$H = 18.0$
$k = 1.0$
$\alpha = 0.037$
$\beta = 1.08$

Case Eleven:
- Elevated, viaduct section
- Four-lane divided roadway
- Neutral atmospheric stability

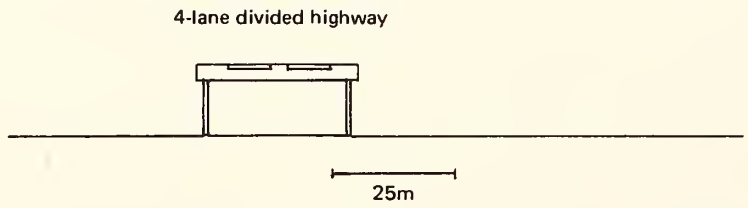

The values of normalized concentration are quite small at and below the 8-m level for all separations tabulated. At the 15-m level (close to roadway height), concentrations are comparable with peak-values for some of the other cases. With little aerodynamic drag from the open viaduct section there is no downwash (as occurs behind the fill) and subsequently the centerline of the roadway plume is maintained at the height of the roadway. Consequently, ground-level concentrations are lower than in the case of the fill section although plume-centerline concentrations would be expected to be larger (due to the reduced turbulence compared with the fill case). As with many other cases examined, peak concentrations are found to be associated with winds perpendicular to the roadway.

$\chi U/Q(m^{-1})$

		z(m)			
θ(deg)	x(m)	1	3	8	15
0.	15.	.028	.028	.028	.035
0.	20.	.028	.028	.028	.033
0.	30.	.028	.028	.028	.031
0.	40.	.029	.029	.029	.030
15.	15.	.028	.028	.029	.081
15.	20.	.028	.028	.030	.073
15.	30.	.028	.028	.031	.056
15.	40.	.035	.034	.035	.046
30.	15.	.028	.028	.031	.131
30.	20.	.028	.028	.031	.114
30.	30.	.029	.029	.035	.082
30.	40.	.042	.039	.041	.062
60.	15.	.028	.028	.033	.205
60.	20.	.028	.028	.034	.177
60.	30.	.029	.029	.039	.122
60.	40.	.052	.047	.051	.087
90.	15.	.028	.028	.033	.233
90.	20.	.028	.028	.034	.200
90.	30.	.029	.029	.041	.136
90.	40.	.055	.050	.055	.096

MODEL INPUTS

$a_1 = 0.00005$
$b_1 = 3.14$
$c_1 = 3.07$
$a_2 = -0.0018$
$b_2 = 2.20$
$c_2 = 1.44$
$a_3 = 0.040$
$b_3 = 3.78$
$c_3 = 4.93$
$W = 11.4$
$H = 18.0$
$k = 1.0$
$\alpha = 0.028$
$\beta = 1.07$

C. Special Considerations

1. Variation in Median Width for Grade-Level Roads

The ROADMAP coefficients given in Table 10 are based on atmospheric and wind tunnel experiments where the median widths were 9.1 m and 7.6 m, respectively. As these already represent significantly wide median strips, it is suggested for strips >12 m wide that the road be considered as two roads (one in either direction). Concentration computations would then be made separately for each traffic stream and the two values added. As an example consider a 15-m median separating two 12-m wide traffic streams. A 1.5-m high receptor located 10 m downwind of the downwind edge of the downwind traffic stream (x = 16 m) would be located 43 m downwind of the center of the upwind stream. Thus if there was neutral stability and a perpendicular wind, ROADMAP would yield normalized concentrations (χ U/Q) of 0.94 m^{-1} from the downwind traffic and 0.36 m^{-1} from the upwind traffic, and the total would be 1.31 m^{-1}. However, if the road had not been considered as two distinct parts then x = 29.5 m and the calculated normalized concentration would have been 0.89 m^{-1}.*

Assume further that the wind speed is 1.5 m s^{-1} and that both traffic streams have CO emissions of 0.015 g m^{-1} s^{-1}. It then follows that the emission flux for the total roadway is 0.030 g m^{-1} s^{-1}. The downwind traffic stream thus contributes a CO concentration of 9.4 mg m^{-3} to the air at the receptor, while the upwind lanes add another 3.6 mg m^{-3} to give a total concentration of 13.0 mg m^{-3} using the "two-stream" approach. On the other hand, the "total-roadway" approach yields a CO concentration of only 8.9 mg m^{-3}. This smaller value is due to the non-linear relationship between concentration and distance.

---

*It should be noted that since both of the above cases deal with the same average emission flux, the total flux for the latter "compound" case is twice as large as either of the individual traffic streams and hence the normalized concentration has been doubled for the compound case. In practice, one would normally deal with absolute rather than normalized concentrations, and the intercomparison would be more straightforward as actual values of wind speed and emissions would be used to calculate the actual concentration directly.

2. Depressed Sections Resembling the ROADWAY Prototypes

The width of the median strip affects depressed section concentrations in two ways: (1) as the median becomes narrower, the height-to-width aspect ratio of the cut becomes greater and thus may affect the overall wind circulation in the cut; and (2) as with grade-level roads, very wide medians can affect the basic assumptions of emissions uniformity that are implicit in the model. Unlike the grade-level case, the road cannot be treated with the model as two traffic streams in that the diffusion coefficients would no longer be representative or meaningful. On the other hand, it would not be economical to build cut sections with wide medians. Therefore, the following guidelines are suggested for estimating concentrations in the downwind half of cut sections and further downwind: Cut sections having widths or depths within a factor of two of the scale model (i.e., width $\leq$80 m and height 6 to 12 m) can have the concentration field estimated by introducing scale and shape factors into the ROADMAP calculations in the following manner. First, where horizontal distance (x) is used in ROADMAP, substitute instead the equivalent distance (or shape factor) ℓ, where

$$\ell \equiv x\left(\frac{x^*}{\ell^*}\right) \tag{24}$$

and x is the actual horizontal distance from centerline of the cut; x* is the x-distance in the prototype from centerline to the vertical wall (i.e., 19 m) or to the mid-point of the sloped cut (i.e., 21 m); and ℓ^* is the corresponding distance (to x*) in the cut being considered. In the same way, an equivalent height h is introduced,

$$h = z\left(\frac{z^*}{h^*}\right) \tag{25}$$

where z is the actual height above the base of the cut, z* is the depth of the prototype cut (i.e., 6.1 m), and h* is the depth of the cut under study. Then, use ℓ to estimate σ_z, z', and f and compute an equivalent (χU/Q) using these parameters and h (in place of z) in ROADMAP. Next, these equivalent values must be scaled, using the relationship

$$\left(\frac{\chi U}{Q}\right)_{scaled} = \left(\frac{\chi U}{Q}\right)_{equivalent} \cdot \left(\frac{x^*}{\ell^*}\right) \cdot \left(\frac{z^*}{h^*}\right) \quad . \qquad (26)$$

3. Broad and Shallow Cut-Sections

In the case of very broad cut-sections with low height-to-width aspect ratios (i.e., less than 1:20), it would most likely be adequate to simply consider the configuration equivalent to a grade-level roadway, with one exception. At all receptor locations, the height of the receptor (z) should be considered as the height above the immediate (or local), underlying terrain. The roughness may be either smooth or rough depending on the environmental conditions, the depth of the cut, and the aspect ratio. If the configuration has an aspect ratio between 1:10 and 1:20 and the user cannot definitively classify it as a broad cut, then the average of the values given in these two procedures (i.e., Subsections 2 and 3) may be used. Note, however, that when the cut is less than 2 m deep it will normally be sufficient to consider the section as an equivalent grade-level configuration (regardless of the aspect ratio). This follows as a result of the vertical mixing that is induced by the thermal and mechanical effects of the traffic; the grade-level, atmospheric experiment reported in Volume I indicated that this enhanced mixing extends to a height of at least 4 m.

4. Variations in Height and Width of Elevated Sections

ROADWAY explicitly considers the height (H) of the roadway above grade-level for both viaduct and fill sections. Variations in the width of actual study cases from the ROADMAP prototypes should not be particularly troublesome for fill sections in that these are usually built with narrow medians and no separation of traffic streams. Viaduct sections, on the other hand, will likely fall into one of two categories: narrow or no median divider and separated traffic streams (in effect, two viaducts). The former case, which does not represent a problem, requires a straightforward application of ROADMAP. The latter can also be treated with the assessment methodology provided that viaducts with "significant" separation are treated as separate sections (which in

reality they are). It will not usually be necessary to consider secondary effects on the dispersion caused by the presence of the second adjacent viaduct. The open construction of the viaducts tends to minimize any significant impacts.

In using the assessment methodology, it is important that the height of the viaduct or fill section be determined properly. The methodology uses the height of the roadway above the aerodynamic displacement height (D) of the surrounding terrain. D is the height above ground level at which a period-average horizontal wind flow is first established and is computed as the sum of the average physical height of the roughness elements (e.g., houses) and the aerodynamic roughness (z_o) of the surface. As an example, a very smooth surface would have a negligible value of D compared to the height of a 7-m high fill section, for example. Thus, H = 7 m and the ground surface is located at z = 0. If, however, the same viaduct were located in a dense surburban development with an average house-height of 4 m, then the concentration pattern would be different. The corresponding value of z_o from Eq. (4) would be about 1 m, and thus D = 5 m, H = 2 m, and the ground surface has a value in ROADMAP of -5 m. For a perpendicular wind, ($\chi U/Q$) has ground-level values at x = 50 m of 0.16 m^{-1} for the smooth-terrain case and 0.17 m^{-1} for the rough-terrain case. Note that nothing has been done to the dispersion coefficients; this reflects the implicit assumption that the dispersion near the roadway is dominated by the obstruction of the elevated section and not by the ground roughness. This assumption is certainly more appropriate to the fill section than to the viaduct section. When the user suspects that rough terrain near a viaduct will have a significant effect on the microscale dispersion pattern, it is suggested that the σ_z-term be increased as a function of the increase z_o.

5. Stacked Viaducts

Viaducts that are stacked one above the other are accommodated simply by applying the assessment methodology twice--once for each level. The only difference would be in the values of H. The resulting concentration values would then be added. The guidance given earlier

in Subsection 4 should be consulted regarding the determination of H and the possible modification of σ_z.

6. Curved Roadways

The objective assessment procedure given by ROADMAP has no provision for treating curved roadways. However, the gradual curves encountered on the interstate and most major intrastate roadway systems can be approximated by ROADMAP by simply considering the roadway as a straight line oriented perpendicular to the wind streamline that passes through the receptor of interest. Figure 37 illustrates an example using a roadway with a 45° curve over 300 m (1000 ft). When the road is concave with respect to the receptor there will be a slight underestimate in the predicted concentration (about 10% for this example) and a slight overestimate with a convex orientation.

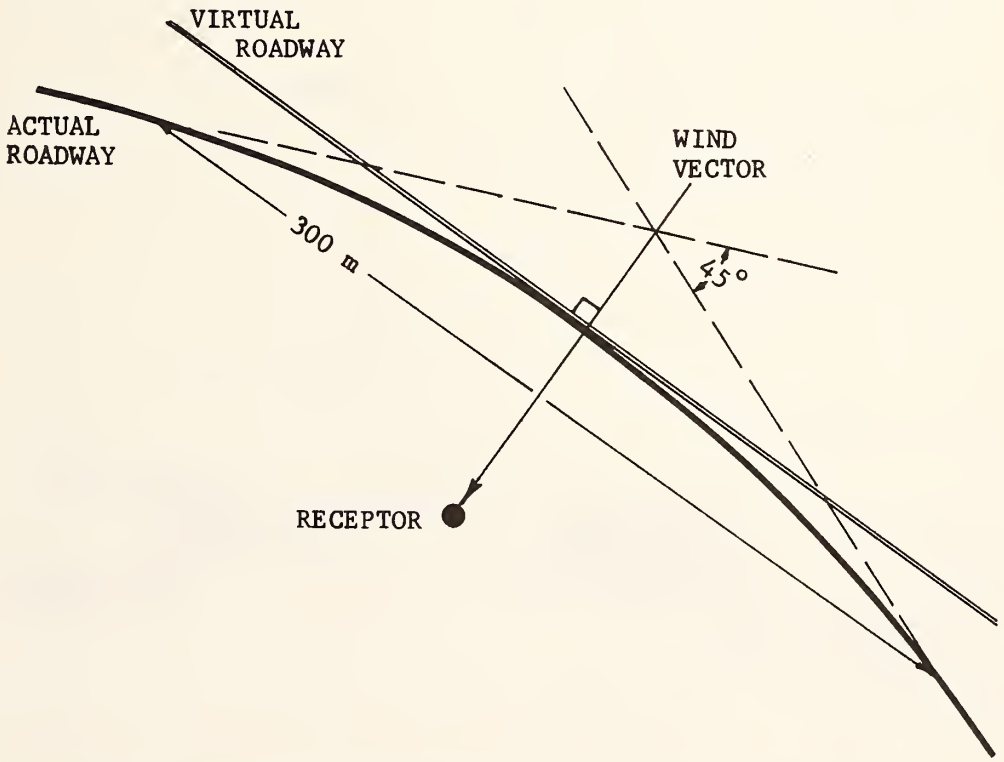

FIGURE 37 SCHEMATIC ILLUSTRATION OF THE USE OF A VIRTUAL ROADWAY IN APPLYING ROADMAP TO A GENTLE CURVE

Should the curvature be significantly greater, a correction may be necessary. This can be done by first computing the concentration as indicated above. Next, apply a numerical line source model (such as HIWAY; see Zimmerman and Thompson, 1973) to compute the ratio of the relative concentration for the curved configuration to the straight configuration. Apply this ratio as a corrective factor to the ROADMAP estimate.

7. Grade Separations

a. Overpass and Grade-Level Crossing

Complex interchanges (such as multi-level crossings) can be evaluated with the assessment methodology by summing the pollutant concentrations from each roadway. While this approach will undoubtedly not describe all the local peculiarities of each configuration, it should provide a representative picture of the significant features.

As an example, consider the two-level interchange illustrated in Figure 38. The overpass, on a fill section, is evaluated as though it were elevated along its entire length. The surrounding terrain is smooth, the atmospheric stability neutral, and the wind is parallel to

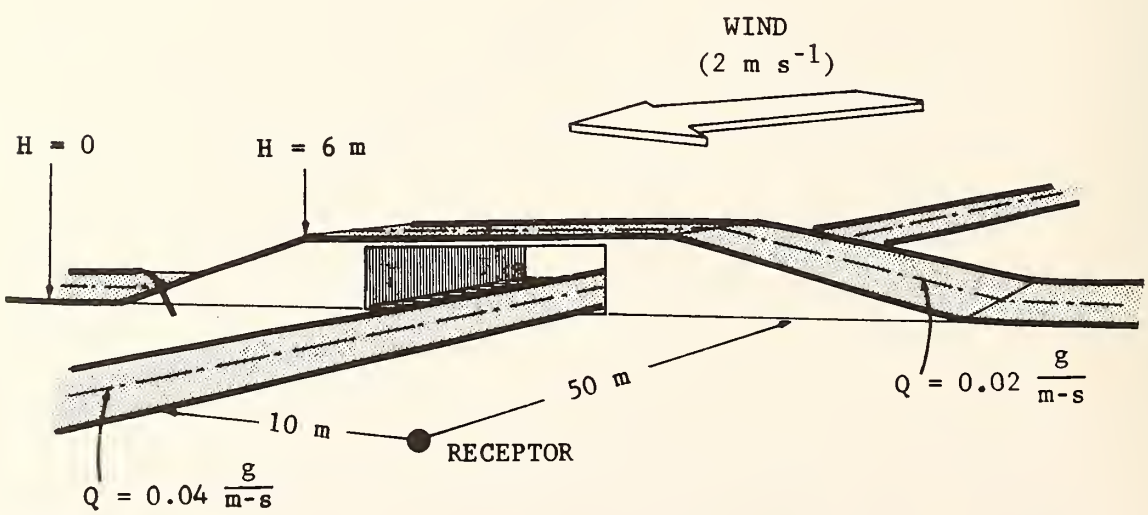

FIGURE 38 SCHEMATIC ILLUSTRATION OF RECEPTOR NEAR INTERCHANGE OF GRADE-LEVEL ROADWAY AND ELEVATED CROSSING ON FILL

the grade-level road at a speed of 2 m s^{-1}. Computing the CO concentration at the surface receptor due to emissions from the elevated section, we estimate a value of 1.6 mg m^{-3}. To this we add the contribution from the grade-level roadway which is estimated to be 6.3 mg m^{-3}, yielding a total concentration at the receptor of 7.9 mg m^{-3}.

Although the surrounding terrain is smooth, it may be argued that the aerodynamic effect of the upwind overpass is sufficient to produce a dispersion pattern from the grade-level roadway that more nearly resembles a rough-terrain situation. Accepting this hypothesis results in a ROADMAP estimate of the CO contribution from the grade-level roadway of only 2.1 mg m^{-3}. Thus the total CO concentration due to both roads would be 3.7 mg m^{-3}, or only about 50% of the previous estimate. In practice, both estimates are useful as they help to identify the bounds that the actual concentration would have. The total ambient concentration would (as in all cases) require the ambient or background concentration to be added to the value of the local contribution that has just been estimated.

b. Underpass and Grade-Level Crossing

Another type of multi-level interchange is the grade-level roadway that is intersected by a depressed roadway in the sloped-wall cut section. Figure 39 illustrates the configuration. The following conditions are again assumed: neutral stability, smooth terrain, windspeed of 2 m s^{-1}, and wind direction parallel to the grade-level road.

ROADMAP is used as in the preceding case. As before, the CO contribution from the grade-level roadway is 6.3 mg m^{-3}. There is no strong argument to be made here for considering the surface to be aerodynamically rough, for while there is some effect from the cut, it is not apt to be particularly significant. From the cut section, the receptor receives a CO contribution of 1.0 mg m^{-3}. The total local CO concentration at the receptor is therefore 7.3 mg m^{-3}. This value is only 0.6 mg m^{-3} less than the larger estimate made for the comparable overpass situation discussed above, indicating that this particular receptor is dominated by the emissions from the adjacent grade-level roadway. Also, the

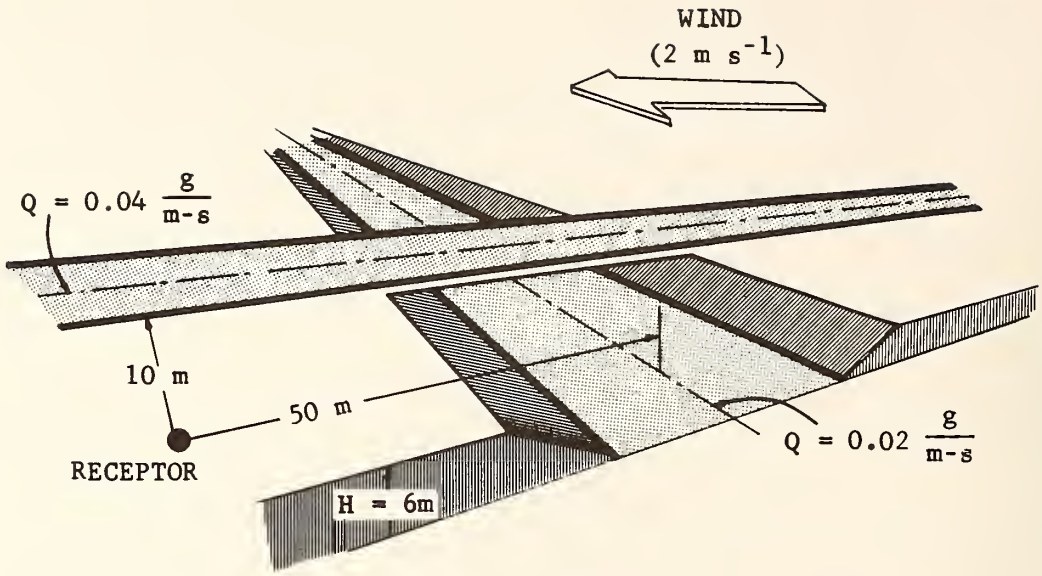

FIGURE 39 SCHEMATIC ILLUSTRATION OF RECEPTOR NEAR INTERCHANGE OF GRADE-LEVEL ROADWAY INTERSECTED BY A DEPRESSED ROADWAY IN A SLOPED-WALL CUT SECTION

overpass may offer some environmental advantage in the near vicinity where it increases the vertical dispersion (this influence region is likely to extend downwind for a distance on the order of 10 times the height of the fill section). When the downwind turbulence effect of the overpass is considered, the concentration at the receptor is twice as large for the underpass situation. Stating the comparison a little differently, we see that the underpass-crossing has a slightly smaller air pollution impact if one ignores any consideration of the downwind turbulence effect of the fill section. When one considers this effect of the overpass, then the underpass situation has a significantly greater impact at the receptor evaluated. As always, the total air pollution picture must be assessed by evaluating the concentration at all sensitive receptor locations near the project site.

8. Artificial Dispersion Control

a. Turbulence Enhancement

It has occasionally been suggested that artificial methods be employed to enhance the turbulent mixing of vehicular emissions on and near roadways. In effect this is already the case, for the initial mixing is presently increased significantly by: (1) the mechanical mixing from vehicular movement, (2) mechanical mixing due to the shelterbelt, (3) waste heat emissions from vehicles, and (4) differential sensible heat transfer to the atmosphere between the roadway surface and the adjacent terrain. Further increases in initial mixing are not feasible through processes (1) and (3) above, although (2) and (4) may at times be viable methods by which dispersion can be enhanced and near-roadway concentrations reduced.

Impact of Roadway Surface Construction--The thermal characteristics of the roadway pavement help regulate the diurnal cycle of atmospheric stability over the roadway. In particular, it is the so-called thermal admittance (μ, cal cm^{-2} $s^{-1/2}$ $°K^{-1}$) that best describes the way in which the surface heats up by day and cools off at night. The thermal admittance is a convenient way to describe the joint influence of the thermal conductivity (λ, cal cm^{-1} s^{-1} $°K^{-1}$) and the volumetric heat capacity (C, cal $°K^{-1}$ cm^{-3}), where

$$\mu \equiv \sqrt{\lambda C} \quad .$$

The following tabulation lists values of λ, C, and μ for several substances. Also listed are typical values of the albedo--the fraction of the incoming solar energy reflected at the surface. To illustrate the effect that the roadway surface type can have on local surface temperatures (and hence stability and mixing), we have estimated the diurnal cycle of surface temperature for sandy clay, dry sand, concrete, and asphalt according to Lettau's climatonomy theory as described by

Substance	Density ($g\ cm^{-3}$)	Heat Capacity C ($cal\ cm^{-3}K^{-1}$)	Thermal Conductivity λ ($mcal\ s^{-1}K^{-1}cm^{-1}$)	Thermal Admittance μ ($mcal\ K^{-1}cm^{-2}s^{-1/2}$)	Albedo
Quartz sand, dry	1.65	0.31	0.63	14	0.1-0.2
Quartz sand, 8% moisture	1.58	0.39	2.3	30	0.1-0.15
Sandy clay, 15% moisture	1.78	0.58	2.2	36	0.1-0.15
Concrete	2.30	0.54	2.9	40	0.20
Asphalt	2.12	0.50	1.6	28	0.05

Dabberdt and Davis (1977). These estimates indicate the following diurnal temperature changes (ΔT, shown in parentheses) at the surface of each of these media under clear skies, moderate winds, and smooth surface roughness:

	Concrete (7.3°C)	Asphalt (9.4°C)
Sandy clay (7.3°C)	0.0°C	2.1°C
Dry quartz sand (9.6°C)	-2.3°C	-0.2°C

These diurnal temperature amplitudes are given in a matrix format where the values at the four matrix intercepts represent the differences between the roadway and environmental values of ΔT. Thus, it follows that the asphalt roadway has a greater diurnal amplitude (by 2.1°C) than does the sandy clay surface. Assuming both surfaces to have the same average diurnal temperature, it follows that the roadway surface is warmer by day than the overlying air that has first passed over the sandy clay; this unstable configuration may thus aid in enhancing near-roadway dispersion. On the other hand, nighttime and early-morning conditions are reversed as the asphalt cools off more quickly, and a corresponding decrease in mixing is to be expected.

As a word of caution, it should be stressed that the absolute magnitude of this effect of surface structure has not yet been analyzed by researchers for in situ conditions. This brief, qualitative discussion has been given only as an introduction to the subject. Application of these concepts on the highway-project level should be substantiated with more detailed theoretical analyses and experimental observations.

Impact of Turbulence Enhancement with Shelterbelts--Earlier in this report (Section I-C-4,6) the fundamentals of the shelterbelt effect were discussed in relation to aerodynamic effects that can occur as the ambient wind flow encounters a "wall" of vehicles on a highway. Historically, shelterbelts have been considered and applied for agricultural and snow-control purposes (see, for example, the comprehensive summary prepared by the World Meteorological Organization, 1964). The apparent similarities between the impacts of highway traffic and traditional windbreaks/shelterbelts raise the possibility that the initial dispersion of highway emissions can intentionally be enhanced by the use of fixed shelterbelts constructed along the axis of highway medians.* As with the scenario presented above on the potential impacts of roadway-surface construction, we will present here some tentative examples of the enhanced mixing that may be achieved by a "medianbelt" (i.e., a median shelterbelt) and the resulting impact on near-roadway air quality.

Using the framework of ROADMAP, we may postulate two effects of a medianbelt: one on the vertical dispersion term (σ_z) and the other on the height-offset term (z'). These effects we propose to quantify by assuming:

$$\sigma_z = (\sigma_z)_{original} + (p - \sigma_{z\text{-}orig})^{1/2} \quad ; \; p \geq \sigma_{z\text{-}orig} \tag{27}$$

$$z' = (z')_{original} + (p + z'_{orig})^{1/2} \quad ; \; p \geq z'_{orig} \tag{28}$$

---

*Note that sound barriers are themselves a double-row shelterbelt. However, from an air pollution perspective, the single-line shelterbelt may be equally or more effective while offering secondary benefits of both reduced costs and aesthetic impacts.

where p is the actual height of the medianbelt. Figure 40 illustrates the values of (χU/Q) that are estimated at x = 20 m for the values of σ_{z-orig} and z'_{orig} from ROADMAP for a perpendicular wind, neutral conditions and an at-grade roadway for each of three heights of the medianbelt: p = 0 m (i.e., no medianbelt); p = 2 m; p = 3 m. Several noteworthy observations are given by this example. First, the surface concentration is relatively insensitive to the height of the medianbelt; (χU/Q) ranges from 0.20 m^{-1} with no medianbelt to 0.17 m^{-1} for p = 3 m. However, the peak concentration is significantly reduced by the medianbelt, decreasing from 0.88 m^{-1} with p ≤ 0.9 m to 0.41 m^{-1} with p = 2.0 m and 0.35 m^{-1} with p = 3.0 m. At the same time, the height and width of the peak are also affected.

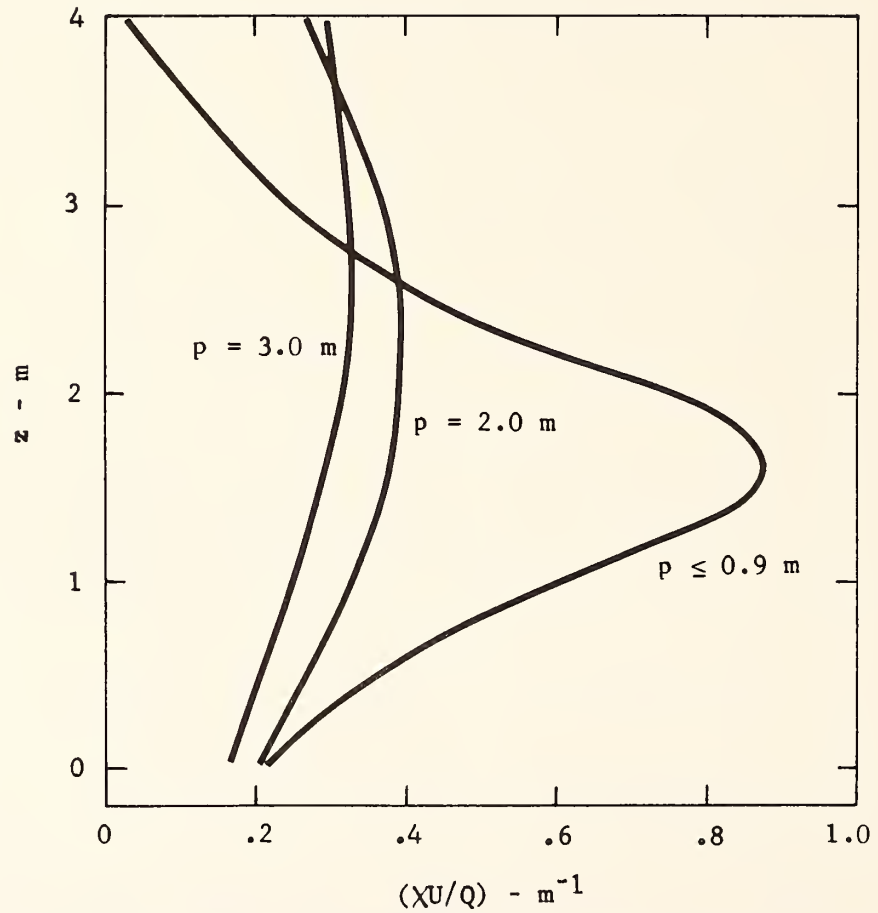

FIGURE 40 NORMALIZED CONCENTRATION PROFILES FOR VARIOUS MEDIAN BELT HEIGHTS (p). AT-GRADE ROADWAY, NEUTRAL STABILITY, X = 20 m

As with the preceding discussion on thermal effects, it is recommended that the application of these concepts be supported by empirical measurements before they are applied to specific project-level analyses.

Dispersion Modification by Active Means--The medianbelt concept discussed above may be thought of as a passive method of altering the turbulence (and hence dispersion) characteristics of the air flow near the roadway--passive because the total energy of the fluid has not been changed; rather its form has been changed in that some of the energy of the mean (or steady) flow has been converted to turbulent energy which in turn disperses the emissions more quickly and to greater heights. As a result, peak concentrations are reduced (while minima are increased). Active methods have been employed in fluid dynamics to alter or modify certain flow phenomena. The methods used have included suction, flow discharge (or pressurization), and movement of the surface (e.g., rotation of a circular cylinder); a good summary of these techniques has been prepared by Goldstein (1938). The application of these active methods has been restricted to relatively "simple" surfaces, such as airfoils, flat plates, and circular cylinders. The flow around the surfaces and configurations characteristic of highways is infinitely more complex and inhomogeneous. Moreover, the scale is significantly larger so that the corresponding kinetic energy required to modify the flow is similarly much greater. Also, an adequate description of the flow structure is needed to make consideration of active modification plausible. In summary, active control of the dispersive characteristics of the atmosphere on and near roadways is neither feasible nor practical, and should not be considered as a viable alternative for attaining air quality goals.

Another aspect of active modification of the near-roadway environment, the use of ventilation to directly reduce pollutant concentrations, is considered below.

b. Ventilation Considerations

There may be a few occasions when artificial ventilation is a practical solution for minimizing locally large pollution concentrations. A few examples are apparent; for example, tunnels and street canyons. Tunnel ventilation has been used for some time but is, however, outside the scope of this report. On the other hand, the street-canyon configuration may on occasion be a suitable candidate for ventilation for two reasons: (1) ambient pollution concentrations are often quite large, and (2) they are also quite localized and may thus be more easily controlled by ventilation.

Thorough analysis of the effectiveness of ventilation is quite complicated in the ambient atmosphere where steep concentration gradients exist and where natural ventilation by both the ambient wind and vehicle effects can be difficult to quantify. Accordingly, this discussion is limited to a general treatment of the scope of the problem and its necessary considerations.

In the absence of artificial ventilation, the profile of normalized concentration for a grade-level roadway in smooth, uniform terrain with neutral atmospheric stability is shown in Figure 40. Assuming a CO emission rate of 0.04 g $m^{-1}s^{-1}$ and a 2 m s^{-1} ambient windspeed, the concentrations at x = 20 m range from 4.0 mg m^{-3} at the ground surface to a peak of 17.5 mg m^{-3} at a height of 1.5 m. As a simplifying assumption, we will consider this profile to be representative of average conditions all across the road (i.e., x = -18 m to x = +18 m).

The relationship between concentration and ventilation rate for a rigid chamber is given by Givoni (1969) as:

$$\chi = \frac{Q}{VR}\left[1 - \exp\left(-\frac{VR \cdot t}{VOL}\right)\right] \qquad (29)$$

where Q is the emission rate (g $m^{-1}s^{-1}$), VR is the ventilation rate (m^3 $s^{-1}m^{-1}$), VOL is the volume of the chamber (m^3), and t is the time (s) that the emission has taken place. As t become large, a steady-state situation develops where

$$\chi = \frac{Q}{VR} \cdot \qquad (30)$$

Recalling Figure 40, we compute the average concentration between the surface and z = 4 m as 8.8 mg m^{-3}. We further assume that the ventilation is effective to a height of 4 m and then use Eq. (30) to compute the natural or ambient ventilation rate (VR) as equal to 4.5 $m^3 s^{-1} m^{-1}$. We next postulate the specifications of an artifical ventilating system. For illustration, we assume such a system consists of 0.5-m wide vents located in the center and aligned with the longitudinal axis of each of the six hypothetical traffic lanes; it is assumed further that each vent withdraws air from the roadway surface at a speed of 4 m s^{-1}. The total artificial ventilation (i.e., suction) rate is 12 $m^3 s^{-1} m^{-1}$ as calculated from the product of the individual (artificial) ventilation rate, the number of vents, and the cross section of the vent openings. Provided that the artificial ventilation does not interact with or impair the natural ventilation, then the two may be added (i.e., 16.5 $m^3 s^{-1} m^{-1}$). Using Eq. (30), the "post-ventilated" average CO concentration is estimated to be 2.4 mg m^{-3}.

As was the case with the passive control systems, the example given here should not be interpreted as an endorsement of artificial ventilation in ambient roadway environments. The example is rather a thumbnail sketch of what might be possible at selected, localized areas with high concentrations. Unfortunately, no definitive analyses are available to serve as models for how the complexities of this dispersion-ventilation problem can be treated in a comprehensive and realistic fashion in the ambient atmosphere. In addition to these technical problems there are at least three other aspects that would need to be considered: cost, subsequent venting or control of the withdrawn air, and energy consumption and pollution emissions of the power source for the ventilating system.

D. Semi-quantitative Applications

This subsection addresses a wide range of conditions not explicitly covered by the quantitative methodology. These "departures" have effects that fall into one or both of two categories: emissions and dispersion. Not intended to be all inclusive, the discussion suggests ways in which

the air pollution potential of alternative traffic and roadway conditions may be approached.

1. Noise Barriers

Walls are now frequently constructed along one or both sides of freeways in urban areas for the purpose of muffling the noise in adjacent residential neighborhoods. Of the configurations explicitly incorporated into the assessment methodology, two are similar to the double noise barrier: the vertical-walled cut section, and the "leaky street canyon" configurations. We know of no experimental studies of dispersion near noise barriers and must postulate that there exists a greater similarity with the leaky street canyon. Recalling the background discussion of shelterbelt effects, we suggest that the noise barrier serves to effectively increase turbulent mixing in the local environment of the roadway in much the same way as a field of houses. Furthermore, the wind recirculation characteristic of the vertical-walled cut section is not apt to be present because of the shallow notch formed by the relatively short height of the walls in comparison with their horizontal separation. A six-lane urban freeway with a narrow median and 5-m barriers would likely have height-to-width aspect ratios on the order of 1:8. Accordingly, it is suggested that the porous street-canyon configuration be used to estimate concentrations near a roadway with two noise barriers; for a single noise barrier, one of the two rough-smooth, grade-level configurations is appropriate.

2. Air-right Structure

An air-right structure is a building constructed over the roadway right-of-way. Examples can be seen most often over cut sections, although some also exist over grade-level roadways. One of the experimental configurations tested in the wind tunnel (see Volume I) was an air-right building located over a vertical-walled cut section, shown in the sketch (plan view) below. Wind/roadway angles were varied in the tests: $\theta = \pm 30°$ with the building first located upwind, then downwind of the sampling array used to measure pollutant concentrations.

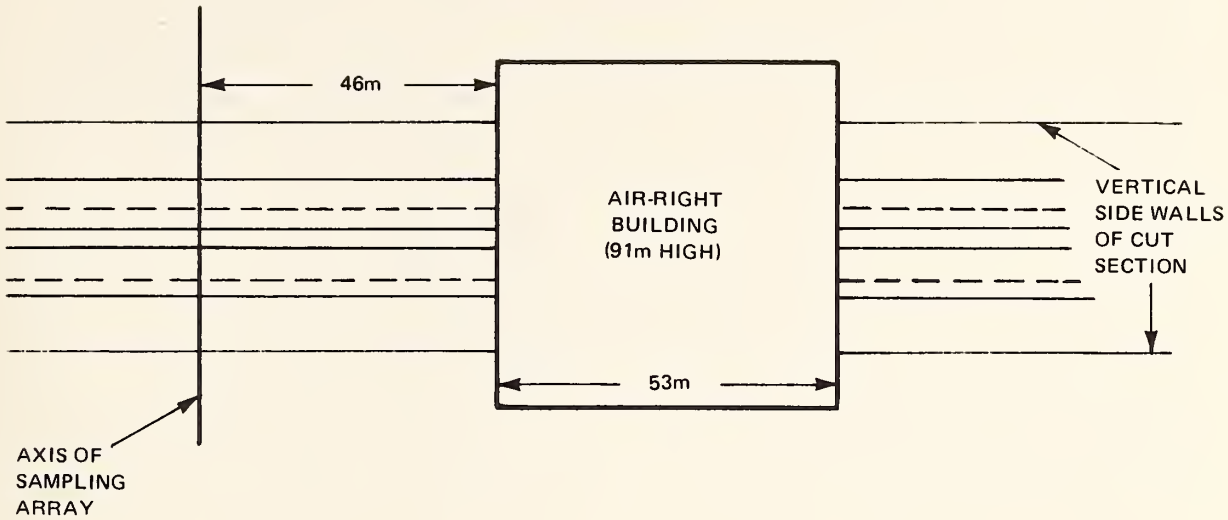

As reported in Volume I (Section VI, Subsection B-1) the aerodynamic effect of the structure resulted in an overall increase of about 70% in concentration levels compared to the same cut-section configuration without the building. However, the ratios at individual locations vary significantly with wind direction relative to roadway and building. Figures 101 (a) and (b) in Volume I illustrate concentration contours for four wind/building/roadway orientations (but at a fixed locus across the roadway 46 m from the building), both in the presence and absence of the air-right structure. Estimates of the concentration can be approximated, first by applying the ROADMAP methodology with inputs appropriate to a vertical-wall cut, and then multiplying these by the ratio of values with and without the structure as estimated for the appropriate location using Figures 101 (a) and (b) in the Volume I report.

3. Large Isolated Buildings Near Roadways

Often, large buildings such as schools and hospitals are located within 50-100 m of major roadways. As these buildings are "sensitive receptors," it is important to quantify the concentrations that can be expected nearby and the influence of the buildings on the dispersion process. Again, virtually no studies have been done to ascertain the magnitude of this effect with the exception of the air-right data reported above. As a rule of thumb, it is suggested that the 70 percent

increase-factor be used as an upper limit of the dispersion impact of the building. The actual effect could be less since the building is not located over the source. Also, the horizontal constraint on dispersion imposed by the walls of the cut section may have served to magnify the relative effect of the turbulence created by the air-right structure.

4. Traffic Congestion

Traffic congestion can affect local concentrations two ways: (1) increasing the emission rate, and (2) decreasing the dispersion. The CO emission flux (g s^{-1}) per vehicle is relatively independent of speed in the range 0-15 mph; the 1975 low-altitude non-California reference value is 0.308 g s^{-1}, as shown in Table 11. Knowing the year and location, the reference flux can be obtained; then the temperature/cold-start and grade correction factors from Tables 6 and 8 should be applied. Lastly, the emission flux density (g $m^{-1}s^{-1}$) is obtained by dividing the flux value by the average length of roadway "occupied" by a single car. This flux density would then be used in Step 4 of the dispersion worksheet (No. 2).

Wind tunnel tests have shown (Volume I) that moving vehicles disperse pollutants appreciably more than idling vehicles, although once a nominal vehicle speed has been attained (e.g., 10 mph) the effect is significantly reduced. Compared to freely moving traffic, pollutant concentrations are about 25 percent greater for idling vehicles. This increase was essentially independent of the near-roadway locations sampled.

5. Grade

Grade is defined as the change in roadway elevation in meters per 100 meters of horizontal distance. Provision was made in Worksheet 1 (see Table 8) for a grade correction factor to the emission flux density. However, the Environmental Protection Agency has not formally issued such factors, and the factors given in Table 8 should be used cautiously. The traffic literature does report some data on the effects of grade on

*See Vol. I, page 163

**This assumes that the spacing and rates of emissions of vehicles are unchanged for idling compared to moving vehicles. If idling vehicles have much closer spacing and higher emission rates per vehicle the difference could be far greater than 25%.

Table 11

CO EMISSION FLUX FACTOR (F)
FOR SLOW-MOVING VEHICLES

Year	Flux Factor (gm/s-veh)			
	Low Altitude (Non-California)	High Altitude (Non-California)	Low Altitude (California)	High Altitude (California)
1975	0.038	0.544	0.302	0.533
1976	0.268	0.484	0.252	0.455
1977	0.245	0.433	0.232	0.410
1978	0.204	0.375	0.189	0.347
1979	0.167	0.314	0.159	0.299
1980	0.135	0.255	0.131	0.247

emissions. These were recently summarized in a report by Technical Committee on Road Tunnels of the Permanent International Association of Road Congresses* at the XV Congress held in 1975 in Mexico City. Illustrated in Figure 41, their values show a nearly ±20 change in emissions for grades of ±4 percent, respectively. In the absence of better data, these have been cited in Table 8 for use in Worksheet 1.

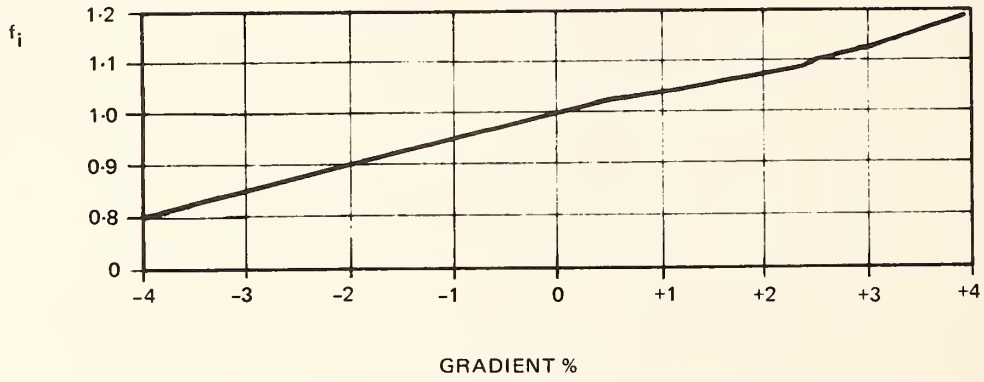

FIGURE 41 SLOPE CORRECTION FACTOR FOR CO EMISSIONS

6. Street Canyons and Cut Sections

The cut sections evaluated experimentally (Volume I) were each 6.1 m deep; the vertical-walled configuration was 38.1 m wide (1:6 aspect ratio), and the base of the sloping (30°) configuration was 29.0 m wide. It would be difficult to extrapolate the generalized outputs of the assessment methodology to significantly deeper cut sections.

One special type of cut which does, however, lend itself to wider analysis is the high-aspect-ratio, urban street-canyon configuration discussed earlier in Section II (C-3). Johnson et al. (1971) reported on a simple model of pollutant concentrations which can be used to describe concentrations within these relatively deep cuts. The model treats the concentration (χ) at a receptor as having two superimposed components.

*43 Avenue du Président-Wilson, Paris, 16, France.

One component is the concentration (χ_b) of the air entering the street canyon from above. The other component ($\Delta\chi$) arises from the locally generated CO emissions within the street. Hence, we have

$$\chi = \chi_b + \Delta\chi \quad . \tag{31}$$

Equations for calculating the $\Delta\chi$ components on both the leeward side ($\Delta\chi_L$) and the windward side ($\Delta\chi_W$) were derived by Johnson et al. (1971) and modified by Ludwig and Dabberdt (1972). The leeward component is calculated by

$$\Delta\chi_L = \frac{K\, Q_s}{(u + 0.5)\left[(x^2 + z^2)^{1/2} + L_o\right]} \quad . \tag{32}$$

In this equation, K is an empirical nondimensional constant ($K \simeq 7$); L_o is a dimension representing the vehicle size ($L_o \simeq 2$ m); and x and z are the horizontal and vertical distance of the receptor relative to the center of the traffic lane (see Figure 42). Also, u is the rooftop wind speed (m s^{-1}), generally estimated from the airport wind speed U_a by a regression relationship, and Q_s is the average rate of emission of CO (g $m^{-1} s^{-1}$) in the street. Values of Q_s are computed by Worksheet 1. The windward-side component ($\Delta\chi_W$) is calculated by

$$\Delta\chi_W = \frac{K\, Q_s (H^* - z)}{W(u + 0.5)H^*} \tag{33}$$

where W is the street width, and H^* is the average building height. When the wind direction is such that neither a leeward nor a windward case is appropriate, an intermediate concentration ($\Delta\chi_I$) is calculated by combining the above two equations,

$$\Delta\chi_I = 1/2\ (\Delta\chi_L + \Delta\chi_W) \quad . \tag{34}$$

Figure 43 defines the range of windward, leeward, and parallel wind directions.

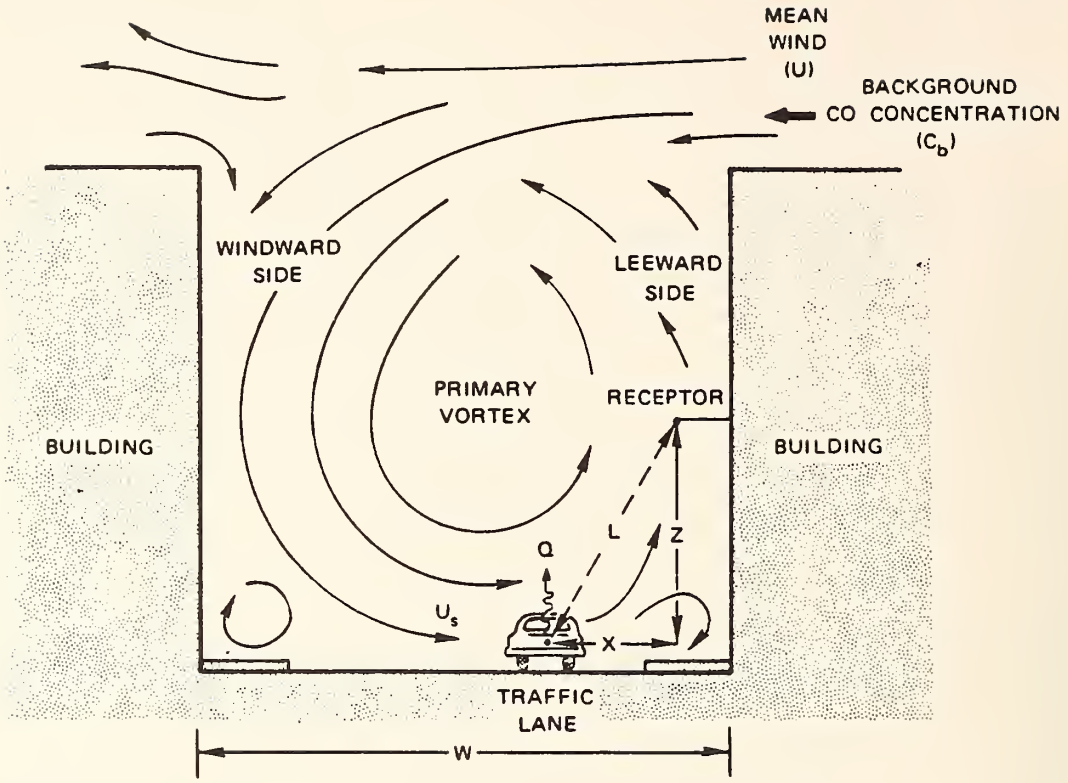

FIGURE 42 SCHEMATIC OF CROSS-STREET CIRCULATION BETWEEN BUILDINGS

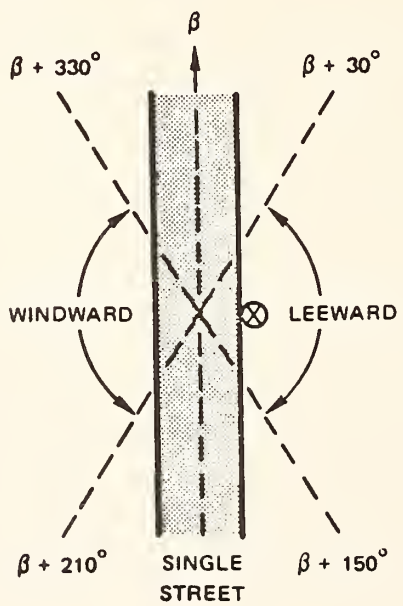

FIGURE 43 SPECIFICATION FOR LEEWARD AND WINDWARD CASES ON THE BASIS OF RECEPTOR LOCATION, STREET ORIENTATION, AND WIND DIRECTION

7. Hillsides

A roadway located at the base or on the side of a semi-infinite ridge is a special type of fill section. Maximum concentrations are comparable to those estimated from the assessment methodology. However, experimental wind tunnel tests described in Volume I have indicated that the distribution pattern of concentration levels is markedly different, a direct consequence of the eddy circulations that are associated with wind flow over a hill or ridge (see Section II). When the roadway is located on the upwind side of the hill the dispersion is enhanced and concentrations are both relatively low and decrease quickly downwind. Figure 44(a) illustrates CO concentrations (ppm) for a 30° slope with moderate traffic that is uniform in both directions and a 3-m s^{-1} cross-wind. When the roadway is on the downwind side of the same hill, a different pattern emerges. An eddy circulation develops in the lee of the hill as is seen in the concentration pattern in Figure 44(b). The backflow extends nearly to the top of the hill for the case studied. Moreover, the wind speed in the lee of the hill is reduced accordingly, and the transport of pollutants away from the roadway is retarded. Over the roadway, pollutant concentrations are increased by over 50 percent.

E. Remarks

In this section we have tried to illustrate some of the many ways that the assessment methodology can be used to evaluate the effects on pollution concentrations of variations in meteorology, traffic, and roadway configuration. More often than not, an actual site requiring evaluation would not fit one of the nine basic configurations for which the methodology has been derived. A number of these departures have been discussed with the idea of providing guidance for the extended application of the methodology. In the final analysis, it will be the judgment and experience of the user that will ultimately determine the exact approach to be followed and the subsequent representativeness of the results.

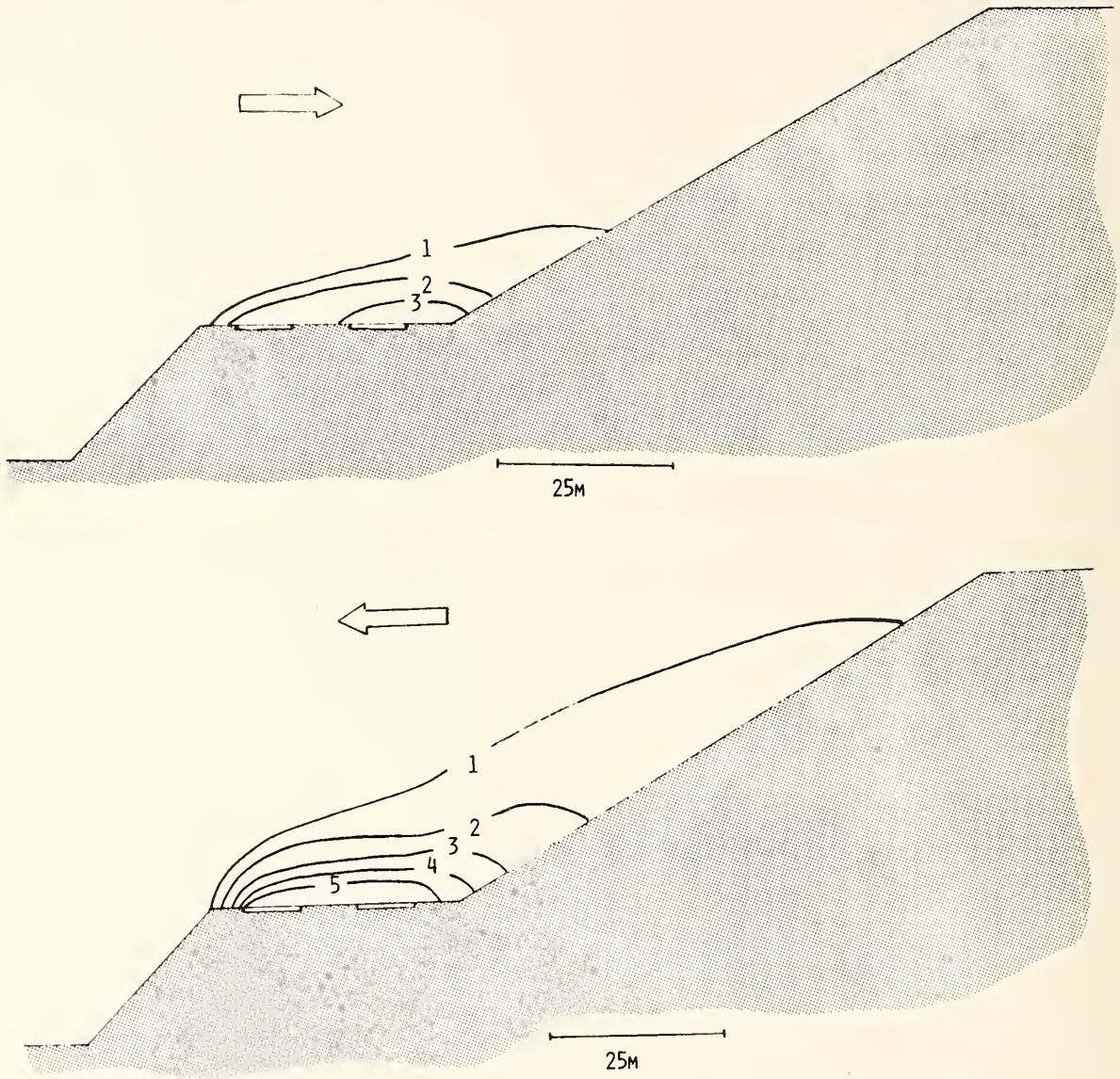

FIGURE 44 WIND TUNNEL RESULTS OF CARBON MONOXIDE CONCENTRATIONS (ppm) FOR A ROADWAY ON A HILLSIDE WITH A 3-m s^{-1} AMBIENT CROSSWIND AND MODERATE TRAFFIC MOVING AT 25 MPH

A last caution: The assessment methodology as presented here is designed for use as a planning and evaluation tool. It can be used to weigh the air pollution potential of alternative roadway designs or locations or to obtain a first cut at the absolute value of the near-roadway CO levels. In most cases it should not be used to make detailed evaluations of the type required in environmental impact statements unless the site is nearly identical to one of the nine tested. Even then, the detailed model evaluations reported in Volume I should be considered.

V AIR QUALITY MANAGEMENT THROUGH ROADWAY DESIGN AND LOCATION

A. Use of the ROADMAP Assessment Procedure

Section III provided a description of the rationale for and the basis of the ROADMAP assessment methodology. Worksheets, tables, and instructions were given to facilitate the use of ROADMAP. Apart from the mechanics of the application of the procedure, the user must bear in mind the purposes for which the model can properly be applied (i.e., when and where ROADMAP should be used). Many aspects of the proper use of the model have already been discussed in Section IV; others will be addressed here.

Perhaps the most important feature of the model is the scale over which it may be used. ROADMAP is by design a microscale model; its use is most appropriate out to distances of 50-100 m from the roadway edges. Accordingly, it would be inappropriate to assess the larger scale effects due, for example, to local circulations in mountain-valley regimes where the characteristic length scale may be on the order of kilometers. To be sure, the model could be used to assess microscale impacts near the roadway, but not throughout the valley.

In analyzing the local air pollution aspects of any highway project (existing or proposed), it is essential that the user identify and address both (1) the background and (2) the local components of the total air pollution concentration at the site. For the purposes of this study, the local component results entirely from vehicular pollutant emissions of the project under review; ROADMAP addresses only the local component. The so-called background component is the portion of the total pollution concentration that is produced by pollutant emissions other than those from vehicles that are using or would use the project under review. Several interesting and important aspects should be considered: (1) the background component may not be uniform

throughout the project site when other, non-local emission sources are close by; and (2) the magnitude of the background component may change as a result of interactions between traffic flow at the project site and in the immediate vicinity which may alter the density and/or dynamics of the traffic (and hence the resulting emissions) away from the project site.

There are two similar yet distinct ways in which the ROADMAP methodology may usefully be applied. In the first application, ROADMAP may be used to estimate the absolute magnitude of the concentration of inert pollutants emitted from an existing or proposed project. If the highway project is already completed and the (total) pollution concentration is known, then this will provide useful information on the relative magnitudes of the local and background components. In this way, it is possible to address the degree of local control necessary to improve existing air quality conditions to the point where they may, for example, comply with the National Ambient Air Quality Standards (NAAQS). Or, alternatively, such analysis could also be used to address proportional controls of both local and background emission sources.

The second use of ROADMAP involves the assessment of the local air pollution impacts of alternative designs or locations of proposed or existing roadways. Such air pollution "benefits" can then be evaluated in conjunction with their corresponding costs against other environmental, engineering, and aesthetic considerations to assess the optimal project design. In the remaining portions of this section, we will address these types of air management considerations. But throughout, one concept should be remembered--that is that no broad and firm generalizations can be made applicable to all sites. As emphasized in Section II, there are many processes that control local dispersion and subsequently air quality, and depending on the configuration of the local project, any one or more of these factors may dominate.

B. Guidelines for the Management of Local Air Quality

One of the more revealing findings of the experimental studies reported in Volume I is the complex manner in which atmospheric stability and wind/roadway orientation are interrelated with the magnitude of the pollution concentration. Some examples of this complex relationship are given in Table 12; the values are computed from ROADMAP for a grade-level roadway for three stability types, two wind directions (θ), two cross-roadway distances (x), and three heights (z). Referring to the table, the highest concentration at z = 1 m occurs with θ = 90°, x = 15 m, and neutral stability; whereas at z = 3 m the highest concentration occurs again at x = 15 m, yet under unstable conditions and with little dependence on θ. Thus in seeking to manage air quality by varying the height or separation of sensitive receptors, it is necessary to consider the joint effects of wind/roadway orientation and atmospheric stability for the time of peak local emissions. Also, the example given in Table 12 is only for a grade-level roadway in smooth terrain; similar considerations are necessary for each roadway configuration.

Table 12

COMPARISON OF ROADMAP COMPUTATIONS OF $\chi U/Q(m^{-1})$ FOR AN AT-GRADE ROADWAY, ILLUSTRATING THE VARIATION WITH STABILITY, HEIGHT, CROSS-ROADWAY DISTANCE, AND WIND-ROADWAY ORIENTATION

θ (deg)	x (m)	z = 1 m			z = 3 m			z = 8 m		
		U*	N*	S*	U	N	S	U	N	S
0	15	.314	.246	.254	.453	.111	.142	.040	.111	.015
0	40	.192	.329	.275	.204	.300	.246	.079	.119	.134
90	15	.297	.985	.092	.416	.112	.054	.040	.111	.010
90	40	.200	.383	.063	.212	.347	.057	.091	.121	.034

*U = unstable, N = neutral, S = stable.

On occasion, alternative locations for a proposed project may be considered where there is a marked difference in surface roughness.

In these situations, surface roughness may be considered as an air management device. For example, scale-model tests in the wind tunnel indicate that a surface with roughness typical of single-story housing developments can reduce concentrations near grade-level roads by 30-40% from their counterparts in flat and open terrain. Comparisons are given in Table 13 for several variations in θ, x, and z (all with neutral stability).

Table 13

COMPARISON OF ROADMAP COMPUTATIONS OF $\chi U/Q(m^{-1})$ FOR AN AT-GRADE ROADWAY, ILLUSTRATING THE VARIATION WITH SURFACE ROUGHNESS, HEIGHT, CROSS-ROADWAY DISTANCE, AND WIND-ROADWAY ORIENTATION DURING NEUTRAL ATMOSPHERIC STABILITY

θ (deg)	x (m)	z = 1 m		z = 3 m		z = 8 m	
		Smooth	Rough	Smooth	Rough	Smooth	Rough
0	15	.254	.138	.207	.134	.073	.090
0	40	.128	.076	.120	.076	.079	.074
90	15	.263	.943	.212	.139	.073	.092
90	40	.201	.092	.169	.092	.092	.089

Grade-level roadways are candidates for at least two types of passive dispersion-enhancement techniques. As discussed earlier in Section III-C, both the selection of the roadway surface-type and the use of medianbelts (shelterbelts or windbreaks erected along the roadway median) offer at least some potential for enhancing the initial dispersion of roadway emissions. By varying the thermal properties of the roadway surface relative to the properties of the adjacent terrain, it is conceivable that the local stability can be modified measurably. Rough estimates indicate the magnitude of this effect could approach that of the waste heat from the traffic (i.e., a few degrees Celsius across the roadway). Similarly, there are theoretical indications that medianbelts could also enhance the initial mixing process significantly. However, in both cases the user is cautioned that these techniques are as yet unproven and should not be employed without further study.

Whereas passive control techniques would require no continuous, artificial input of energy, active control measures have the disadvantage of being energy consumers. As such, they are less attractive. Two types of active systems have been considered: (1) those that seek to modify the air flow or turbulence levels, and (2) filtering systems. Apart from the disadvantages of heavy energy consumption, those of the first kind are not thought to be feasible for any but the most localized situations. This is because of the following: (1) increasing the turbulence intensity within a given layer will not be effective if the emissions are already well-mixed--as they usually are; and (2) modification of the mean flow structure is impractical, particularly in view of the large amounts of mean and turbulent kinetic energy already existent in the ambient flow as well as the drag flow from the vehicles.

On the other hand, active control using a filtering system may occasionally be attractive. As discussed in Section III-C, a small-scale system that withdraws high-concentration air from the near-roadway environment may be quite effective. Even so, there would be the additional problem of either purifying or safely venting the highly polluted air so as not to create a new pollution problem elsewhere. Similar to the passive techniques, this type of active system requires additional study to support its usage in that it has not been used outside of the confines of tunnels and parking garages.

A more direct approach to the management of local air quality conditions near highways is through the minimization of vehicular emission rates by optimizing traffic operations. In the case of CO and hydrocarbons, this means increasing the average vehicle speed. However, emission of nitrogen oxides vary in the opposite way, increasing with increasing speed. Insofar as adverse local air quality conditions mainly involve CO, we will focus on the relationship between vehicle speed and CO emissions. In the limit, a single traffic lane can accommodate a demand volume of 1067 vehicles per hour traveling at 5 mph*--provided they all move in unison with a headway equal to 5 m (i.e., one vehicle length per 10-mph increment of speed). Similarly, the corresponding hypothetical capacity at 15 mph is 1920 vehicles per hour per lane. Of course the

---

*1 mph = 1.6 kmph

actual capacity will be less than these hypothetical estimates. But for illustrative purposes, we have tabulated the hypothetical CO emission flux densities (Q) that correspond to various speeds (with the help of Figure 23) assuming: (1) all vehicles are 1975, non-California models, (2) the cold-start percentage is zero, and (3) the vehicles are at low altitude. Also included in the tabulation are values for several different roadway grades.

Cruise Speed (mph)	CO Emission Flux Density ($g\ m^{-1} s^{-1}$)		
	0% Grade	+10% Grade	-10% Grade
5	.0267	.0395	.0134
10	.0191	.0283	.0096
15	.0149	.0221	.0075
20	.0130	.0192	.0065
25	.0121	.0179	.0090

Referring to the tabulation, several air management strategies emerge. For example, on a level roadway Q decreases 22% when speed is increased from 10 to 15 mph. Uphill traffic on a 10% grade has a CO flux nearly three times greater than does the downhill traffic. Combining these two concepts it becomes immediately apparent that it is essential that uphill traffic flow be optimized to avoid excessively large CO emissions. It may also be advisable to consider diverting the roadway into two widely separated uphill sections in urban areas to avoid creating a single section with a very large emission flux. Better yet, steep uphill grades should be avoided on high-demand roadways in areas with poor air quality conditions (i.e., high background).

The configuration of the roadway itself can be very important. Perhaps the most dramatic example of this is the comparison of concentrations that were observed in the wind tunnel tests on the upwind sides of two cut sections. With a cross-roadway wind, peak concentrations just upwind of the roadway in a vertical-walled cut were four times larger then comparable values in an equally deep cut with sloping (30°) side walls. Downwind differences are not as dramatic, though they can still

be significant. In Table 14, concentrations are compared at common receptors for each of five roadway configurations (all with smooth adjacent terrain) tested in the wind tunnel experiments reported earlier: (1) grade-level, (2) vertical-walled cut, (3) sloping-walled cut, (4) fill section, and (5) viaduct section. In the near-downwind vicinity of the roadway, pollutant concentrations are generally comparable among the grade-level and two cut sections. The height-dependence is also similar among these three configurations: values at z = 1 and 3 m are about the same, while at z = 8 m they fall off toward zero. The principal difference between these three configurations and the two elevated cases is mainly the offset in the height of the plume centerline. Thus (in the near vicinity of the road) concentrations at ground-level are small and increase toward the roadway height. Further downwind the ground-level concentrations increase as the plume continues to disperse over a wider vertical cross section.

Other examples of possible air management techniques have already been discussed in Sections II and IV. As indicated before, the "air quality manager" must always consider the task of minimizing air pollution impacts in the context of the design of the proposed roadway, the nature of the surrounding terrain, and the magnitude of the background pollution concentration. Only then can a meaningful assessment of alternative control measures be undertaken.

Table 14

COMPARISON OF ROADMAP CONCENTRATION ESTIMATES
FOR FIVE ROADWAY CONFIGURATIONS

θ* (deg)	x† (m)	z† (m)	Normalized Concentration ($\chi U/Q, m^{-1}$)				
			Grade Level	Vertical‡ Cut	Sloped‡ Cut	Fill§ Section	Viaduct§ Section
0	15	1	.254	.138	.212	**	.028
0	15	3	.207	.196	.277	**	.028
0	15	8	.073	.137	.110	**	.028
0	15	15	.068	.071	.057	.074	.036
0	40	1	.128	**	**	.040	.029
0	40	3	.120	**	**	.041	.029
0	40	8	.079	.121	.121	.044	.029
0	40	15	.068	.106	.091	.046	.030
90	15	1	.263	.181	.170	**	.028
90	15	3	.212	.276	.217	**	.028
90	15	8	.073	.179	.096	**	.032
90	15	15	.068	.071	.057	.213	.233
90	40	1	.201	**	**	.070	.057
90	40	3	.169	**	**	.083	.053
90	40	8	.092	.143	.110	.123	.057
90	40	15	.068	.121	.083	.143	.096

*0° wind is parallel to the roadway; 90° is perpendicular

†x = 0 at center of roadway median
y = 0 at roadway surface for grade level, and vertical and sloped cut sections
z = 0 at ground level for fill and viaduct sections

‡D = 6.1 m

§H = 18.3 m

**Below ground surface

REFERENCES

Calder, K., 1973: "On Estimating Air Pollution Concentrations from a Highway in an Oblique Wind," Atm. Env., Vol. 7, pp. 863-868.

Chock, D.P., 1977: "General Motors Sulfate Dispersion Experiment: Assessment of the EPA-HIWAY Model," J. Air Poll. Contr. Assoc., Vol. 27, p. 39.

Dabberdt, W.F., et al., 1974: "Studies of Air Quality On and Near Highways," First Interim Report, DOT Contract FH-11-8125, SRI Project 2761, Stanford Research Institute, Menlo Park, California.*

Dabberdt, W.F., 1975: "Studies of Air Quality On and Near Highways,"* Second Interim Report, DOT Contract FH-11-8125, SRI Project 2761, Stanford Research Institute, Menlo Park, California.

Dabberdt, W.F., and R.C. Sandys, 1976: "Guidelines for Evaluating Indirect Sources," Final Report, EPA Contract 68-02-2073, SRI Project 4429, Stanford Research Institute, Menlo Park, California.

Dabberdt, W.F., et al., 1976: "Rationale and Evaluation of Technical Guidelines for the Review of Indirect Sources," Technical Report, EPA Contract 68-02-2073, SRI Project 4429, Stanford Research Institute, Menlo Park, California.

Dabberdt, W.F., E. Shelar, D. Marimont, and G. Skinner, 1979: "Analyses Experimental Studies, and Evaluations of Control Measures for Air Flow and Air Quality On and Near Highways; Vol. I: Experimental Studies, Analyses, and Model Development," DOT Contract FH-11-8125, SRI Project 2761, SRI International, Menlo Park, California.

Dabberdt, W.F., and P.A. Davis, 1977: "Determination of Energetic Characteristics of Urban-Rural Surfaces in the Greater St. Louis Area," Boundary-Layer Meteor., Vol. 14, pp. 105-121.

*Available from NTIS

Dalrymple, P.C., H.H. Lettau, and S.H. Wollaston, 1966: "South Pole Micrometeorology Program: Data Analysis," Antarctic Research Series, Vol. 9 pp. 13-58 (American Geophysical Union, Washington, D.C.).

Environmental Protection Agench, 1978: "Guidelines for Air Quality Maintenance Planning and Analysis; Volume 9 (Rev.): Evaluating Indirect Sources," Report EPA-450/4-78-001 (OAQPS No. 1.2-028R), Research Triangle Park, North Carolina.

Edinger, J., 1966: Watching for the Wind (Doubleday Science Series, Garden City, New York).

Geiger, R., 1965: The Climate Near the Ground (Harvard University Press, Cambridge, Massachusetts).

Georgii, H., E. Busch, and E. Weber, 1967: "Investigation of the Temporal and Spatial Distribution of the Emission Concentration of Carbon Monoxide in Frankfurt/Main," Report No. 11 of the Institute for Meteorology and Geophysics, University of Frankfurt/Main [Translation No. 0477, NAPCA].

Goldstein, S., 1938: Modern Developments in Fluid Dynamics (Oxford Press, England).

Halitsky, J., 1961: "Wind Turbulence in the Lee of a Low Conical Mountain (Local Wind Circulations), Quarterly Progress Report No. 4, New York University, New York; New York.

Highway Research Board, 1971: Highway Capacity Manual, Special Report 87 (National Academy of Sciences, National Research Council, Washington, D.C.).

Johnson, W.B., et al., 1971: "Field Study for Initial Evaluation of an Urban Diffusion Model for Carbon Monoxide," Final Report to Coordinating Research Council and Environmental Protection Agency, Contract CAPA-3-68(1-69), Stanford Research Institute, Menlo Park, California [NTIS No. PB-203469].

Lettau, H.H., 1962: "Notes on Theoretical Models of Profile Structure in the Diabatic Surface Layer," in Final Report on Studies of the Three-Dimensional Structure of the Planetary Boundary Layer, pp. 195-226, Contract DA 36 039 SC-80282, University of Wisconsin, Madison, Wisconsin.

Lettau, H.H., 1969: "Note on Aerodynamic Roughness-Parameter Estimation on the Basis of Roughness-Element Description," J. Appl. Meteor., Vol. 8, pp. 828-832.

Ludwig, F.L., and W.F. Dabberdt, 1972: "Evaluation of the APRAC-1A Urban Diffusion Model for Carbon Monoxide," Final Report to Coordinating Research Council and Environmental Protection Agency, Contract CAPA-3-68 (January 1969), Stanford Research Institute, Menlo Park, California.

Nägeli, W., 1941: "Untersuchungen über die Windverhältnisse im Bereich von Windschutzstreifen," Mitt. Schweiz. Anst. Forstl. Versuchsw., Vol. 23, pp. 221-276.

Plate, E.J., and C.Y. Lin, 1965: "The Velocity Field Downstream from a Two-Dimensional Model Hill," Final Report, Part I, to U.S. Army Material Agency.

Plate, E.J., 1971: Aerodynamic Characteristics of Atmospheric Boundary Layers, AEC Critical Review Series, Oak Ridge, Tennessee [NTIS No. TID-25465].

Slade, D.H., 1968: Meteorology and Atomic Energy, U.S., Atomic Energy Commission, Oak Ridge, Tennessee [NTIS No. TID-24190].

Stearns, C.R. and H.H. Lettau, 1963: "Two Wind-Profile Measurement Experiments in Airflow over the Ice of Lake Mendota," Annual Report, Univ. of Wisconsin, Department of Meteorology, Madison, Wisconsin.

World Meteorological Organization, 1964: Windbreaks and Shelterbelts, Tech. Note 59 (Geneva, Switzerland).

Zimmerman, J.R. and R.S. Thompson, 1975: "User's Guide for HIWAY, A Highway Air Pollution Model," Report No. EPA-650/4-74-008, U.S. Environmental Protection Agency, Research Triangle Park, North Carolina.

*U.S. GOVERNMENT PRINTING OFFICE: 1981-0-728-402/1834

FEDERALLY COORDINATED PROGRAM (FCP) OF HIGHWAY RESEARCH AND DEVELOPMENT

The Offices of Research and Development (R&D) of the Federal Highway Administration (FHWA) are responsible for a broad program of staff and contract research and development and a Federal-aid program, conducted by or through the State highway transportation agencies, that includes the Highway Planning and Research (HP&R) program and the National Cooperative Highway Research Program (NCHRP) managed by the Transportation Research Board. The FCP is a carefully selected group of projects that uses research and development resources to obtain timely solutions to urgent national highway engineering problems.*

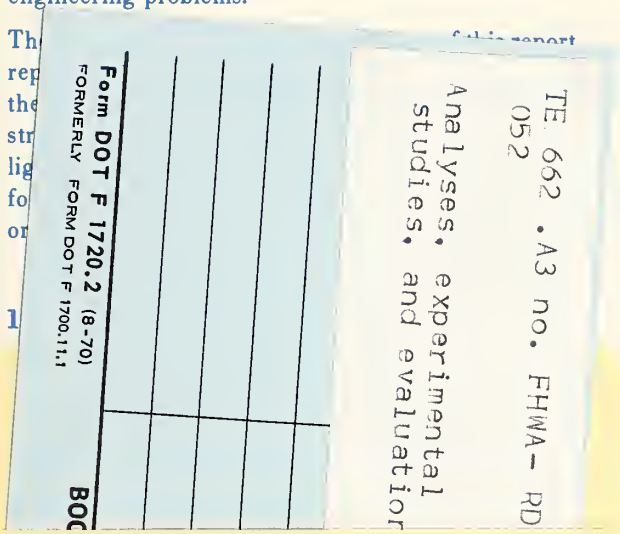

4. Improved Materials Utilization and Durability

Materials R&D is concerned with expanding the knowledge and technology of materials properties, using available natural materials, improving structural foundation materials, recycling highway materials, converting industrial wastes into useful highway products, developing extender or substitute materials for those in short supply, and developing more rapid and reliable testing procedures. The goals are lower highway construction costs and extended maintenance-free operation.

5. Improved Design to Reduce Costs, Extend Life Expectancy, and Insure Structural Safety

Structural R&D is concerned with furthering the latest technological advances in structural and hydraulic designs, fabrication processes, and construction techniques to provide safe, efficient highways at reasonable costs.

5. Improved Technology for Highway Construction

This category is concerned with the research, development, and implementation of highway construction technology to increase productivity, reduce energy consumption, conserve dwindling resources, and reduce costs while improving the quality and methods of construction.

Improved Technology for Highway Maintenance

This category addresses problems in preserving the Nation's highways and includes activities in physical maintenance, traffic services, management, and equipment. The goal is to maximize operational efficiency and safety to the traveling public while conserving resources.

Other New Studies

This category, not included in the seven-volume official statement of the FCP, is concerned with HP&R and NCHRP studies not specifically related to FCP projects. These studies involve R&D support of other FHWA program office research.